Methamphetamine-induced Cell Death in the Striatum and the Role of Neurokinin-1 Receptor in its Pathogeny

by

Judy Peng Qiao Zhu

A dissertation submitted to
the Graduate Faculty in Biology
in partial fulfillment of the requirements for the degree of

Doctor of Philosophy

at

THE CITY UNIVERSITY OF NEW YORK

2006

UMI Number: 3205014

ProQuest Information and Learning Company
300 North Zeeb Road
P.O. Box 1346
Ann Arbor, MI 48106-1346

This manuscript has been read and accepted for the
Graduate Faculty in Biology in satisfaction of the
dissertation requirement for the degree of Doctor of Philosophy.

January 24th, 2006	Jesus A. Angulo
Date	Chair of Examining Committee
January 30th, 2006	Richard L. Chappell
Date	Executive Officer

Syed F. Ali

Maria E. Figueiredo-Pereira

Thomas Schmidt-Glenewinkel

Christoph P. Wiedenmayer
Supervision Committee

THE CITY UNIVERSITY OF NEW YORK

ABSTRACT

Methamphetamine-induced Cell Death in the Striatum and the Role of Neurokinin-1 Receptor in its Pathogeny

by

Judy Peng Qiao Zhu

Adviser: Professor Jesus A. Angulo

Methamphetamine (METH) is a potent psychostimulant known to cause extensive neural damage in the central nervous system. Continued characterization of its neural effects showed that single intraperitoneal injection of METH (10-40 mg/kg of body weight) induces striatal apoptosis (assessed by terminal deoxynucleotidyl transferase-mediated dUTP nick end labeling [TUNEL]) dose-dependently. Single bolus doses of METH generated higher levels of TUNEL-positive neurons compared to a binge of METH (4 x 10 mg/kg of body weight at 2-hour intervals). METH-induced (30 mg/kg of body weight) apoptosis peaks at 24 hours after treatment, and occurs prior to the depletion of dopamine nerve terminal markers and the increases in reactive astrocytes. Nissl staining confirmed neuronal loss at this time point. Since the striatum is a heterogeneous structure known to exhibit selective vulnerabilities

towards different insults, a series of immunohistochemical and cell quantification studies were carried out to identify the phenotypes of cells affected by METH. METH induced death of GABAergic projection neurons. METH also damaged GABAergic and cholinergic interneurons in the dorsal striatum. Interestingly, somatostatin interneurons were spared.

Since METH augments striatal substance P (SP) levels, it was hypothesized that signaling through the neurokinin-1 (NK-1) receptor by SP activates the apoptotic cascade. To determine the role of NK-1 receptor in METH-induced apoptosis, the effects of pharmacological blockade and local ablation of receptor-expressing neurons were examined. Administration of NK-1 receptor antagonist, WIN 51,708, 30 minutes prior to METH exposure, prevented METH-induced apoptosis and peroxynitrite generation. Pretreatment with WIN 51,708 had no effect on METH-induced hyperthermia. To confirm that local activation of NK-1 receptors within the striatum are contributing to METH-induced apoptosis of striatal neurons, NK-1 receptor-expressing interneurons were selectively ablated by intrastriatal injections of NK-1 receptor agonist, [Sar^{9},$Met(O_2)^{11}$]substance P, conjugated to a ribosomal-inactivating cytotoxin saporin (SSP-SAP). Ablation of NK-1 receptor-expressing striatal interneurons prevented METH-induced apoptosis. These results provide the first pharmacological evidence that tachykinins, particularly SP, acting through NK-1 receptors, play a crucial role in the pathogenesis of METH-induced cell death in the striatum. These findings also suggest a novel approach for therapeutic interventions in the treatment of neurodegenerative disorders including Parkinson's and Huntington's

diseases.

ACKNOWLEDGEMENTS

I would like to thank my mentor, Jesus Angulo, for all his guidance, encouragement and support. His persevering and zealous spirit in science has guided and encouraged me throughout my graduate training. When most needed, he has helped me see that a butterfly flapping its wings on the other side of the world can change the climate of the globe. His confidence in me as a student has helped shaped me into the independent thinker that I am today.

I wouls also like to extend my gratitude to the other members of my thesis committee, Drs. Syed F. Ali, Jean Lud Cadet, Maria E. Figueiredo-Pereira, Thomas Schmidt-Glenewinkel, and Christoph P. Wiedenmayer for their time, resources, and advice throughout my graduate training. I am especially indebted to Dr. Thomas Schmidt-Glenewinkel for helping me find my way to science.

I would like to thank my colleague, Dr. Wenjing Xu, for her friendship and for her collaborative work on the SSP-SAP model. I would also like to express my appreciation to my other colleagues Dr. Pierre Noailles, Dr. Thomas Loonam, Dr. Jing Yu, Xu Han, and Jing Wang for generating a creative and supportive environment in which to work. I would like to thank Gertrude Rivera for her generous and kind spirit.

I would like to dedicate this thesis to my family. To my parents, who has loved and sacrificed for me tremendously. They are a constant source of strength to which I can always look to for motivation. To my siblings, Jenny, Mary, and Vincent, who has unending faith in me. Their endless love and support has given me great encouragement. To my husband, Tom, who has inspired courage. I am blessed by his endearing love and constant support.

TABLE OF CONTENTS

LIST OF FIGURES

Number *Page*

LIST OF ABBREVIATIONS

3-NT	3-nitrotyrosine
5-HT	Serotonin
AMPA	Alpha-amino-3-hydroxy-5-methyl-4-isoxazolepropionic acid
ChAT	Choline acetyltransferase
CPu	Caudate-putamen
CuZnSOD	cooper-zinc-dependent superoxide dismutase
DA	dopamine
DARPP-32	Dopamine and cyclic adenosine 3',5'-monophosphate-regulated phosphoprotein, 32 kDa
DAT	Dopamine transporter
DL	Dorsal lateral
DM	Dorsal medial
GABA	Gamma-aminobutyric acid
GFAP	Glial fibrillary acidic protein
HPLC	High performance liquid chromatography
i.p.	Intraperitoneal
METH	Methamphetamine
MnSOD	Manganese superoxide dimutase
NeuN	Neuronal nuclei
NGS	Normal goat serum
NKA	Neurokinin A
NKB	Neurokinin B
NK-1	Neurokinin-1
NK-2	Neurokinin-2
NK-3	Neurokinin-3
NMDA	N-methyl-D-aspartate
NO	Nitric oxide
NOS	Nitric oxide synthase
NRS	Normal rabbit serum

$ONOO^-$	Peroxynitrite	SST	Somatostatin
O_2^-	Superoxide	STN	Subthalamic nucleus
PBS	Phosphate buffered saline	TH	Tyrosine hydroxylase
		TUNEL	Terminal deoxynucleotidyl transferase-mediated dUTP nick end labeling
PPT-A	Preprotachykinin-A		
PPT-B	Preprotachykinin-B		
SAP	Saporin		
SN	Substantia nigra	Tyr	Tyrosine
SOD	Superoxide dismutase	VL	Ventral lateral
SP	Substance P	VM	Ventral medial
SSP-SAP	$[Sar^9,Met(O_2)^{11}]$ substance P-saporin		

Chapter 1

Introduction

1.1 History and Prevalence of the Methamphetamine Problem

Methamphetamine (METH) is an addictive and very potent central nervous system stimulant. Since first synthesized in 1919 by Japanese chemist A. Ogata (Ogata, 1919), METH's use, distribution, and place in society has changed from insignificant to controversially beneficial to terrible infamy in the past eight decades (Lukas, 1985; Anglin et al., 2000). METH was first marketed as an anorectic drug under the trade name Methedrine®. During the 1940's, METH (under the name Pervitin) and amphetamine-related stimulants were widely distributed by Allies and Axis troops to combat fatigue and increase endurance during WWII. It is a practice used by the military that has continued through the present day (Emonson and Vanderbeek, 1995). In the 1950's and 1960's, it was widely prescribed to the American public for depression and obesity, reaching a peak of 31 million prescriptions in the United States in 1967 (Anglin et al., 2000).

The start of illicit METH manufacture by clandestine laboratories also began in the 1960's. Unlike cocaine and marijuana which needs to be directly harvested from coca and cannabis plants, METH is synthetic and is produced with ease using inexpensive chemicals that are readily available in household products and over-the-counter medicines (ephedrine and pseudoephedrine). This has made METH a drug of choice for illegal synthesis and has contributed to its widespread use. Today, in addition to the clandestine "super labs" run by drug traffickers in Mexico and California, numbers of small-scale "mom and pop" clandestine METH labs have increased all over the United States; especially in poor suburban and rural areas of the Southwest and the Midwest (DEA, 2005).

Until the late 1980s, illicit consumption and production of METH was endemic to California and Hawaii. Today, the consumption and distribution of this popular recreational drug of abuse has broadened in nature and in regional distribution. Epidemic proportions of use and abuse have spread from Hawaii and the west cost to the southwestern areas and Midwestern states; along with a trend that is continuing to move eastward in the country (CEWG, 2005). According to SAMHSA's (Substance Abuse and Mental Health Services Administration) *2004 National Survey on Drug Use and Health*, an estimated 11.7 million Americans, aged 12 or older, had used METH at least once in their lifetime; with an estimated 300,000 initiates of METH abuse every year (SAMHSA, 2005). According to the United Nations Office of Drugs and Crime, more than 33.4 million individuals regularly use and abuse amphetamine and/or METH in the world (UNODC, 2003), with

amphetamine and METH being the most widely abused illicit drugs after marijuana (Rawson et al., 2002).

The consumption and abuse of METH is a serious and growing problem that has extensive negative economic, social and health consequences. Abuse of drugs exhausted a staggering $143.4 billion from the U.S. economy in 1998 and showed an estimated 5.9% increase annually (ONDCP, 2001). METH abuse results in decreased productivity, crime and violence (ONDCP, 2001). Children of METH abusers are at risk of neglect and abuse, and the use of METH by pregnant women can cause growth retardation, premature birth, and developmental disorders in neonates and enduring cognitive deficits in children. Use among homosexual men is expanding, and with it, unsafe sex behaviors that increase the transmission of human immunodeficiency virus (HIV) (Halkitis et al., 2001). Short- and long-term health effects of METH use include stomach cramps, shaking, anxiety, hypertension, cardiac arrhythmia, aggression, insomnia, paranoia, memory loss, stroke, seizures, hallucinations, drug addiction, and long term structural changes to the brain which are manifested as neurological deficits and psychiatric conditions. In addition, the neurological deficits induced by long term METH abuse may be relevant to the neurodegeneration seen in Parkinson's disease and Huntington's chorea. Such destructive consequences of METH abuse have made it a major focus of the war on drugs in the United States (CEWG, 2005) and therefore critical to identify and characterize the biochemical pathways through which METH acts to rectify the damage it causes the nervous system.

1.2 Methamphetamine and the Brain

1.2.1 Pharmacology

Methamphetamine (METH, $C_{10}H_{15}N$) is a synthetic drug and is the common name for *N*,α-dimethylphenethylamine. It is also referred to as desoxyephedrine, methylamphetamine, phenylisopropylmethylamine, and a variety of other similar systematic names. METH is an amine derivative of amphetamine and belongs to the class of amphetamines, a group of psychoactive drugs that can elevate mood, produce euphoria, and increase mental stamina.

In its purest form, it is commonly referred to as "glass" or "ice" on the streets. This is because it appears as broken shards of glass or crushed ice. Other popular terms in use today include “crystal” and “tina” for purer forms and “chalk”, “crank”, or “speed” for the less pure crystalline powder.

METH exists in two isomeric forms, levorotatory (*l*-) and dextrorotatory (*d*-). In the United States, *l*-methamphetamine (under the label *l*-desoxyephedrine) is the active ingredient in the over-the-counter Vicks Inhaler decongestant drug. The dextrorotatory isomer is a legal US DEA schedule II prescription drug (Desoxyn®) (21 CFR 1308.12) and has 3-4 times the central nervous system stimulant effects that of the *l*-enantiomer (Hardman and Limbird, 1996). The free base of METH (pKa 9.9) has a molecular weight of 149.24 a.m.u., and is a liquid at room temperature. Thus, it is invariably supplied and used as a hydrochloride salt ($C_{10}H_{15}N \cdot HCl$, 185.74 a.m.u.), which has a melting point of 170–175^{o}C and becomes volatile without pyrolysis at

300–305^{o}C; a temperature readily achieved in a butane lighter flame, meaning that it can be smoked in the salt form without the tedious conversion to the base like cocaine.

METH is taken orally or intranasally (snorting powder), by intravenous injection, or by smoking. As with heroin, nicotine, or cocaine, the potential for addiction is greater when it is delivered by methods that cause the concentration in the blood to rise quickly, principally because the effects desired by the user are felt quicker and with a higher intensity than a moderated delivery mechanism. The intense sensations of the drug are felt 5 min after snorting, 20 min after ingestion, and almost instantaneously when smoked or injected. The elimination half-life in humans is estimated to be 10.1h for oral administration, 11.1 h for smoking, and 12.2 h for IV injection. Although the half-life of METH appears to be independent of the route of administration, the ranges for half-life were found to be broad (extremes of 6.4 and 18.2 h) in some studies (Cook et al., 1992; Cook et al., 1993). In rats, METH's plasma half life is between 68-75 minutes (Riviere et al., 2000; Cho et al., 2001). Studies involving rats also indicate that METH rapidly accumulates in the brain, with a ratio of brain concentration to plasma concentration of 7:1, 2 minutes after exposure, peaking at a ratio of 13:1, 20 minutes after exposure, and plateaus at average ratios of 8-10:1 (Melega et al., 1995; Riviere et al., 2000).

The pharmacological effects of METH are extremely complex and involve the actions of both the peripheral and the central nervous systems. Primarily mediated through the augmented release of catecholamines like dopamine (DA),

norepinephrine, and epinephrine, METH causes vasoconstriction, elevates blood pressure, accelerates heart rate, and increases body temperature. At acute low-dose administrations, METH has alerting, anorectic, and locomotor stimulating effects. With increased dosing and duration of use, METH causes more disorienting effects on cognition, reasoning, psychomotor ability, and can lead to seizures, rhadomylolysis and cardiovascular problems including myocardial infarction, stroke, and dilated cardiomyopathy (Hong et al., 1991; Albertson et al., 1999; Perez et al., 1999; Richards et al., 1999; Varner et al., 2002). Withdrawal from METH use has a depressant-like profile and is often compounded by delusions and psychotic episodes (Ellinwood and Kilbey, 1980).

1.2.2 The Striatum

Methamphetamine (METH) acts in the brain by augmenting the release of the neurotransmitter dopamine (DA) from vesicular and nerve terminal stores into the synapses of the striatum; a brain area associated with disorders of movement (DeLong et al., 1984; Hickey and Chesselet, 2003; Singer and Minzer, 2003), and has been implicated in the control of attention, executive function, motivated behaviors (Alexander et al., 1986) as well as neuropsychiatric conditions such as obsessive compulsive disorder, psychoses, and addictive behaviors (Calabresi et al., 1997a).

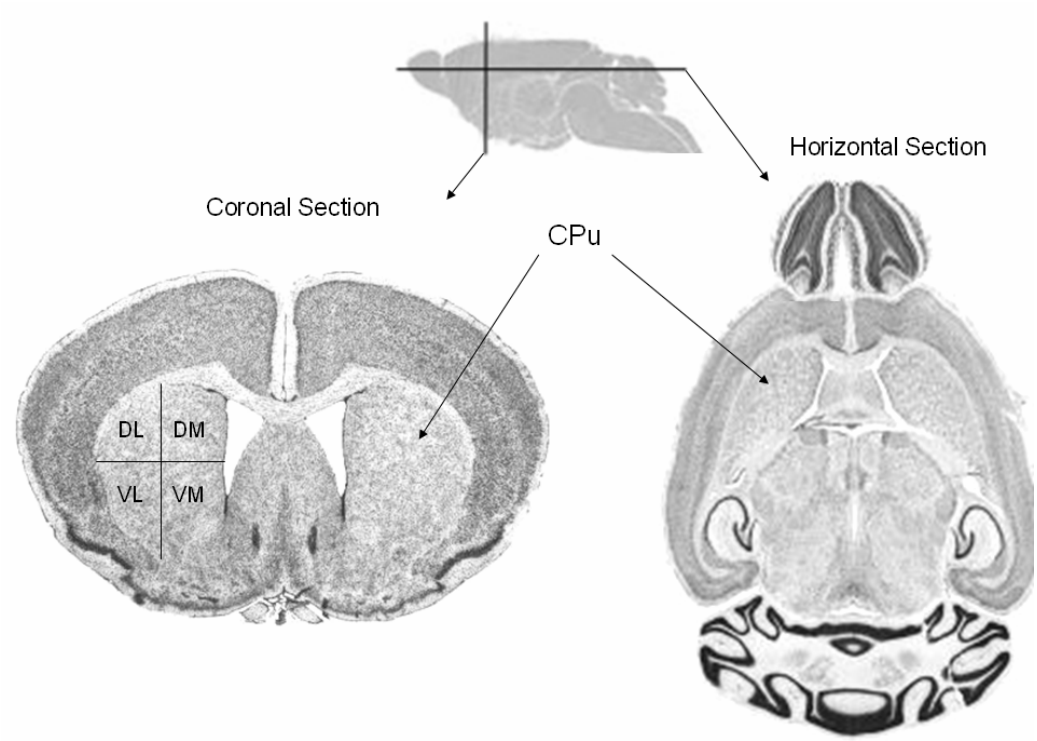

Figure 1-1. The mouse striatum in coronal and horizontal sections. The striatum is also referred to as the caudate-putamen (CPu). It is subdivided here into four regions in the coronal section: dorsal-medial (DM), ventral-medial (VM), dorsal-lateral (DL), and ventral-lateral (VL). Adapted from *High Resolution Brain Atlas* (Sidman et al., 2005) and *Brainmaps.org* (Jones et al., 2005).

In some mammals like the mouse, the striatum is a single structure and is referred to as the caudate-putamen (CPu) (See Figure 1-1). In humans, the striatum consists of two portions, the medial caudate nucleus and the lateral putamen. This structure is heterogeneous in its internal organization as well as in its afferent and efferent connections. 90-95% of the neuronal population in the striatum is gamma-

aminobutyric acid (GABA)ergic medium spiny projection neurons that are further subdivided into direct pathway striatonigral projections containing substance P (SP) and dynorphin and indirect pathway striatopallidal projections containing enkephalin. The remaining 5-10% make up the various striatal interneurons; of which GABA-, somatostatin (SST)- and cholinergic-containing interneurons are considered the most prevalent (Gerfen, 1992). This structure also represents a brain area where high concentrations of both the neuropeptide SP and its corresponding receptor, neurokinin-1 (NK-1), can be detected (Otsuka and Yoshioka, 1993) (See Chapter 1.2.5.4 for further discussion).

The striatum is the largest nucleus and the primary afferent structure of the basal ganglia; a group of functionally interconnected brain nuclei involved in a variety of psychomotor behaviors. The striatum receives rich dopaminergic inputs which orginate in the substantia nigra (SN) (See Figure 1-2) (Moore et al., 1971), and essentially all functions ascribed to the striatum are closely linked to its dopaminergic innervations. This structure also receives significant excitatory glutamate inputs from the cerebral cortex (Centonze et al., 1999) (See Figure 1-2) and serotoninergic inputs from the dorsal raphé nucleus (Parent et al., 1983).

Efferents from the striatum control the direct and indirect pathways of the basal ganglia on cortical control of motor behaviors. The direct pathway consists of a distinct population of striatal projection neurons, which send an inhibitory GABA projection directly to the SN. In contrast, the indirect pathway consists of a separate population of GABAergic striatopallidal neurons that transmits an alternate inhibitory

GABA projection to the subthalamic nucleus (STN), which in turn sends an excitatory glutamatergic projection to the SN. The SN then sends another inhibitory GABA projection to motor nuclei of the thalamus, which sends an excitatory glutamate projection to the cortical motor areas. (See Figure 1-2).

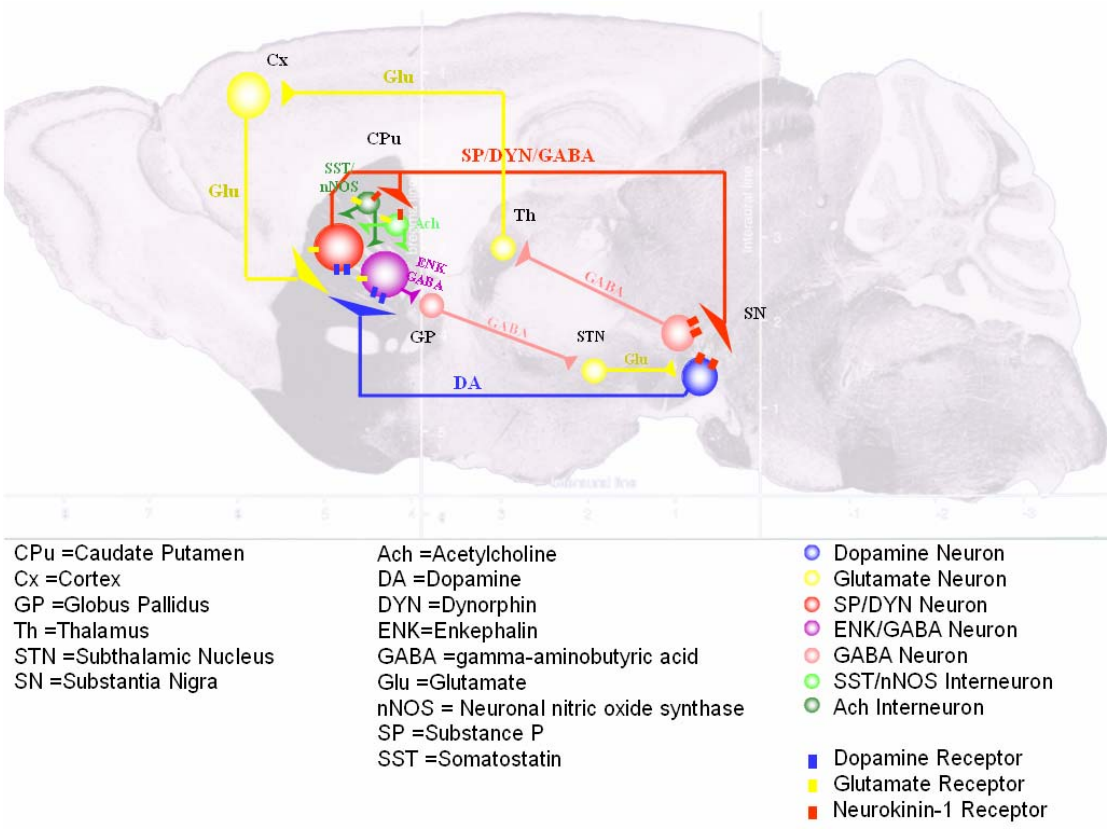

Figure 1-2. Schematic illustration of striatal circuitry. Adapted from *The Mouse Brain in Stereotaxic Coordinates* (Franklin and Paxinos, 1997).

Dysfunction of the striatum and its efferent and afferent pathways are associated with a broad array of clinical phenomena ranging from hypokinesia in

Parkinson's disease to hyperkinesia in Huntington's chorea. Loss of striatal DA or the degeneration of nigrostriatal DA neurons is known to result in Parkinsonism whilst the degeneration of striatal output neurons in Huntington's is associated with choreiform movements. Similarly, lesions in the striatum are associated with dystonia and motor tics seen in Tourette's syndrome (Saka and Graybiel, 2003).

METH exposure disrupts both the afferent and efferent pathways of the striatum, causing neurotoxicity at the nigrostriatal DA nerve terminals (See Chapter 1.2.3) and cell death in the striatal cells (See Chapter 1.2.4). Its actions represent a model of striatal injury which can mimic the dysfunctions seen in these neurodegenerative diseases.

1.2.3 Neurotoxicity: Neurochemical Alterations at the Presynaptic Nerve Terminal

The stimulant properties of methamphetamine (METH) on the central nervous system, however pleasurable, have been widely documented to damage brain dopamine (DA) and serotonin (5-HT) neurons. Similar to neurochemical depletions seen in Parkinson's disease (Kita et al., 2003), humans exposed to recreational doses and laboratory animals given repeated doses of METH show extensive, long-lasting, and persistent depletions of brain DA and 5-HT neurotransmitter levels (Kogan et al., 1976; Seiden et al., 1976; Hotchkiss and Gibb, 1980; Ricaurte et al., 1980; Wagner et al., 1980; Woolverton et al., 1989; Wilson et al., 1996; McCann et al., 1998;

Villemagne et al., 1998; Harvey et al., 2000), as well as marked long-term reductions in the activity of the rate-limiting enzymes responsible for their synthesis (tyrosine hydroxylase and tryptophan hydroxylase respectively) (Hotchkiss et al., 1979; Hotchkiss and Gibb, 1980; Ricaurte et al., 1983; Schmidt et al., 1985), the concentration of DA and 5-HT metabolites (Seiden et al., 1976; Hotchkiss and Gibb, 1980; Ricaurte et al., 1980) and the number of DA and 5-HT transporters (DAT and 5-HTT) (Ricaurte et al., 1980; Wagner et al., 1980; McCann et al., 1998; Yu et al., 2002). Immunohistochemical and anatomical studies also indicate that the loss of these presynaptic DA and 5HT axonal markers and the increases in reactive astrocytes induced by METH treatment are associated with the degeneration of DA and 5HT nerve terminals (Ellison et al., 1978; Lorez, 1981; Nwanze and Jonsson, 1981; Ricaurte et al., 1982; Ricaurte et al., 1984; Fukui et al., 1989; Axt and Molliver, 1991; Pu and Vorhees, 1995; Chapman et al., 2001; Yu et al., 2004).

1.2.4 Cell Death

While neurotoxicity induced by methamphetamine (METH) at nerve terminals have been studied extensively over the past thirty years (Hanson et al., 2004; McCann and Ricaurte, 2004), examinations of postsynaptic neuronal changes induced by METH are just beginning to emerge. Most notable is the emergence of evidence indicating METH-induced apoptosis in the brain. *In vitro* evidence showed METH induced dose-dependent increases in apoptosis in immortalized neural cells and

overexpression of the proto-oncogene, bcl-2, prevented this deleterious effect (Cadet et al., 1997). Similarly, it was shown in rat primary cortical cultures and in mice that METH and amphetamines induced upregulation of proapoptotic genes such as c-myc, l-myc, p53, bad, bax, bid and down regulation of anti-apoptotic genes such as bcl-2 and bcl-xl (Stumm et al., 1999; Imam et al., 2001; Jayanthi et al., 2001; Thiriet et al., 2001). Also, it has been reported that METH activates the cleavage of poly (ADP-ribose) polymerase (PARP) cleavage and increase caspase-3 activity in the striatum; two key proteins in the activation of an apoptotic signaling cascade (Deng and Cadet, 2000). Repeated METH administration in rodents was shown to induced Fluoro-Jade B-positive degenerating neurons in the striatum (Yu et al., 2004). Repeated exposure to METH also resulted in cell body injury in the parietal cortex of rats (Eisch and Marshall, 1998; Eisch et al., 1998). In addition, it has recently been demonstrated that METH can induce TUNEL-positive apoptotic cells in the cortex, striatum, and hippocampus of rodents (Stumm et al., 1999; Deng and Cadet, 2000; Deng et al., 2001; Cadet et al., 2003). Furthermore, significant cortical gray matter and hippocampal deficits are seen in the brains of humans who use METH (Thompson et al., 2004).

These findings all suggest that excessive METH use poses a serious health concern because neuronal loss in the aftermath of METH may lead to the eventual impairment of normal brain function. For example, human chronic METH abusers with long term and perhaps permanent deficits of striatal dopamine indices (Wilson et al., 1996; McCann et al., 1998) may later develop serious movement disorders

resembling Parkinson's disease. Similarly, neuronal cell loss in the striatum of abstinent METH abusers (Ernst et al., 2000) may increase the likelihood of developing symptoms similar to Huntington's chorea. It is, therefore of great importance to clarify and understand the underlying neural mechanisms by which METH exert its adverse effects in the brain so to better treat sequels associated with neural deficits and dysfunction.

1.2.5 Mechanisms of Neural Damage

Methamphetamine (METH)-induced neural damage is a complex phenomenon that may be accounted for by multiple mechanisms operating in parallel, in synergy, and/or separately. These mechanisms include but are not limited to the following: 1) elevation of extracellular dopamine (DA) in the nerve terminal field areas of the forebrain (Frost and Cadet, 2000; Davidson et al., 2001) which gives rise to reactive oxygen and nitrogen species (Cadet and Brannock, 1998; Imam et al., 2000), 2) excitotoxicity via METH-induced release of glutamate (Nash and Yamamoto, 1992) and subsequent neural damage by excitatory amino acids (EAA) (Sonsalla et al., 1989), 3) hyperthermia and 4) the peptidergic system involving the neuropeptide substance P (SP) and its receptor neurokinin-1 (NK-1).

1.2.5.1 Dopamine Overflow and Neuronal Oxidation

The prime causative factor and predominant mediator of the neural damaging effects of methamphetamine (METH) is associated with the augmented aberrant release of dopamine (DA) in the synapse. Excess accumulation of DA in the synapse can lead to excessive DA transmission, oxidative stress (Cadet and Brannock, 1998; Imam et al., 2000) and activation of signal cascades involved in excitotoxicity (Frost and Cadet, 2000; Davidson et al., 2001). DA alone has been shown to be neurotoxic and can induce apoptosis in cultured human neurons (Simantov et al., 1996). Similarly, *in vitro* studies showed that levodopa (L-DOPA), a traditional symptomatic antiparkinsonian drug that supplements the loss of DA activity, can induce oxidative stress-mediated apoptosis in catecholaminergic pheochromocytoma PC12 cells (Migheli et al., 1999).

METH can generate an overflow of DA in the synapse by displacing DA from vesicular and intracellular stores (Raiteri et al., 1979; Liang and Rutledge, 1982; Sulzer et al., 1995). This is due, in part, to METH's sympathomimetic properties,

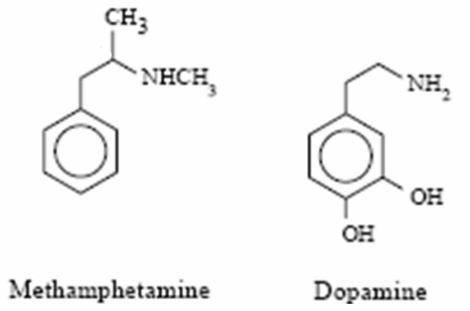

Figure 1-3. Chemical structures of the synthetic sympathomimetic drug methamphetamine and the neurotransmitter dopamine.

meaning that it mimics endogenous neurotransmitters in the sympathetic nervous system by interaction with their receptors. The prototypical sympathetic neurotransmitters are catecholamines like DA, and the structural similiarity of METH to it is clear. (See figure 1-3). Specifically, METH interacts with presynaptic dopamine transporters (DAT) by competitive antagonism, and has minimal, if any, effect as an agonist at postsynaptic dopamine receptors. Acting as an indirect DA agonist, METH can mimic DA, bind to its transporter on presynaptic nerve terminals and is taken up into the cytoplasm. The DAT binding site is now facing inward where it can bind an intracellular DA molecule. Once this has occurred, the DA molecule is transported in the opposite direction for normal reuptake and release into the synapse. This was demonstrated by supporting evidence from studies which showed inhibition of METH-induced DA release by drugs which blocked DA reuptake (Fischer and Cho, 1979; Raiteri et al., 1979; Liang and Rutledge, 1982; Seiden et al., 1993) and from genetic knockouts of the DAT which exhibited neither METH-induced DA release nor locomotor activation (Giros et al., 1996).

METH can also evoke the release of DA through its basic and lipophilic properties. The lipophilicity of METH allows it to diffuse across the plasma membrane of nerve terminals and of acidic catecholamine vesicles. Once sequestered in the acidic vesicles, it acts as a weak base to reduce vesicular pH; changing the pH gradient across the vesicular membrane. This inhibits uptake and promotes efflux of DA from vesicles (Sulzer and Rayport, 1990; Sulzer et al., 1992; Sulzer et al., 1993; Sulzer et al., 1995).

METH induced displacement of DA molecules and its metabolites can readily oxidized by auto-oxidation and be oxidized by monoamine oxidase to reactive quinones and semiquinones. DA auto-oxidized to the ortho-quinone can react with cysteine residues on DATs (Whitehead et al., 2001). In synaptosomal preparations, the auto-oxidation of DA leads to the inhibition of DA uptake by the DAT (Berman et al., 1996) and inhibition of glutamate uptake by the glutamate transporter (Berman and Hastings, 1997). In the presence of tyrosinase, DA induces the covalent modification and inactivation of tyrosine hydroxylase (TH) (Xu et al., 1998).

Oxidation of accumulated DA can also give rise to oxygen-based superoxide (O_2^-) and hydroxyl (OH) free radicals, which can react with nitric oxide (NO) to form the nitrogen based peroxynitrite ($ONOO^-$) free radical (Cadet and Brannock, 1998; Imam et al., 1999b; Ali et al., 2005). Reciprocally, $ONOO^-$ and $ONOO^-$ decomposition products such as nitrite can oxidize DA in a concentration- and pH-dependent manner (LaVoie and Hastings, 1999b). NO can irreversibly inhibit the mitochondrial complex II-III and IV as well as succinate dehydrogenase in the electron transport chain (Bolanos et al., 1997), consequently inhibiting ATP synthesis (Berman and Hastings, 1999; Brookes et al., 1999) and initiating apoptotic cascades (Szabo, 1996b; Heales et al., 1999). These reactive oxygen and nitrogen species can also directly alter protein function by oxidative modifications and destroy cellular membranes by lipid peroxidation (Cadet and Brannock, 1998). Studies showing the suppression of these reactive oxygen and nitrogen-based free radicals have all demonstrated effective protection from METH's damaging effects. METH-induced

striatal DA depletion is attenuated in transgenic mice overexpressing the antioxidant human copper-zinc-dependent superoxide dismutase (CuZnSOD) enzyme (Cadet et al., 1994; Hirata et al., 1996). METH exposure caused overexpression of neuronal nitric oxide synthase (nNOS) in the mouse striatum (Deng and Cadet, 1999) and significant increases in $ONOO^-$ (Imam et al., 1999b). nNOS knockout mice (Itzhak et al., 1998) and selective nNOS inhibitor, 7-nitroindazole (Itzhak and Ali, 1996), offered protection against METH-induced dopaminergic toxicity. Selective peroxynitrate decomposition catalyst, 5,10,15,20-tetrakis (2,4,6-trimethly-3,5-sulfonatophenyl) porphyrinato iron III (FeTPPS), showed protection against METH-induced depletion of DA in the striatum (Imam et al., 1999b). Also, antioxidants like selenium and melatonin can attenuate METH-induced dopaminergic neurotoxicity (Ali et al., 1999; Imam et al., 1999a; Imam and Ali, 2000).

1.2.5.2 Excitotoxicity

Dopaminergic and glutamatergic systems display complex anatomical arrangements in the striatum and striatal transmission of dopamine (DA) and glutamate are often intertwined (Calabresi et al., 1997b). DA can act on presynaptic dopamine receptors located on glutamatergic corticostriatal nerve terminals to regulate glutamate release (Calabresi et al., 1996) and glutamate can act on presynaptic glutamate receptors located on nigrostriatal nerve terminals to regulate DA release (Glowinski et al., 1988). *In vivo* microdialysis studies also indicate that

NMDA-induced striatal glutamate release is dependent on DA and DA receptors (Marti et al., 2002; Marti et al., 2005).

Microdialysis studies in rats demonstrate that methamphetamine (METH)-induced DA release evokes a delayed release of glutamate in the striatum via a cortico-striatothalamo-cortical negative feedback loop (Carlsson and Carlsson, 1990; Nash and Yamamoto, 1992; Abekawa et al., 1994). This delayed aberrant release of glutamate induced by METH can lead to excessive activation of glutamate receptors. Excessive activation of glutamate receptors by excitatory amino acids such as glutamate generates excitotoxicity and is thought to contribute to neuronal death in neurological disorders such as trauma, ischemia, epilepsy, Parkinson's disease, and Alzheimer's disease (Beal, 1992b; Marino et al., 2003; Arundine and Tymianski, 2004; Hynd et al., 2004). Glutamate analogues such as quinolinic acid and kainic acid have been shown to induce excitotoxic lesions of striatal neurons (Vezzani et al., 1991; Qin et al., 1996). Excitotoxicity is mediated by ionotrophic N-methyl-D-aspartate (NMDA) and alpha-amino-3-hydroxy-5-methyl-4-isoxazolepropionic acid (AMPA)/Kainate glutamate receptors (Beal, 1992a; Nakanishi, 1992). Various studies have demonstrated that NMDA receptor activation with selective agonists potentiate the release of DA from synaptosomal preparations, slices of striatal tissue, and from freely moving rats (Araneda and Bustos, 1989; Sonsalla et al., 1989; Kashihara et al., 1990; Krebs et al., 1991b; Krebs et al., 1991a), suggesting that METH-induced glutamate release can exacerbate METH effects by potentiating the release of DA. Agents that block the delayed increase of extracellular glutamate can

prevent METH-induced depletion of DA content (Stephans and Yamamoto, 1994). Administration of NMDA receptor antagonist, MK801, abrogate the effects of METH-induced nerve terminal injury (O'Dell et al., 1992; Weihmuller et al., 1992) Also, application of the glutamate receptor antagonist, MK801 and suppression of the receptor with protein kinase C-ε can block METH-induced apoptosis of pheochromocytoma PC12 cells (Uemura et al., 2003).

1.2.5.3 Hyperthermia

Methamphetamine (METH) treatment produces significant pathological brain hyperthermia in rodents (Sandoval et al., 2000) and in humans (Kalant and Kalant, 1975). METH can dose-dependently increase brain metabolism and diminish heat dissipation by peripheral vasoconstriction (Kiyatkin and Brown, 2004; Kiyatkin, 2005). The thermogenic effects of this drug has been suggested to exacerbate its lethal and toxic effects to neural cells (Ali et al., 1994; Bowyer et al., 1994; LaVoie and Hastings, 1999a; Xie et al., 2000). Exposing laboratory animals to lower environmental temperatures of 4°C have shown attenuation in METH-induced neurotoxicity (Bowyer et al., 1992; Bowyer et al., 1993; Ali et al., 1994). Furthermore, the lethal effect induced by METH is attenuated by immediate cooling after administration (Namiki et al., 2005). Some pharmacological agents, including dopamine (DA) and glutamate receptor antagonists, appear to prevent METH-induced neural damage by attenuating the increase in body temperature caused by METH

(Albers and Sonsalla, 1995), while others have shown protection without affecting the hyperthermic response to METH (Melega et al., 1998; Tsao et al., 1998; El Daly et al., 2000; Itzhak et al., 2000). Also, the vesicular DA-depleting agent reserpine can lower body temperature but does not prevent METH induced neurotoxicity (Albers and Sonsalla, 1995). How hyperthermia plays a role in METH's damaging effects remains to be elucidated. Although it is not solely responsible for METH's actions in the brain, it is a factor that must be taken into consideration while studying and interpreting the mechanisms of action of METH.

1.2.5.4 Substance P and the Neurokinin-1 Receptor

Substance P (SP), neurokinin A (NKA), and neurokinin B (NKB) belong to a family of mammalian tachykinin peptides characterized by the presence of a common C-terminal amidated sequence (Phe-X-Gly-Leu-Met-NH_2) in their structure which is responsible for their fundamental interaction with their corresponding receptors, neurokinin-1 (NK-1), neurokinin-2 (NK-2), and neurokinin-3 (NK-3), respectively (Angulo and McEwen, 1994; Maggi, 1995; Patacchini et al., 2004). cDNA and genomic cloning experiments indicate that SP and NKA are derived from differential RNA splicing of the preprotachykinin-A (PPT-A) gene. NKB is encoded by the preprotachykinin-B (PPT-B) gene (for review see Krause et al., 1990). Although these three neuropeptides and their corresponding receptors have extensive cross-talk

amongst each other, SP and the NK-1 receptor is considered the prototype for the interactions between the tachykinin peptide family and its receptors in the central nervous system.

The neuropeptide SP (Arg-Pro-Lys-Pro-Gln-Gln-Phe-Phe-Gly-Leu-Met-NH2) is found in high concentrations in the striatum and the basal ganglia (Hokfelt et al., 1975). SP binds to all three neurokinin receptors, namely neurokinin-1 (NK-1), neurokinin-2 (NK-2), and neurokinin-3 (NK-3), but has the highest binding affinity for the NK-1 receptor (Maggi, 1995). The NK-1 receptor is a G-protein coupled receptor which can exist in two active conformations (Maggi and Schwartz, 1997; Quartara and Maggi, 1997). One conformation is selective and has high affinity (0.05 nM) for SP. The other conformation binds other tachykinins (0.5nM) like NKA and NKB.

Anatomically, SP and NK-1 receptor are intrinsic components of the neuronal pathways and circuits involving the dopaminergic system of the forebrain. Both are favorably positioned to modulate processing and output of the basal ganglia and METH's deleterious effects on the system (See figure 1-2). SP is expressed by striatal medium spiny neurons that project to the substantia nigra (SN), where they make direct excitatory contact with dopaminergic neurons and can provoke the release of dopamine (DA) in the striatum (Baruch et al., 1988). Reciprocally, a feedback loop is established by dopaminergic projections from the SN onto SP-expressing neurons in the striatum (Angulo and McEwen, 1994). Moreover, SP-containing neurons also extend axon collaterals within the striatum to cholinergic and somatostatin/nitric

oxide synthase-containing (SST/NOS) interneurons in the striatum which express NK-1 receptors (Bolam et al., 1986; Kaneko et al., 1993; Anderson et al., 1994; Li et al., 2000; Li et al., 2002b) (See figure 1-2).

Aside from their favorable anatomical positions in the basal ganglia, SP and NK-1 receptor have been shown to have functional modulatory effects on the dopaminergic and glutamatergic systems. Thus, indicating that the pair may serve as key participants in the deleterious effects of METH. METH treatment has been shown to elevate the striatal (Hanson et al., 1986) and nigral concentrations of SP neuropeptide (Hanson et al., 1986; Sonsalla et al., 1986; Bannon et al., 1987) and increase PPT-A mRNA within striatonigral neurons (Zhang et al., 1997). These increases follow the elevation of extracellular DA levels (Angulo and McEwen, 1994). Microinjections of SP in the SN and microperfusions of a NK-1 receptor agonist in the striatum results in the increased release of DA and glutamate in the striatum (Reid et al., 1990c; Reid et al., 1990b; Reid et al., 1990a; Reid et al., 1991; Tremblay et al., 1992). Also, the firing of SP-containing neurons in the striatum can increase the firing probability of cholinergic and SST/NOS interneurons by receptor-mediated opening of tetrodotoxin-insensitive ion channels (Aosaki and Kawaguchi, 1996). Local perfusion of SP in the striatum can elevate extracellular acetylcholine through NK-1 receptor mediated mechanisms (Anderson et al., 1994). Blockade of the NK-1 receptor prior to METH treatment prevents METH-induced loss of dopamine transporters, DA content, TH, as well as the strong induction of reactive gliosis (Yu et al., 2002; Yu et al., 2004). Moreover, there is evidence of interactions

between glutamate and stimulation of the NK-1 receptor, with subsequent protein kinase C–dependent facilitation of NMDA transmission as well as the formation of NO (Woolf and Doubell, 1994). Intrastriatal infusion of NMDA receptor antagonist, CPP, decreased SP mRNA expression in the striatum in a dose-dependent manner (Jolkkonen et al., 1995). Pharmacological blockade of the NK-1 receptor and genetic knockouts of the substance P gene, preprotachykinin-A (PPT-A), showed reduction and abrogation of excitotoxin-induced seizures (Zachrisson et al., 1998; Liu et al., 1999b). Also, mice lacking the PPT-A do not display kainate-induced cell death in the hippocampus (Liu et al., 1999b). In addition, activation the NK-1 receptor by SP on SST/NOS-containing interneurons (Szabo, 1996a; Li et al., 2000; Li et al., 2001; Li et al., 2002b; Li et al., 2002a) may lead to the activation of NOS to synthesize nitric oxide (NO). NO synthesized in the interneurons, can readily diffuse through the membrane and enter the spines of the striatal projection neurons inducing the synthesis of cGMP (Denninger and Marletta, 1999) and indirectly potentiate the release and actions of glutamate.

Of note are SP and NK-1 receptor's effects on behavior that can be linked to the basal ganglia. Application of SP in the ventral mesencephalon generates a marked increase in locomotion (Kelley et al., 1979; Kelley et al., 1985). Mice lacking the NK-1 receptor showed reduced opiate-induced increases in locomotion (Murtra et al., 2000). Also, NK-1 receptor antagonist, MK-869, was shown to be an effective and well–tolerated antidepressant in clinical trials with human subjects that had major depression (Kramer et al., 1998).

Chapter 2

Central Hypothesis and Research Design

Central Hypothesis: Acute methamphetamine exposure induces selective neuronal cell death in the striatum, in part, by activation of signals through the neurokinin-1 receptor.

2.1 Rationale for the Central Hypothesis

Methamphetamine-induced cell death in the striatum

Methamphetamine (METH)-induced apoptosis in the striatum is a recently identified calamity (Deng and Cadet, 2000; Ernst et al., 2000). However, characterization of this event in the aftermath of METH exposure remains to be investigated in order to identify its underlying mechanisms and to understand how it relates to METH-induced neural damage seen at the dopamine (DA) nerve terminals. Establishing the scope and temporal emergence of METH-induced cell death will provide a framework to gauge possible influencing mechanisms, namely the neuropeptide substance P (SP) and the neurokinin-1 (NK-1) receptor, which may be

at the core of METH's noxious effects in striatal cells. Also, since the striatum is heterogeneous and each subpopulation of striatal cells affect the output of the basal ganglia differently, identifying the phenotypes of striatal cells that are affected and establishing the extent of METH-induced apoptosis in each of the neuronal subpopulations of cells in the striatum will further give insight and direction to identifying its underlying mechanisms of action in the striatum.

Signaling of the neurokinin-1 receptor contributes to methamphetamine-induced cell death in the striatum

There exists now a compelling body of evidence which demonstrates the anatomical associations and functional interactions of the tachykinin neuropeptide SP and the NK-1 receptor with the basal ganglia. Anatomically, SP and the NK-1 receptor are both auspiciously positioned within striatal efferents and afferents to modulate neural responses caused by METH. Multiple administrations of METH have been shown to increase nigral and striatal concentrations of SP (Hanson et al., 1986; Sonsalla et al., 1986; Bannon et al., 1987). Administration of METH can also elevate PPT-A mRNA and SP in striatonigral neurons and with its withdrawal, there is a return to baseline levels (Zhang et al., 1997). The release of SP also follows psychostimulant-induced dopamine release (Noailles and Angulo, 2002), and is therefore contiguous to the neural responses of METH. Furthermore, SP and the NK-1 receptor exerts influence on all major mechanisms of neural damage associated with METH. SP can potentiate the release of both DA and glutamate (Reid et al., 1990c;

Reid et al., 1990b; Reid et al., 1990a; Reid et al., 1991; Tremblay et al., 1992), and antagonists to the NK-1 receptor can block the release of dopamine and hyperlocomotion associated with psychostimulants (Noailles and Angulo, 2002). Genetic knockouts of the SP gene can prevent the excitotoxic effects of glutamate (Liu et al., 1999b). Also, location of the NK-1 receptor on NOS-containing interneurons in the striatum (Li et al., 2001) suggest that it can activate the production of NO, further contributing to oxidative stress involved in METH-induced neural damage. Moreover, blockade of the NK-1 receptor confers protection to METH-induced depletions of the dopamine terminal markers TH, DAT, DA tissue content, and the induction of reactive astrocytes in the striatum (Yu et al., 2002). These findings all presume a role for the NK-1 receptor in METH-induced neuronal damage. Thus, it is reasonable to hypothesize that *tachykinin neuropeptides such as substance P, through their activation of NK-1 receptors, serve as key participants in the neurodegenerative cascades associated with METH-induced cell death in the striatum.*

2.2 Research Design

Specific Aim I. <u>What is the extent of methamphetamine (METH)-induced cell death in the striatum?</u>

A. Assess and standardize the quantification of METH-induced cell death in the striatum.

a) Determine a treatment paradigm (regiment of METH administration) that induces cell death in the striatum.

i) Binge model (4 low dose injections given at 2 hour intervals) vs. bolus dosing model (single high dose injection).

b) Establish dose response relationship.

c) Quantify the amount of cell death occurring.

B. Examine the temporal emergence of METH-induced cell death.

a) Establish a time-course in which METH-induced cell death occurs in the striatum.

b) Establish the temporal relationship between METH-induced postsynaptic cell death and presynaptic dopamine terminal damage in the striatum.

i) Assess time course of select neurochemical and histological markers of METH-induced terminal toxicity in relation to METH-induced cell death.

C. Examine which cells and cell types are dying in the striatum after METH exposure.

a) Assess whether METH induces the death of neurons in the striatum.

b) Assess the types of striatal neurons undergoing METH-induced cell death.

Specific Aim II. <u>Is neurokinin-1 (NK-1) receptor involved in methamphetamine-induced cell death in the striatum?</u>

A. Examine the effects of systemic pharmacological blockade of NK-1 R on METH-induced cell death in the striatum.

a) Establish a dose response relationship for the NK-1 receptor antagonist, WIN 51,708, in METH-induced cell death in the striatum.

d) Examine the effect of NK-1 receptor antagonist, WIN 51,708, on METH-induced hyperthermia.

c) Examine the effect of NK-1 receptor antagonist, WIN 51,708, on METH-induced increase of peroxynitrite ($ONOO^-$).

B. Examine the effects of local striatal ablation of NK-1 receptor-expressing neurons on METH-induced cell death in the striatum.

a) Establish a model which ablates NK-1 receptors and receptor-expressing neurons effectively and consistently in the striatum using the cytotoxin saporin conjugated to NK-1 receptor agonist [Sar^{9},$Met(O_2)^{11}$] substance P.
b) Examine the effect of ablated NK-1 receptors and receptor-expressing neurons on METH-induced cell death in the striatum.

Chapter 3

Materials and Methods

3.1 Animals, Drugs, and Drug Administration

Adult ten-week old ICR/CD-1 male mice weighing 36-44g (Taconic, Germantown, NY) were housed individually with food and water available *ad libitum* on a 12-hour light/dark cycle. These animals were all habituated for approximately two weeks prior to any drug treatment or commencement of surgery.

(+)-Methamphetamine hydrochloride ($C_{10}H_{15}N \cdot HCl$) (Sigma, St. Louis, MI) was dissolved in physiological saline.

The heterosteroid-based nonpeptide NK-1 receptor antagonist, WIN 51,708 (17-hydroxy-17-ethynyl-5--androstano[3,2-*b*]pyrimido[1,2-*a*]benzimidazole; Ki=21nM for rat NK-1 receptor) (Sigma/RBI, St. Louis, MI) was dissolved in 45% 2-hydroxylpropyl-b-cyclodextrin (Sigma/RBI, St. Louis, MI) and phosphate buffered saline (PBS) (1:4).

NK-1 receptor agonist, [Sar^9,$Met(O_2)^{11}$]substance P, conjugated to the ribosomal-inactivating cytotoxin saporin (SSP-SAP) (Advance Targeting Systems,

San Diego, CA) and saporin (SAP) (Advance Targeting Systems, San Diego, CA) was dissolved in saline.

All systemic injections were given intraperitoneally (i.p.). Antagonist is administered 30 minutes prior to METH treatment. After drug treatment, animals were either sacrificed by decapitation or first anesthetized with i.p. injections of ketamine/acepromazine (100mg/kg, 3mg/kg of body weight) and then perfused transcardially with 30 ml of PBS containing heparin followed by 30 ml of 4% paraformaldehyde (PFA) in PBS. Brains were then dissected out and either immediately placed on dry ice or post-fixed in 4% PFA in PBS overnight and cryoprotected in 30% sucrose in PBS at 4 ºC. Tissue was then frozen and stored at –80 ºC until use. All animal use procedures were according to the *National Institutes of Health Guide for the Care and Use of Laboratory Animals* and were approved by the animal care committee at *Hunter College of the City University of New York*.

3.2 TUNEL (terminal deoxynucleotidyl transferase-mediated dUTP nick end labeling)

Fresh frozen or floating 20 μm serial coronal sections were fixed in 4% paraformaldehyde for 30 minutes. After PBS wash, sections were immersed in 0.4% Triton-X-100 in PBS for 5-10 minutes at 70°C. Sections were washed and TUNEL reactions (Roche Applied Science, Indianapolis, IN) were applied directly onto sections and incubated for 1 hour in a humidified chamber at 37°C. After TUNEL,

sections were counterstained with 2-(4-Amidinophenyl)-6-indolecarbamidine dihydrochloride (DAPI). Stained sections were washed in PBS and coverslipped with Vectashield (Vector Laboratories, Burlingame, CA). Images were either taken with a Nikon Eclipse TE200 epifluorescent scope attached with a CE 3.2.0 digital camera using FITC filters or Molecular Dynamics CLSM Multiprobe 2001 scanning confocal system.

3.3 Cell Counts and Quantification

All coronal sections were taken from bregma 0.38 ± 0.1 mm. All cells of interest were quantified from 20 μm sections in an 0.26 mm^2 area (or 5.2 μm^3) for each region of interest in the caudate putamen (CPu) (dorsal-medial [DM], dorsal-lateral [DL], ventral-medial [VM], ventral-lateral [VL]) (See figure 3-1).

Total neuronal cell counts were from taken a total of five serial sections from six control animals immunostained with antibodies against neuronal nuclei (NeuN). The five serial sections were taken from every other section over 0.2 mm. Average neuronal cell counts in each region of interest were taken from counts of these 30 sections. Statistical analysis demonstrated no significance between control animals. The average neuron count from each striatal region of interest was 658, 637, 637, and 639 for DM, DL, VM, and VL regions of the CPu respectively (See figure 3-2).

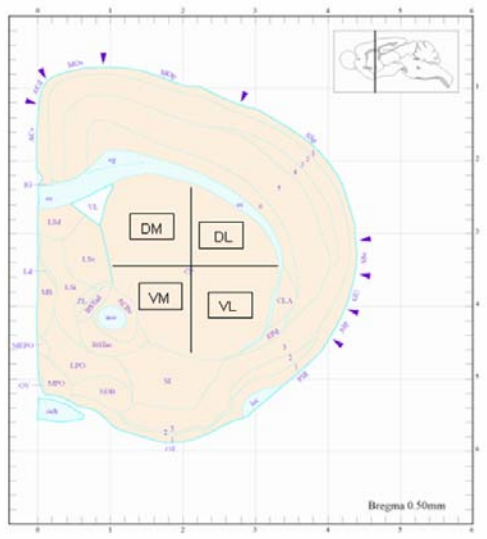

Figure 3-1. Schematic diagram of the striatum showing regions of interest for cell counting and analysis. Black box encompasses 0.26 mm^2 area (or 5.2 μm^3) for dorsal-medial (DM), dorsal-lateral (DL), ventral-medial (VM), ventral-lateral (VL) regions of the caudate putamen (CPu) (Adapted from Hof et al., 2000).

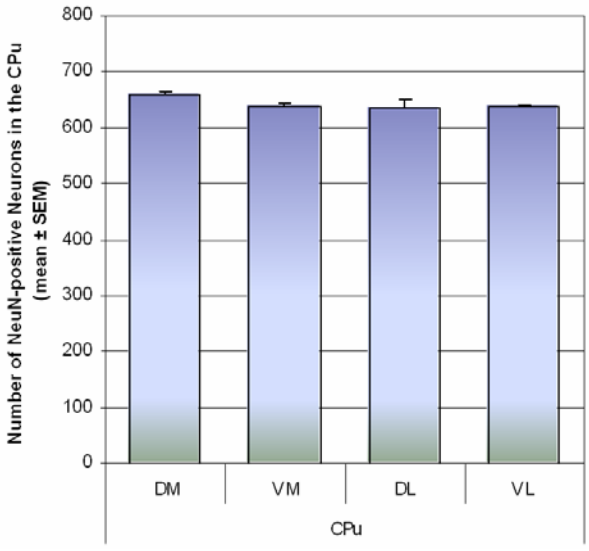

Figure 3-2. Number of neurons in the striatum. Neurons were labeled with antibodies against a neuron-specific protein marker, neuronal nuclei (NeuN). Average number of striatal

neurons is based on cell counts within a 0.26 mm^2 area in each region of the CPu. Dorsal-medial (DM), dorsal-lateral (DL), ventral-medial (VM), ventral-lateral (VL), caudate putamen (CPu).

Average neuronal cell counts were then used to quantify percent of TUNEL positive neurons. TUNEL cell counts were also averaged from five serial 20 μm sections taken from every other section over 0.2 mm in every animal.

Number of nissl-, SST-, CHAT-, parvalbumin-, DARPP32-, GFAP-positive and cells were quantified from three serial 20 μm sections per animal. All cell counts were blinded to experimental treatment.

3.4 Immunohistochemistry of NeuN, Parvalbumin, ChAT, SST, DARPP32, NK-1 receptor, and Double-labeling with TUNEL

Immunohistochemistry was processed by the free-floating method. Serial 20 μm coronal sections were collected between bregma 0.38 mm ± 0.1 mm. Tissue was washed in phosphate buffered saline (PBS) and then immersed in heated 0.4% Triton X-100 in PBS for 5 minutes and immediately washed in PBS.

For neuronal nuclei (NeuN) or parvalbumin immunohistochemistry, nonspecific binding sites were blocked with M.O.M. ® Mouse Ig Blocking Reagent (Vector Laboratories, Burlingame, CA) for 1 hour. Sections were washed and

incubated with M.O.M. ® diluent for 15 minutes. Sections were them incubated in mouse anti-NeuN (1:500, Chemicon, Temecula, CA) or mouse anti-parvalbumin (1:2000, Chemicon, Temecula, CA) in M.O.M. ® diluent in 0.1% Triton-X-100 in PBS overnight at 4 ºC. Sections were washed in PBS and blocked again with 5% normal goat serum (NGS) in 0.1% Triton X-100 in PBS for 30 minutes. After PBS washes, sections were incubated with Cy3-conjugated goat anti-mouse (1:1000, Chemicon, Temecula, CA) in 1% NGS in 0.1% Triton X-100 in PBS for 1 hour and washed with PBS.

For somatostatin (SST) or dopamine and cyclic adenosine 3',5'-monophosphate-regulated phosphoprotein, 32 kDa (DARPP32) or neurokinin-1 (NK-1) receptor immunohistochemistry, nonspecific binding sites wre blocked with 10% NGS in 0.2% Triton X-100 in PBS for 1 hour. Sections were washed in PBS and incubated with rabbit anti-SST (1:500, Chemicon, Temecula, CA) or rabbit anti-DARPP32 (1:200, Cell Signal) or rabbit anti-NK-1R (1:1000, Chemicon) in 2% NGS in 0.1% Triton X-100 in PBS overnight at 4 ºC. After washing with PBS, sections were incubated with Cy3-conjugated goat anti-rabbit (1:1000, Chemicon, Temecula, CA) in 1% NGS in 0.2% Triton X-100 in PBS for 1 hour and washed with PBS.

For choline acetyltransferase (ChAT) immunohistochemistry, nonspecific binding sites were blocked with 10% normal rabbit serum (NRS) in 0.2% Triton X-100 in PBS for 1 hour. Sections were washed in PBS and incubated with goat anti-CHAT (1:500, Chemicon, Temecula, CA) in 2% NRS in 0.2% Triton X-100 overnight. After washing with PBS, sections were incubated with Cy3-conjugated

rabbit anti-goat (1:1000, Chemicon, Temecula, CA) in 1% NRS in 0.2% Triton X-100 in PBS for 1 hour and washed with PBS.

No staining was observed when primary antibody was left out or when primary antibody was preabsorbed with either SST or ChAT. For double-labeling with TUNEL, sections were washed in PBS then incubated in the TUNEL reaction at 37 ºC for 1 hour. Sections were washed in PBS, mounted on slides, and overlaid with a coverslip with Vectashield (Vector Laboratories, Burlingame, CA). All incubations and washes are performed at room temperature unless otherwise stated. Images are viewed and taken with a Nikon Eclipse E400 epifluorescent scope attached with a Hamamatsu digital camera C4742-95 using rhodamine and FITC filters.

3.5 GFAP Immunohistochemistry

Fresh frozen 20 μm coronal sections from bregma 0.38 mm ± 0.1 mm were air-dried and fixed in absolute ethanol at -20ºC for 10 minutes. Sections were allowed to air-dry again and washed in PBS. Nonspecific sites were blocked with M.O.M. ® Mouse Ig Blocking Reagent (Vector Laboratories, Burlingame, CA) in 0.3% Triton X-100 in PBS for 1 hour. After being washed with PBS, sections were incubated with M.O.M. ® diluent for 15 minutes and then with Cy3-conjugated mouse anti-glial fibrillary astrocytic protein (GFAP) (1:25, Sigma, St. Louis, MO) for 3 hours. After washing, slides were mounted with Vectashield (Vector Laboratories, Burlingame,

CA). All incubations were performed at room temperature with gentle rocking. Images were taken with a Nikon Eclipse TE200 inverted-epifluorescent scope attached to a CE 3.2.0 digital camera using rhodamine filters.

3.6 Nissl Staining

Coronal 20 μm sections of the striatum from bregma 0.38mm ± 0.1mm were fixed with 4% paraformaldehyde and defatted. Slides were then rinsed with water followed by incubation in 0.2% cresyl violet for 2 minutes. Sections were then washed with water and dehydrated in a graded series of alcohol/water solutions. Tissue was place in xylene for 5 minutes and mounted under coverslips.

3.7 Western Blot Analysis of TH

Striata were dissected out after decapitation and separated into dorsal-medial (DM), dorsal-lateral (DL), ventral-medial (VM), and ventral-lateral (VL) parts. Tissues were then homogenized with lysis buffer (50 mM Tris-HCL pH 7.4, 150 mM NaCl, 320 mM sucrose, 5 mM HEPES, 1mM EDTA, 1mM EGTA, 1mM PMSF, 1mM DTT, 1% Inhibitor Cocktail [1.04 mM AEBSF, 0.8 μM aprotinin, 0.02 mM leupeptin, 0.04 mM bestatin, 0.015 mM pepstatin A, 0.014 mM E-64 (Sigma, St. Louis, MO)]). Homogenates were centrifuged at 800 x g for 5 min at 4°C.

Supernatants were further centrifuged at 3000 x g for 20 min at 4°C and supernatants were then used for western analysis. After determining protein concentration using the Bradford assay, samples were denatured in Laemmli sample buffer containing 20% β-mercaptoethanol for 10 minutes at 85°C. Samples are then subjected to 10% SDS-PAGE gel and proteins are transferred onto PVDF membranes. Membranes are blocked with 5% non-fat dry milk and probed with mouse anti-tyrosine hydroxylase (TH) (1:1000, Chemicon International Inc., Temecula, CA) overnight at 4°C with gentle rocking. Membranes are washed with TBS and incubated with HRP-conjugated goat anti-mouse (1:1000, Santa Cruz Biotech, Santa Cruz, CA) for 1 hour at room temperature. After wash with TBS, proteins are detected using the SuperSignal® West Pico Chemilumescent Substrate (Pierce, Rockford, IL) and exposed on Hyperfilm™ ECL film (Amersham Biosciences Corporation, Piscataway, NJ). For internal standards, membranes were stripped and reprobed with mouse anti-β-actin (1:10,000, Sigma, St. Louis, MO). Densitometry was performed using a NIH image analysis system and relative density of each band is normalized again that of β-actin.

3.8 Autoradiographic Binding Analysis of DAT

Fresh frozen 20 μm coronal sections were dried in a dessicator and then incubated in 0.073nM [^{125}I]RTI-121 (2200Ci/mmol, New England Nuclear, Boston,

MA) buffered solution (137 mM NaCl, 2.7 mM KCl, 10.14 mM Na2HPO4, 1.76 mM KH2PO4, 10 mM NaI) for 1 hour at room temperature. Non-specific binding was determined using 10 μM GBR-12909 (Sigma, St. Louis, MO). After incubation, sections were washed twice with chilled buffer for 20 minutes and then quickly rinsed with chilled distilled water. Slides were allowed to air-dry overnight and exposed on Hyperfilm MP (Amersham Pharmacia, Piscataway, NJ) together with a [^{125}I] microscale. Binding of [^{125}I]RTI-121 was quantified by densitometry using a computer-based NIH image analysis system.

3.9 Temperature Measurements

Core body temperature was determined using a BAT-12 thermometer coupled to RET-3 mouse rectal probe (Physitemp Instruments, Clifton, NJ). Ambient room temperature was maintained at 20-22 °C.

3.10 HPLC-EC Detection of 3NT and Tyrosine Concentration

3-nitrotyrosine (3-NT) and tyrosine (TYR) concentration in mouse striatum was measured by high performance liquid chromatography (HPLC-Coularray electrochemical detection method). Striatal tissue was dissected out and sonicated in

400 µl of 10 mM sodium acetate NaOAc, pH 6.5. A 25 µl aliquot of the homogenate was used to determine protein concentration (BCA method). The remaining homogenate was centrifuged at 14,000 rpm (Eppendorf 5403 centrifuge) for 10 minutes at 4°C. The supernatant was removed and treated with 100 ml of 1 mg/ml pronase for 18 hours at 50°C. Enzymatic digests were then treated with 0.5 ml of 10% TCA and centrifuged at 14,000 rpm for 10 minutes at 4°C. Supernatants were then passed through a 0.2 µm PVDF filter before injection onto the HPLC instrument. Samples were analyzed on an ESA (Cambridge, MA, USA) CoulArray HPLC equipped with 8 electrochemical channels using platinum electrodes arranged in line and set to increasing specified potentials [channel (potential): 1 (180 mV); 2 (240 mV) ; 3 (350 mV) ;4 (500 mV) ; 5(550 mV) ; 6(690 mV) ; 7(875 mV) ; 8(900mV)] . The analytical column was a TSK-GEL ODS 80-TM reverse-phase column with a column size of 4.6 mm x 25.0 cm (TOSOHAAS, Mongtomeryville, PA, USA). The mobile phase was 50 mM NaAc, 5% (v/v) methanol, pH 4.8. HPLC was performed under isocratic conditions. 3-NT and Tyr were quantified relative to known standards. 3-NT values were represented as 3-NT per 100 Tyr.

3.11 Intrastriatal Microinjections

Mice were anesthetized with inhaled isoflurane (2.5% for induction, 2% for maintenance) and their heads were placed in a stereotaxic frame (Model 5000, David

Kopf Instruments, and Tujunga, CA). A hole was drilled in the skull and a 25 gauge 2 µl Hamilton microinjection syringe was lowered into the striatum. Distance of injection sites from bregma was determined using a mouse brain atlas (Franklin and Paxinos, 1997): anteroposterior + 0.5 mm; mediolateral ± 2.0 mm; dorsoventral -2.5 mm. The microinjection needle was left in position for 5 minutes prior to drug injection of 1.0 µl PBS (pH 7.4), 1.0 µl 4 ng/µl saporin (SAP) (Advance Targeting Systems, San Diego, CA), or 1.0 µl 4ng/µl [Sar^{9},$Met(O_2)^{11}$]substance P conjugated to the ribosomal-inactivating cytotoxin saporin (SSP-SAP) (Advance Targeting Systems, San Diego, CA). Drugs were injected over a 10 minute (~0.1µl/minute) period and the needle was left in place for an additional 5 minutes before removal from the striatum.

3.12 Statistical Analysis

Analysis is performed from mean ± SEM. Differences between groups were analyzed by ANOVA followed by post hoc comparison using Fisher's protected least significance test. Differences between two groups were analyzed by Student's *t*-test. A significance criterion is set at $p< 0.05$.

Chapter 4

Characterization of Methamphetamine-induced Cell Death in the Striatum

Methamphetamine (METH)-induced cell death in the striatum is a relatively recent discovery that represents a model of striatal injury at the level of the postsynaptic neurons. In using this model to study the underlying mechanisms of METH-induced striatal injury, it is first necessary to characterize striatal damage in the aftermath of METH exposure. The location and scope of damage will give insight into the mechanisms involved. Thus, the first aim of this thesis project is to evaluate and quantify the extent of METH-induced cell death in the striatum.

4.1 Establishing a Paradigm

Human METH abuse patterns include single and multiple dosing of the drug. In the laboratory, the binge (usually in a 5-10 mg/kg of body weight dose range given 4 times at two-hour intervals) and the single bolus (20-40 mg/kg of body weight) drug

administrations of METH have been used to reflect human abuse patterns and understand the underlying neurobiological mechanisms of METH-induced neural damage (Cho et al., 2001). Both drug regimens have been equally effective in inducing depletion of dopamine (DA) nerve terminal markers in the striatum (Frost and Cadet, 2000; Davidson et al., 2001) and each has contributed to the understanding of striatal injury at the terminals in various animal models. METH-induced cell death and degeneration in the striatum are relatively recent discoveries (Deng and Cadet, 2000; Deng et al., 2001). Both binge and bolus drug administrations of METH have been able to induce some form of neuronal apoptosis or degeneration in the brain. However, comparison between the efficacies of these two paradigms in their ability to induce injury at the level of postsynaptic cells and neurons in the striatum is needed.

Apoptosis of striatal cells is used as an indication for injury and is detected using terminal deoxynucleotidyl transferase-mediated dUTP nick end labeling (TUNEL). The technique's principle involves the labeling of 3'-OH nicks of cleaved genomic DNA that occurs as one of the late key biochemical events in apoptosis (Gavrieli et al., 1992). METH-induced apoptotic cell death was assessed in coronal sections of the striatum. Cells that display green fluorescence are apoptotic and have accumulated extensive nicks on their DNA which are tagged by TUNEL with FITC-conjugated dUTP's (Figure 4-1A). The striatum was subdivided into four quadrants (dorsal-medial, dorsal-lateral, ventral-medial, and ventral-lateral) and cell counts were taken from each region of the striatum when necessary to assess the potential differences in the dorsal-ventral and medial-lateral aspects of the striatum in response

to METH (See Chapter 3.3). The amount of TUNEL-positive neurons is expressed as a ratio of TUNEL-positive cells relative to a predetermined number of neurons in each of the striatal quadrants (See Chapter 3.3). It was demonstrated that all TUNEL-positive cells colocalized with the neuron specific marker neuronal nuclei (NeuN). Thus, establishing that METH-induced apoptosis occurs in neurons (See Chapter 4.4.1).

An acute bolus drug administration (30 mg/kg of body weight, i.p.) of METH induces considerably more TUNEL-positive neurons 24 hours after the treatment than a binge of METH at 10 mg/kg of body weight x 4 at 2 hour intervals (Figure 4-1A, B). At 24 hours post-METH treatment, an acute bolus drug administration of METH induced on average 16-23% TUNEL-positive neurons in the striatum, while a binge drug administration induced just an average of 4–7% cell death (Figure 4-1B). The bulk of the cell death which can be detected with TUNEL occurs 24 hours after METH treatment and few scattered TUNEL-positive cells are visible three days after the treatment for both drug delivery schedules (Figure 4-1A, B; See also Chapter 4.3.1). METH-induced apoptotic cell death at day 3 post-treatment fell between averages of 2–4% of total striatal neurons (Figure 4-1B). On average, all striatal quadrants displayed proportional levels of TUNEL staining although not all animals displayed proportional levels of apoptosis within treatment groups (Figure 4-1C). Interestingly, an acute bolus drug administration of METH induces apoptosis in the striata of more mice than a binge of METH (Figure 4-1C).

(A)

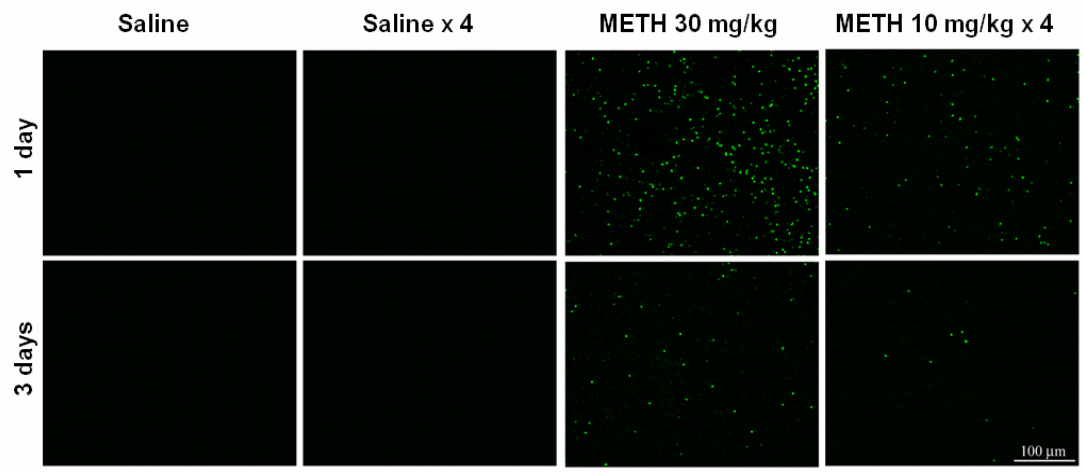

(B)

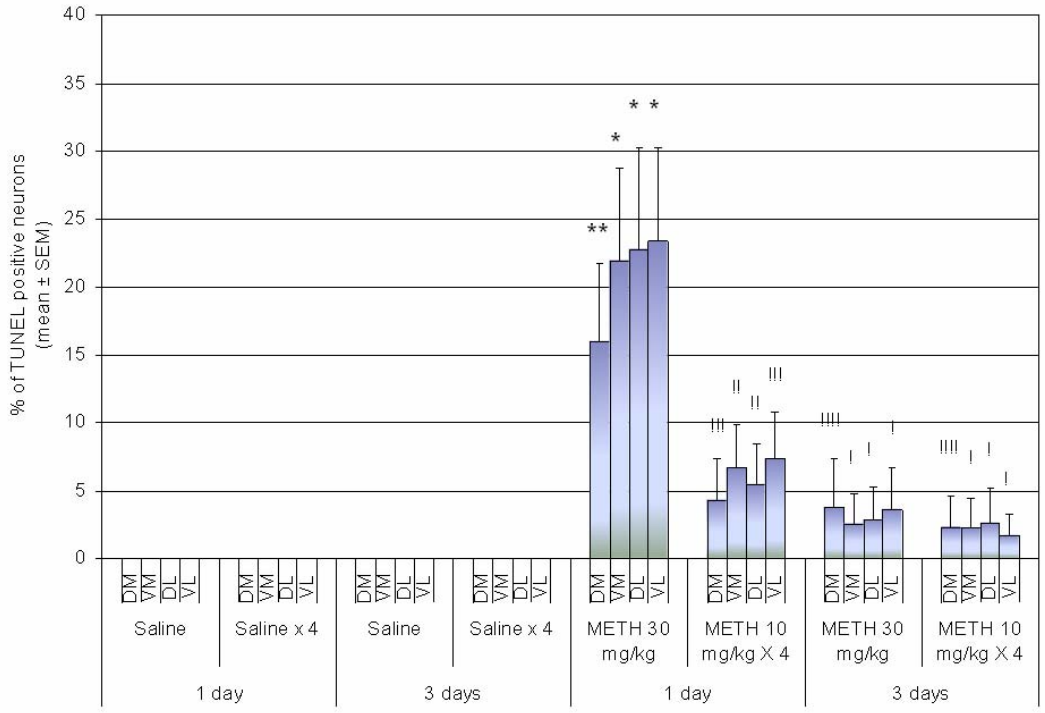

Figure 4-1 continues on next page→

(C)

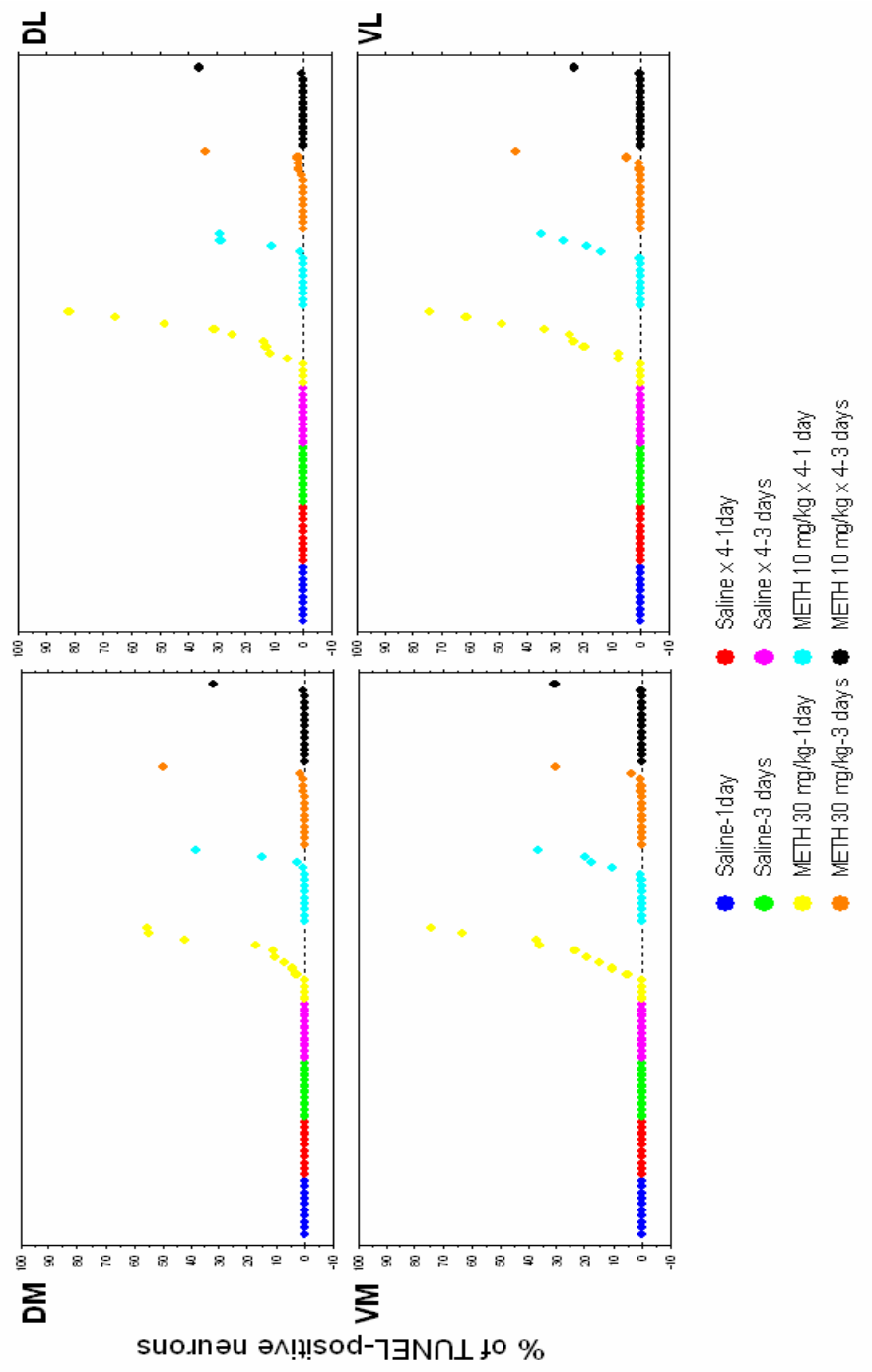

Figure 4-1. Comparison between bolus (30 mg/kg of body weight, i.p.) and a binge (10 mg/kg of body weight x 4 at 2 hour intervals, i.p.) administrations of methamphetamine

on the induction of cell death in the striatum. Animals were treated with methamphetamine (METH, i.p.) and sacrificed 1 day or 3 days after. Cell death is detected with TUNEL with FITC conjugated dUTP's on 20 µm coronal brain tissue sections of the striatum. (**A**) Epifluorescent micrographs of TUNEL-stained mouse striata. Scale bar = 40 µm. (**B**) Percent of TUNEL-positive neurons (mean ± SEM) were determined from cell counts in an area of $0.26mm^2$ for each of the four quadrants of the caudate putamen (CPu, dorsal-medial [DM], dorsal-lateral [DL], ventral-medial [VM], and ventral-lateral [VL]). * $p< 0.0001$ compared to all saline treatments. ** $p< 0.001$ compared to all saline treatments. ! $p< 0.0001$, !! $p<0.0005$, !!! $p< 0.001$, !!!! $p< 0.005$ compared to METH 30 mg/kg. (**C**) Scattergraphs for DM, DL, VM, and VL regions of the CPu demonstrate the percent of TUNEL-positive neurons are variable within treatment groups. Each dot represents one animal within each treatment group. ● Saline-1day, ● Saline x 4-1 day, ● Saline-3 days, ● Saline x 4-3 days, ● METH 30 mg/kg-1 day, ● METH 10 mg/kg x 4-1 day, ● METH 30 mg/kg-3 days, ● METH 30 mg/kg-3 days. n=10 for all saline groups. n=13 for METH treatment groups at day 1. n=14 for METH treatment groups at day 3.

4.2 Dose-Response

Various doses of METH (10-40 mg/kg of body weight) were tested to assess the effects of METH dose on the induction of apoptosis in the striatum. METH-induced apoptosis was assessed on coronal tissue sections of striatum using TUNEL 24 hours after METH injection. The striatum was again subdivided into four compartments in order to assess their potential differences. To determine the percentage of neurons undergoing METH-induced apoptosis, we first established a consistent and reliable baseline of the total number of neurons within each aspect of the striatum (See Chapter 3.3). This was accomplished by labeling the neurons with an antibody against the neuron-specific marker neuronal nuclei (NeuN). Five striatal sections (bregma 0.38 mm ± 0.1 mm) from each animal (total of 6 animals) were processed for immunofluorescence for NeuN and all fluorescent neurons were counted under the microscope. The average number of NeuN-positive neurons from the 30 sections was taken from each of the four quadrants of the striatum and later used to determine the percentage of TUNEL-positive neurons in the aftermath of METH. The total number of NeuN-positive neurons in each aspect of the striatum were consistent between animals.

A dose-dependent response was observed with increased METH dosing. Figure 4-2A shows representative photomicrographs of TUNEL-positive neurons from the striatum of mice that had been exposed to increasing doses of METH (b-e). There is a sharp increase in the amount of TUNEL-positive neurons going from 20 to

30 mg/kg of METH (Figure 4-2A, B). The average amount of neuronal apoptosis induced by METH 30mg/kg was between 13-25% amongst the four quadrants of the striatum (Figure 4-2B). Continued increase of METH dosing at 40 mg/kg did not show any significant increase from 30 mg/kg. Also, an increased dose of METH caused higher mortality in animals (*data not shown*). Thus, a 30 mg/kg dose of METH was chosen for subsequent studies. Although the dorsal-medial aspect of the striatum consistently displayed lower levels of METH-induced apoptosis relative to other striatal quadrants, no significance was found between the four different regions of the striatum (Figure 4-2B). Again, METH-induced (30 mg/kg, i.p.) striatal apoptosis detected by TUNEL has large inter-animal variability within treatment groups, ranging from 3% to 82% in the four regions of the striatum (See scattergraphs in Figure 4-2C). Some animals do not have any TUNEL-positive neurons. Due to this inter-animal variability, a large number of animals (n) were used throughout the subsequent studies.

(A)

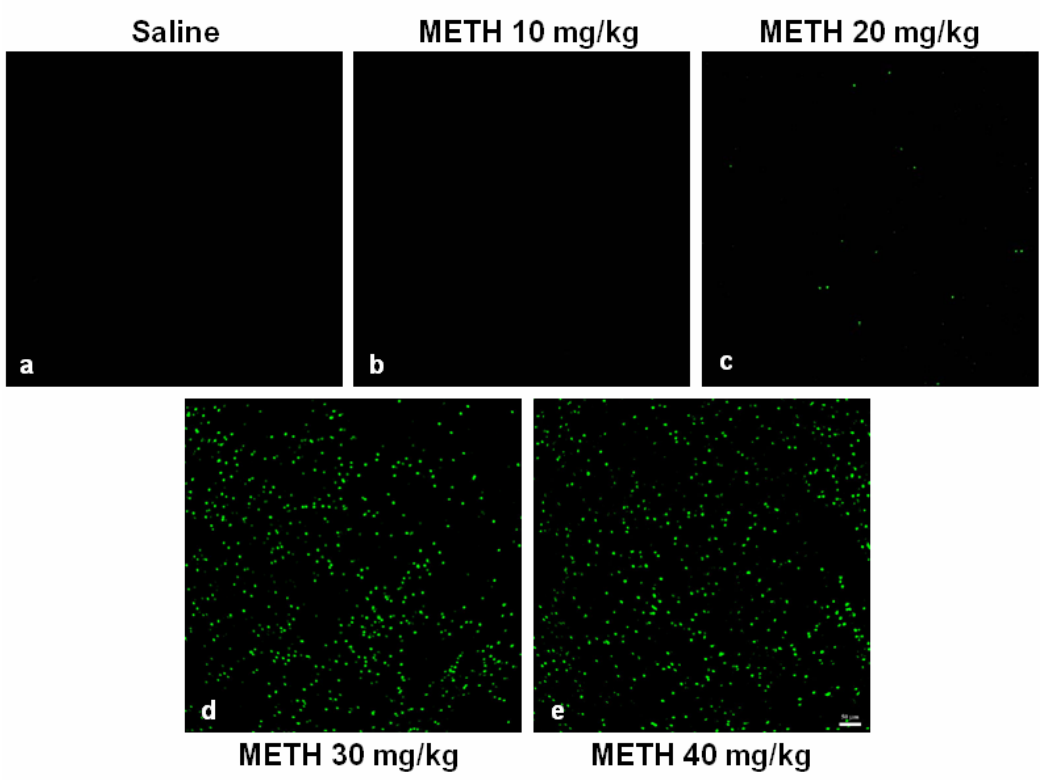

(B)

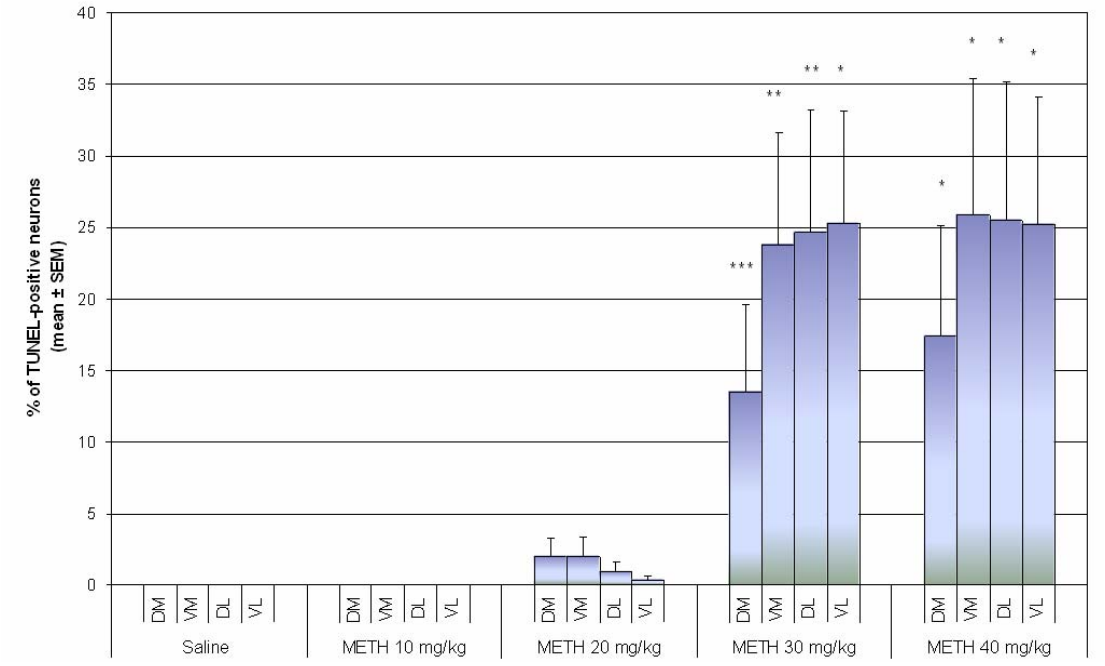

Figure 4-2 continues on next page→

(C)

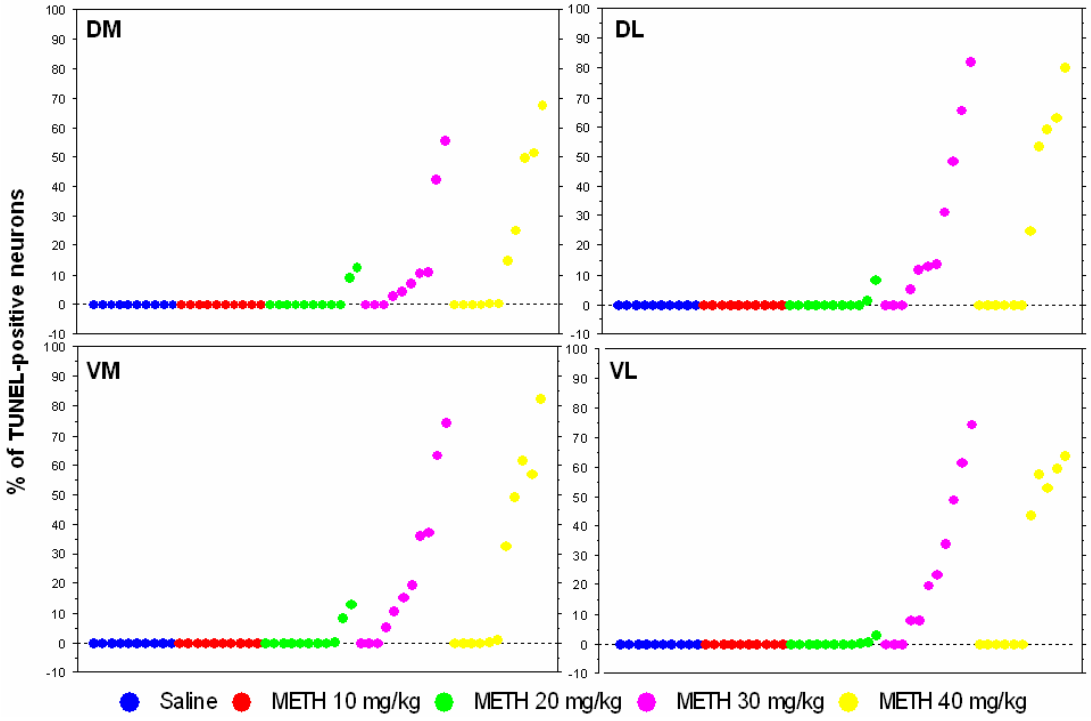

Figure 4-2. Effect of methamphetamine dose on the induction of striatal apoptosis. ICR mice received single bolus injection of methamphetamine (METH, i.p.) and were sacrificed 24 hours after. Coronal sections of brain tissue at the level of the striatum were processed for TUNEL with FITC-conjugated dUTP's. **(A)** Scanning confocal micrographs of TUNEL-positive neurons in the striatum of mice treated with increasing doses of METH (10, 20, 30, or 40 mg/kg of body weight, i.p.) **(a-e)**. Scale bar=50 μm. **(B)** Percent of TUNEL-positive neurons (mean ± SEM) were determined from cell counts in an area of 0.26mm^2 for each of the four quadrants of the caudate putamen (CPu, dorsal-medial [DM], dorsal-lateral [DL], ventral-medial [VM], and ventral-lateral [VL]). * $p< 0.005$, ** $p< 0.01$, *** $p<0.05$ compared to saline control. **(C)** Scattergraphs indicate percent of TUNEL-positive neurons for each animal within each treatment group. Each dot represents one animal. ● Saline, ● METH 10 mg/kg, ● METH 20 mg/kg, ● METH 30 mg/kg, ● METH 40 mg/kg. n=10-11 per experimental group.

4.3 Temporal Assessments

4.3.1 Time Course of METH-induced Cell Death

Multiple time points (16 hours, 1 day, 2 days, and 3 days) were assessed in order to determine the time when apoptosis occurs in the striatum after METH administration (30 mg/kg of body weight, i.p.). Apoptosis is detected by TUNEL. Apoptotic cells were detectable by TUNEL (2-6%) at 16 hours after METH treatment. The peak of apoptosis occurs at 24 hours after METH administration in all aspects of the striatum (Figure 4-3A). METH induced 25-32% of TUNEL positive neurons 24 hours post-treatment. METH-induced apoptosis is barely detectable at 2 days post-METH treatment (Figure 4-3A). Some TUNEL-positive neurons are apparent (2-4%) at 3 days post-METH treatment(Figure 4-3A). This however is due to one animal that displayed high levels of apoptosis on day 3 (Figure 4-3B). This animal may represent a delayed onset of apoptosis or a second phase of apoptosis induced by the initial apoptosis seen at day 1 post-METH treatment. The majority of the animals displayed only residual levels of apoptosis on day 3 (Figure 4-3B). This is possibly due to secondary effects cause by the initial apoptosis at day 1. No significance was found between the four quadrants of the striatum.

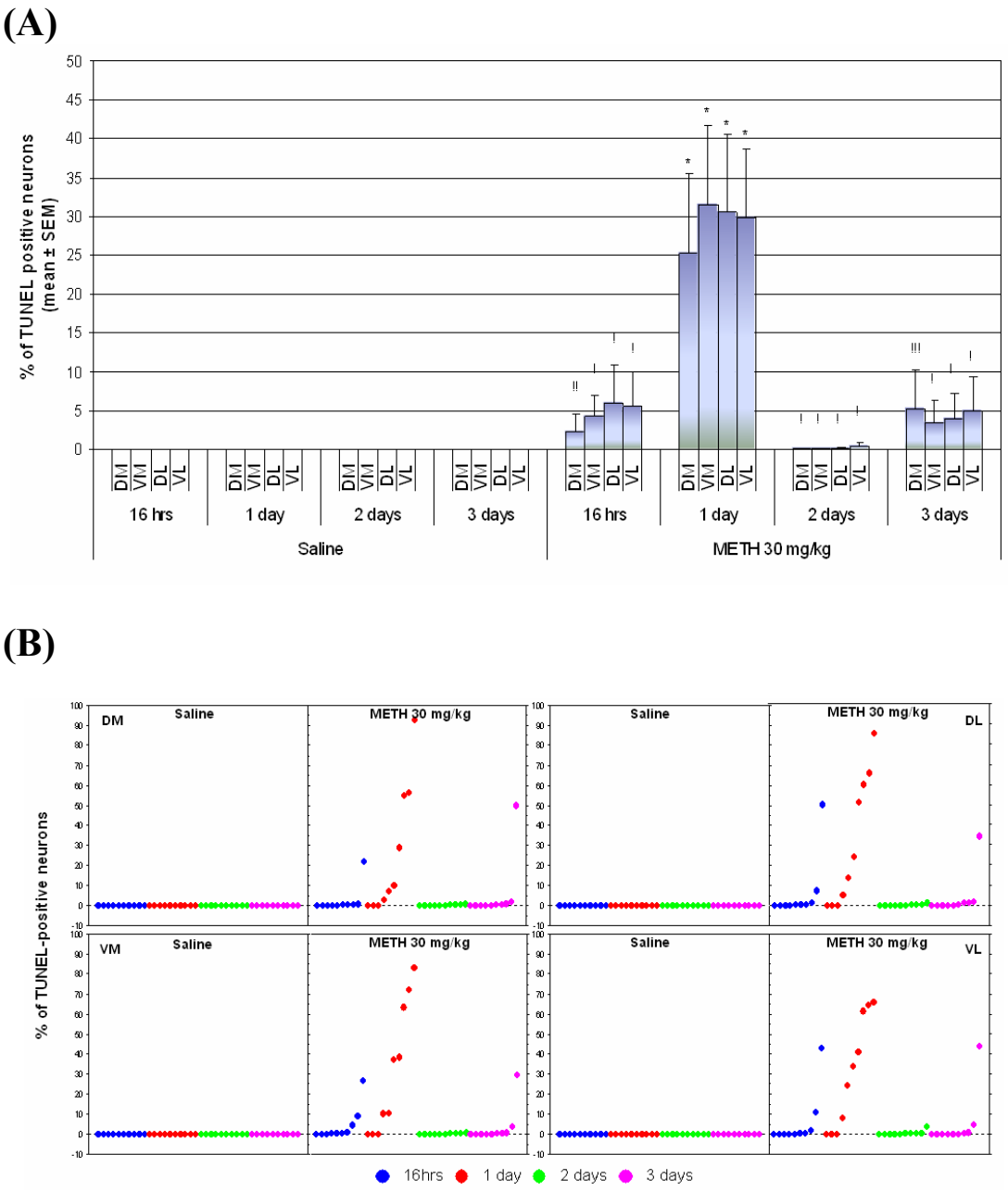

Figure 4-3. Time course of methamphetamine-induced cell death in the striatum. Animals received a single injection of methamphetamine (METH 30 mg/kg of body weight, i.p.) and were sacrificed at various times (16 hours, 1 day, 2 days, or 3 days) after the treatment**.** Striatal tissue sections were processed for TUNEL with FITC-conjugated dUTP's. **(A)** Percent of TUNEL-positive neurons (mean ± SEM) were determined from cell counts in

an area of 0.26 mm^2 for each of the four quadrants of the caudate putamen (CPu, dorsal-medial [DM], dorsal-lateral [DL], ventral-medial [VM], and ventral-lateral [VL]) at 16hrs, 1 day, 2 days, and 3 days post METH treatment. * $p<0.0001$ compared to all saline treatment groups and regions. ! $p<0.0001$, !! $p<0.0005$, !!! $p<0.001$, compared to corresponding region of METH 30 mg/kg-1 day. No significance was found between regions of the CPu. **(B)** Scattergraphs show percent of TUNEL-positive neurons for each animal within each treatment group. Each dot represents one animal. ● 16hrs, ● 1 day, ● 2 days, ● 3 days post-treatment. n=10 per experimental group.

4.3.2 Temporal Relationships to Presynaptic Terminal Damage

4.3.2.1 Tyrosine Hydroxylase

Tyrosine hydroxylase (TH) is the rate-limiting enzyme for the synthesis of dopamine. Depletion of TH is used as a neurotoxic marker to indicate injury at dopamine nerve terminals. Protein levels of TH from four striatal quadrants were assessed at various times (16 hours, 1 day, 2 days, and 3 days) by Western blot after an acute bolus dose of METH (30 mg/kg of body weight, i.p.) (Figure 4-4A). After stripping the blots and reprobing for β-actin, the protein bands corresponding to TH protein were quantified by densitometry and normalized against β-actin. At 16 hours and 1 day after METH treatment, TH protein levels were reduced by 24-38% below control in the dorsal striatum (both medial and lateral aspects). However, TH protein levels were not appreciably decreased at these time points in the ventral striatum (Figure 4-4B). At days 2 and 3 post-METH treatment, TH protein levels were decreased 74-88% below control in all aspects of the striatum (Figure 4-4B). Note that when the peak of TH depletion is reached at day 2, the peak of apoptosis preceded it by approximately 24 hours (Compare Figure 4-3A and Figure 4-4B).

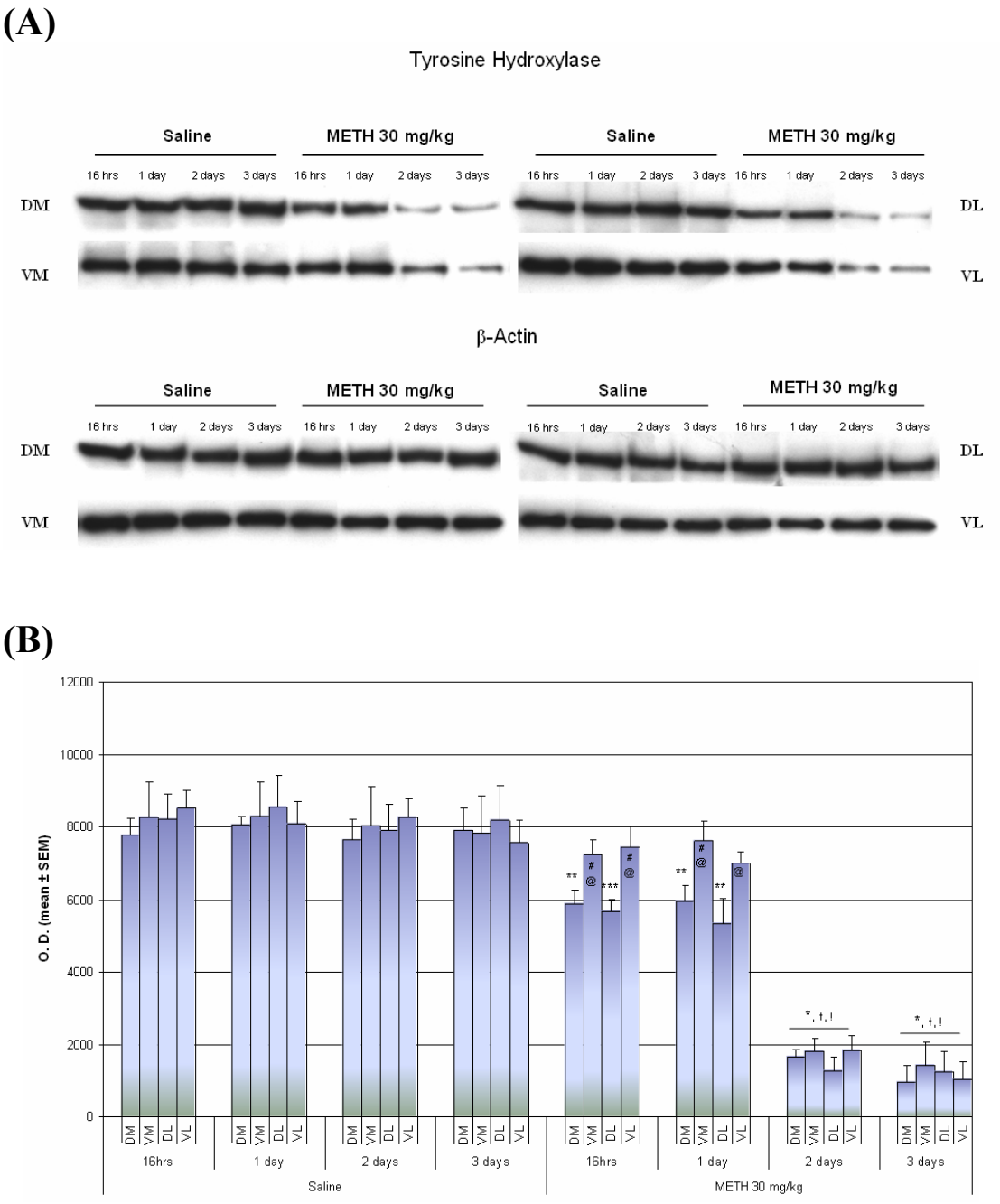

Figure 4-4. Time course of methamphetamine-induced depletion of tyrosine hydroxylase (TH) in the striatum. Animals received a single injection of methamphetamine (METH 30 mg/kg of body weight, i.p.) and were sacrificed at the various times indicated after the treatment**. (A)** Western blots of TH and β-actin from four different quadrants of the caudate

putamen (CPu) (dorsal-medial (DM), ventral-medial (VM), dorsal-lateral (DL), and ventral-lateral (VL) at 16hrs, 1 day, 2 days, and 3 days post-METH treatment. **(B)** Optical densities (O.D.) (mean ± SEM) of TH western blot bands from six separate blots. At 16 hrs post-treatment, METH induced a loss of 24.2%, 12.7%, 30.9%, 12.9% in the DM, VM, DL, VL quadrants of the CPu respectively. At 1 day post-treatment, METH induced a loss of 25.9%, 8.1%, 37.5%, 13.5% in the DM, VM, DL, VL quadrants of the CPu respectively. At 2 days post-treatment, METH induced a loss of 78.2%, 77.4%, 83.8%, 77.6% in the DM, VM, DL, VL quadrants of the CPu respectively. At 3 days post-treatment, METH induced a loss of 87.8%, 81.8%, 84.8%, 86.2% in the DM, VM, DL, VL quadrants of the CPu respectively. * $p<0.0001$, ** $p<0.005$, *** $p<0.01$ compared to corresponding regions of saline treatment groups. † $p<0.0001$ compared to corresponding regions of METH 30 mg/kg-16hrs. ! $p<0.0001$ compared to corresponding regions of METH 30mg/kg-1 day. # $p<0.05$ compared to the DM region within each experimental group. @ $p<0.05$ compared to the DL region within each experimental group. n= 6 per experimental group.

4.3.2.2 Dopamine Transporters

The dopamine transporter (DAT) is located at dopamine terminals in the striatum. It is a reliable and sensitive neurochemical marker that has been used extensively to assess injury at dopamine terminals. Loss of striatal DAT binding sites in the four regions of the striatum were assessed by autoradiography with DAT [^{125}I]RTI-121 at 16 hours, 1 day, 2 days, and 3 days after METH (30 mg/kg, i.p.) administration (see Figure 4-5A). DAT binding sites were stable at 16 hours after METH treatment but decreased by 21-36% of control 1 day post-METH treatment (Figure 4-5B). By days 2 and 3, METH induced 50-71% depletion in DAT binding sites. Similar to TH, DAT sites were decreased at 1 day post-METH treatment, but the peak of depletion was reached 2 days after METH treatment (Compare Figure 4-3A, Figure 4-4B, and Figure 4-5B).

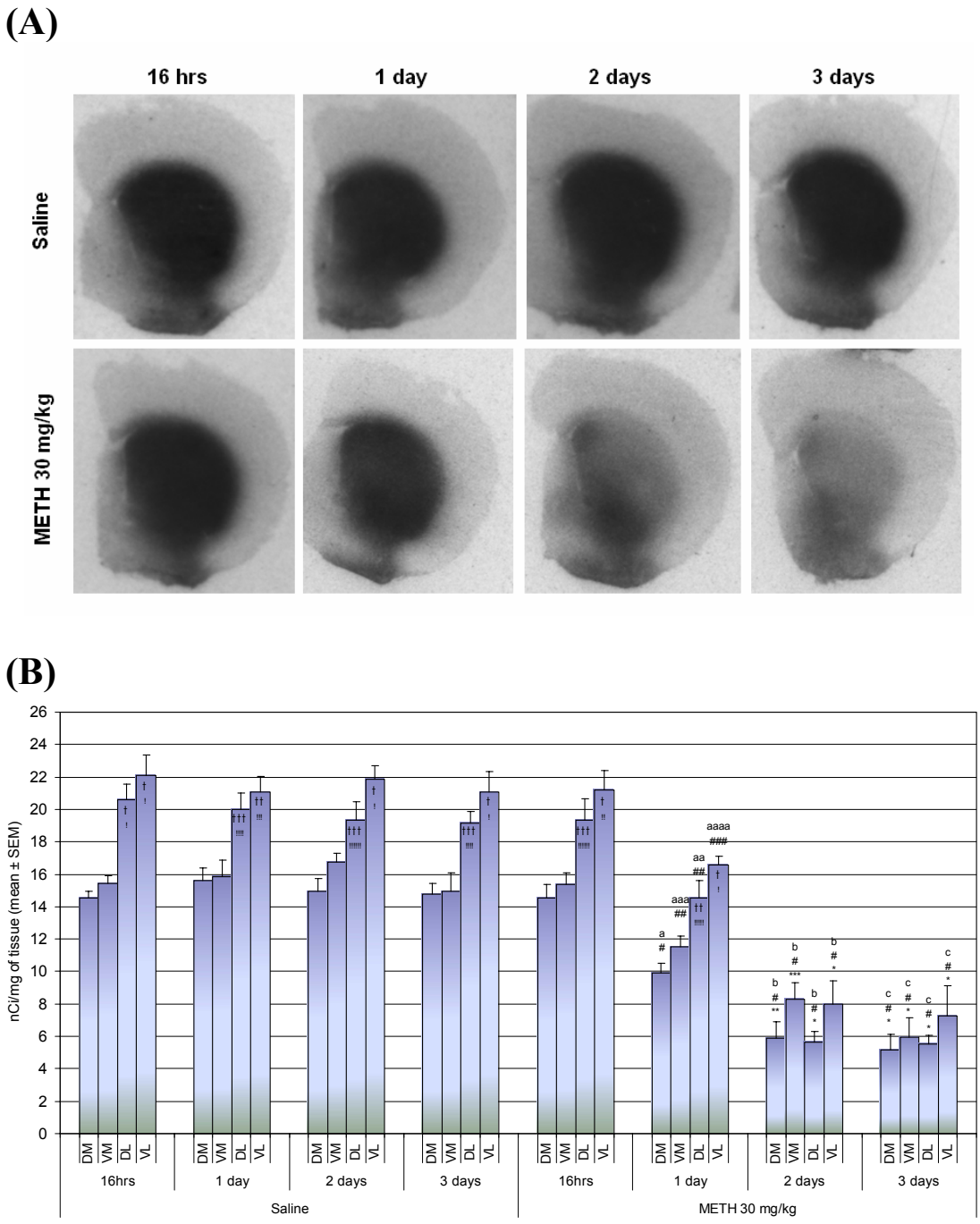

Figure 4-5. Time course of methamphetamine-induced loss of striatal dopamine transporter (DAT) binding sites in the striatum. Animals received a single injection of METH (30 mg/kg, i.p.) and were sacrificed at various indicated times after the treatment.

Striatal tissue sections were process for receptor autoradiographic analysis of DAT using [^{125}I]RTI-121. **(A)** DAT [^{125}I]RTI-121 receptor autoradiographs of METH-induced depletion of DAT binding sites in the striatum at 16hrs, 1 day, 2 days, and 3 days post treatment. **(B)** METH-induced a progressive loss of [^{125}I]RTI-121 binding sites (mean ± SEM). In the DM region, METH induced a loss of 0%, 36.43%, 60.62%, and 65.13% of DAT levels at 16 hrs, 1 day, 2 days, and 3 days post-treatment respectively. In the VM region, METH induced a loss of 0.45%, 27.43%, 50.51%, and 60.16% of DAT levels at 16 hrs, 1 day, 2 days, and 3 days post-treatment respectively. In the DL region, METH induced a loss of 6.35%, 27.20%, 70.76%, and 70.29% of DAT levels at 16 hrs, 1 day, 2 days, and 3 days post-treatment respectively. In the VL region, METH induced a loss of 4.16%, 21.33%, 63.42%, and 65.5% of DAT levels at 16 hrs, 1 day, 2 days, and 3 days post-treatment respectively. Regional comparisons showed the lateral portion of the CPu has an average of 35% higher distribution of DAT sites than its medial portion. The DL region displayed the highest vulnerability to METH-induced DAT depletion. † $p<0.0001$, †† $p<0.0005$, ††† $p<0.005$ compared to the DM region within each experimental group. ! $p\leq0.0001$, !! $p\leq0.0005$, !!! $p<0.001$, !!!! $p<0.005$, !!!!! $p<0.01$, !!!!!! $p<0.05$ compared to the VM region within each experimental group. a $p<0.0001$, aa $p\leq0.0005$, aaa $p<0.001$, aaaa $p<0.05$ compared to the corresponding region of saline-1 day. b $p<0.0001$ compared to the corresponding region of saline-2 days. c $p<0.0001$ compared to the corresponding region of saline-3 days. # $p\leq0.0001$, ## $p<0.005$, ### $p<0.05$ compared to the corresponding region of METH 30 mg/kg-16 hrs. * $p<0.0001$, ** $p<0.001$, *** $p<0.05$ compared to the corresponding region of METH 30 mg/kg-1day. n=8 per experimental group.

4.3.2.3 Reactive Astrocytes

In addition to the DA terminal markers, we also assessed the induction of striatal astrocytes at various times after METH (30 mg/kg of body weight, i.p.) treatment by immunohistofluorescence using a monoclonal antibody against glial fibrillary acidic protein (GFAP) (Figure 4-6A). GFAP is a cytoskeletal protein prominently expressed in immature and reactive astrocytes. Elevated expression of the GFAP protein is an indicator of injury in the central nervous system. The numbers of reactive astrocytes were counted in an area of 0.26 mm^2 in each striatal quadrant (See Chapter 3.3). In sections from control mice, the levels of GFAP are at the threshold of detection by immunohistofluorescence (Figure 4-6A, a,c,e & g). Thus, the control number of astrocytes was arbitrarily set as zero. The induction of GFAP in astrocytes is significantly (average 14-40%) above control at day 2 post-METH treatment. The peak (58-74% above control) of GFAP induction occurs at 3 days after METH treatment (Figure 4-6B). This contrasts sharply with the peak of apoptosis occurring 1 day after METH treatment (Compare Figure 4-3A and Figure 4-6B). This data suggests that loss of postsynaptic striatal neurons may contribute to the induction of presynaptic nerve terminal depletions of TH and DAT binding sites and the induction of an astrocytic response.

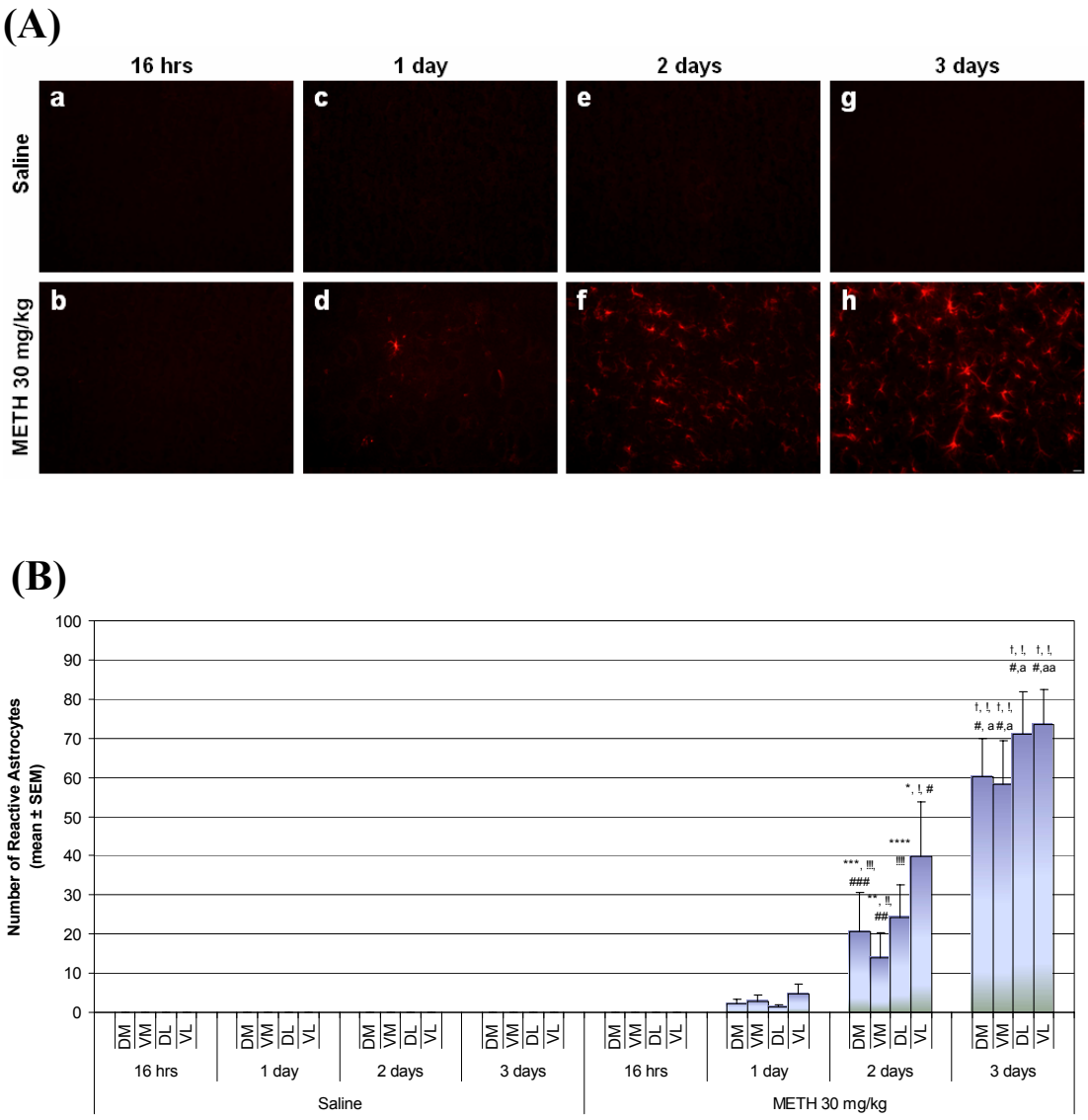

Figure 4-6. Time course of methamphetamine-induced increase in reactive astrocytes in the striatum. Animals received a single injection of methamphetamine (METH 30 mg/kg of body weight, i.p.) and were sacrificed at various times after the treatment. Striatal tissue sections were labeled with a Cy3-conjugated antibody against glial fibrillary acidic protein (GFAP). **(A)** Epifluorescent images of GFAP-stained mouse striata at 16hrs, 1 day, 2 days, and 3 days post METH treatment. Scale bar = 20 μm. **(B)** Number of METH-induced reactive astrocytes (mean ± SEM) were determined from cell counts in an area of 0.26 mm^2 for each

of the four quadrants of the striatum (dorsal-medial [DM], dorsal-lateral [DL], ventral-medial [VM], and ventral-lateral [VL]) * $p<0.0001$, ** $p<0.005$, *** $p<0.01$, **** $p<0.05$ compared to the corresponding region of saline-2 days. † $p<0.0001$, †† $p<0.005$, ††† $p<0.05$ compared to the corresponding region of saline-3 days. ! $p<0.0001$, !! $p<0.005$, !!! $p<0.01$, !!!! $p<0.05$ compared to the corresponding region of METH 30 mg/kg-16 hrs. # $p<0.0001$, ## $p<0.005$, ### $p<0.05$ compared to the corresponding region of METH 30 mg/kg-1day. a $p<0.0001$, aa $p<0.0005$ compared to the corresponding region of METH 30 mg/kg-2 days. No significance was found between the DM, VM, DL, and VL regions of the striatum. n=6 per experimental group.

4.4 Selective Neuronal Vulnerabilities

The striatum is a heterogeneous structure that is composed of various neuronal cell types (See Chapter 1.2.2). These striatal neurons have shown selective vulnerability towards various chemical insults and in neurodegenerative diseases. For example, striatal atrophy and choreiform movements seen in Huntington's disease are attributed to the progressive degeneration of striatal medium spiny projection neurons (Reiner et al., 1988; Albin et al., 1990). Considerable evidence now shows that it is the enkephalin-positive striatopallidal neurons that are the most vulnerable (Albin et al., 1992; Richfield et al., 1995; Mitchell et al., 1999; Richfield et al., 2002; Deng et al., 2004) while striatal aspiny interneurons are spared in this disease (Ferrante et al., 1985; Reiner et al., 1988; Cicchetti et al., 1996; Hickey and Chesselet, 2003). Excitotoxic lesions by quinolinic acid are associated with increased concentrations of somatostatin (SST) and neuropeptide Y (NPY) as a result of preferential sparing of striatal interneurons (Beal et al., 1986; Beal et al., 1991). Damage to the striatum by mitochondrial inhibitor, 3-nitropropionic acid (3NP), is specific to projection neurons while dopaminergic axons and nicotinamide adenine dinucleotide phosphate (NADPH)-diaphorase positive interneurons are spared (Guyot et al., 1997). Interneurons that contain NADPH-diaphorase, SST and NPY are also less vulnerable in ischemia models (Uemura et al., 1990). In light of these findings, immunohistochemistry and cell quantification was utilized to assess how each neuronal cell type in the striatum is affected by METH exposure.

4.4.1 Neurons

To determine whether METH (30 mg/kg, i.p.) induces apoptosis in neurons of the striatum, we combined TUNEL with immunofluorescence of neuronal nuclei (NeuN). NeuN is a DNA-binding, neuron-specific nuclear protein (Mullen et al., 1992). This marker was chosen over other neuronal markers because the labeling of this protein occurs in the nucleus like TUNEL. METH treatment causes NeuN staining to be less pronounced (Figure 4-7; d). This is probably an indication that these neurons have already incurred severe deficits in molecular markers such as receptors and peptides. Double-labeling reveals TUNEL-positive nuclei colocalized with NeuN (Figure 4-7; g-i).

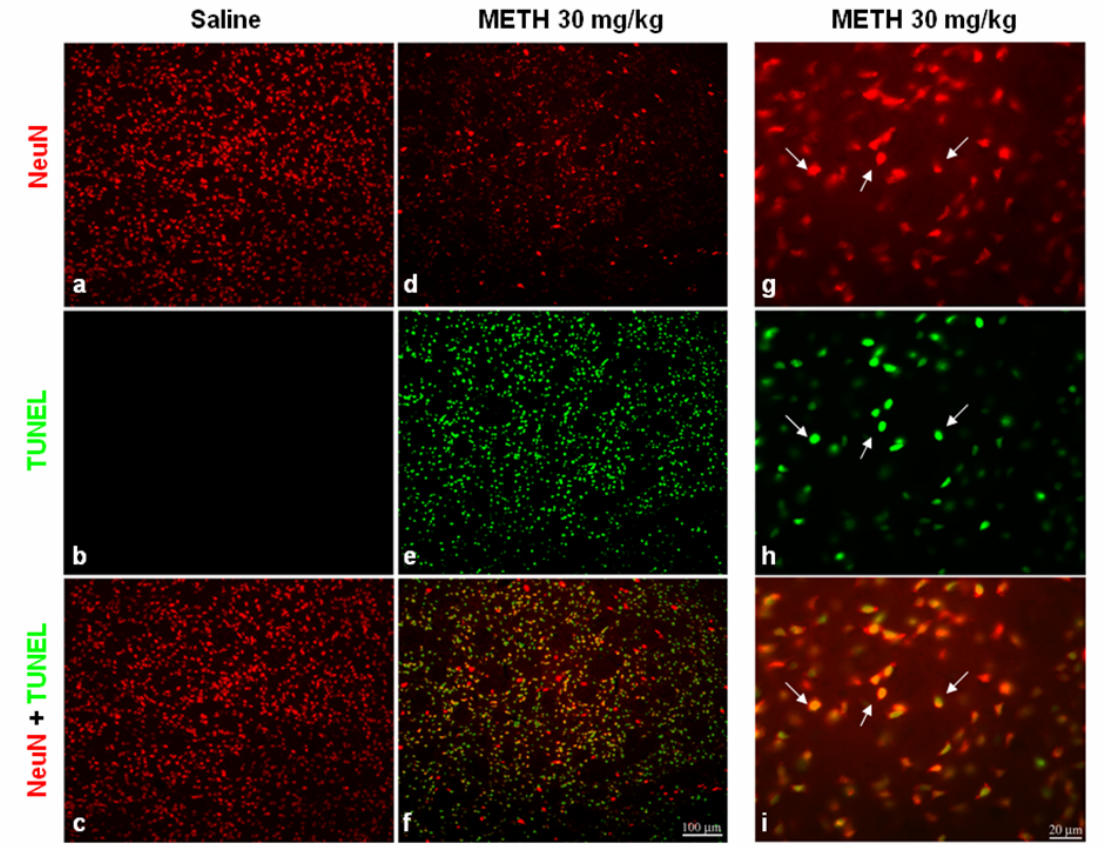

Figure 4-7. Methamphetamine induces apoptosis in striatal neurons. Animals were treated with methamphetamine (METH 30 mg/kg of body weight, i.p.) and sacrificed 24 hours after. Coronal sections of the striatum were labeled with TUNEL and neuronal nuclei (NeuN). **(A)** Double-labeled epifluorescent micrographs of striatal tissue stained with Cy3-labeled antibodies against neuron-specific nuclear protein NeuN and TUNEL with FITC-conjugated dUTP's in control **(a-c)** and METH treated animals **(d-i)**. Bottom panels **(c,f,i)** are overlays of both TUNEL and NeuN staining. Higher magnifications in METH treated animal indicated that NeuN positive neurons colocalized with TUNEL-positive cells **(g-i).** White arrows point to examples of overlapping TUNEL and NeuN-positive cells. Scale bar=100 µm **(a-f)**, 20 µm **(g-i)**.

4.4.2 GABAergic Projection Neurons

Approximately 90% percent of the striatum is composed of the striatonigral and the striatopallidal gamma-aminobutyric acid (GABA)ergic projection neurons. METH-induced apoptosis of projection neurons was demonstrated by using immunofluorescence for dopamine cAMP-regulated phosphoprotein 32kDa (DARPP32), a reliable protein marker found in both striatopallidal and striatonigral projection neurons.

There was no colocalization of DARPP32 with TUNEL-positive neurons observed (Figure 4-8A; g-i). However, immunoreactivity of DARPP32 showed significant decreases with METH treatment (Figure 4-8A; a-f). Closer observation showed that within a given area where TUNEL-labeling was observed, it was very difficult to also find DARPP32 staining (Figure 4-8A; d-f). This is dramatically different in controls where there is abundant DARPP32 staining and no TUNEL (Figure 4-8A; a-c). Cell counts of DARPP32-positive neurons showed that METH caused a 15.4% ± 2.5% decrease of DARPP32-positive neurons in the DM region, 23.8% ± 3.8 % in the VM region, 22.8% ± 3.8 % in the VL region and 24.4% ± 3.9 % in the DL region compared to controls (Figure 4-8B). These decreases correspond with the METH-induced increases in percentage of TUNEL-positive neurons in figures 4-1B, 4-2B, and 4-3A. This demonstrates that the loss of DARPP32 correlates with the increase in TUNEL-positive cells, consistent with an interpretation that METH induces the loss of some projection neurons in the striatum.

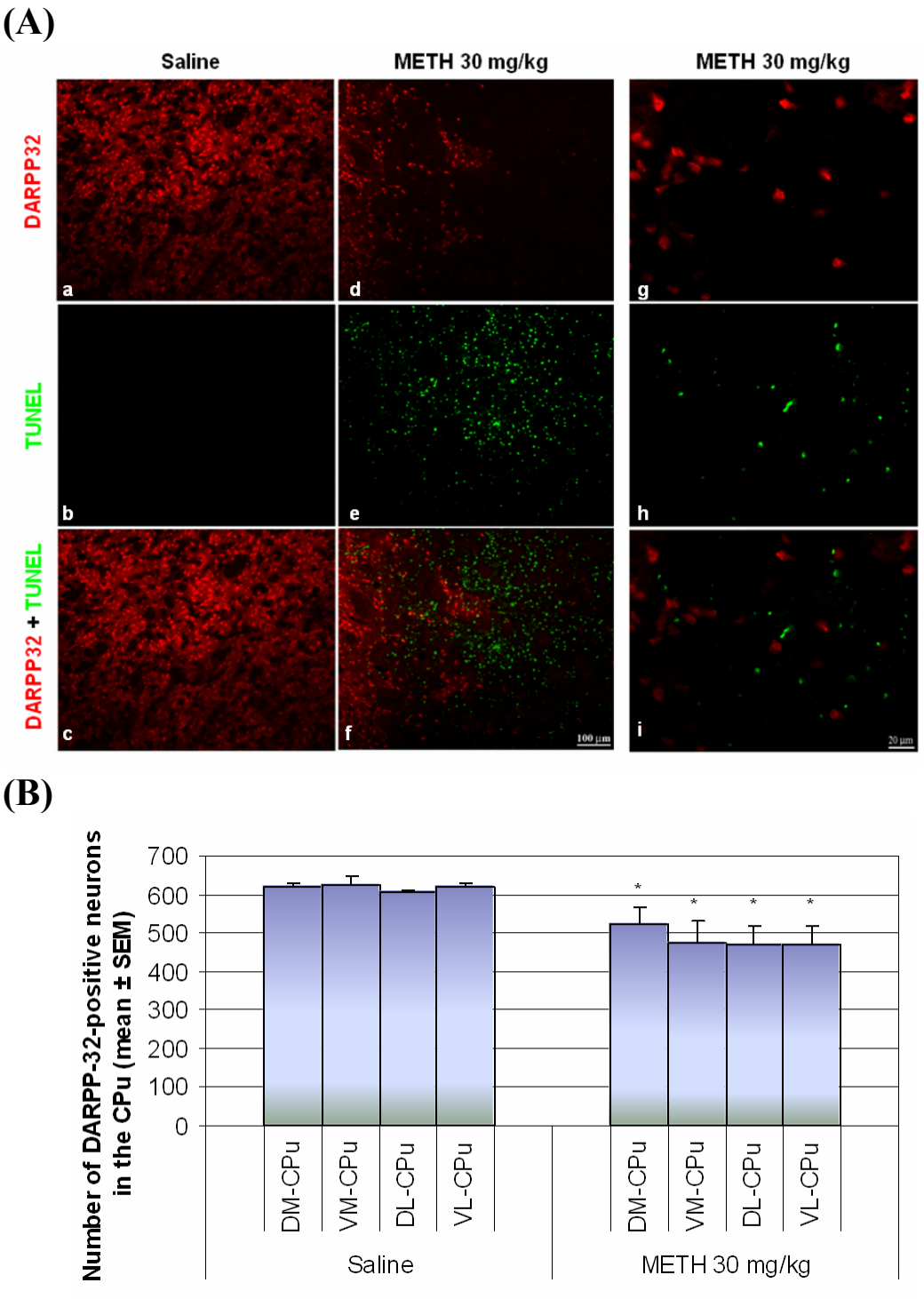

Figure 4-8. Loss of DARPP32-containing projection neurons in the striatum after methamphetamine treatment. Animals received a single injection of methamphetamine

(METH 30 mg/kg of body weight, i.p.) and were sacrificed 24 hours later. Striatal tissue sections were processed for immunofluorescence and TUNEL. **(A)** Double-labeled epifluorescent micrographs of striatal tissue stained with Cy3-labeled antibodies against DARPP32 and TUNEL with FITC-conjugated dUTP's in control **(a-c)** and METH treated animals **(d-i)**. Bottom panels **(c,f,I,l)** are overlays of both TUNEL and DARPP32 staining. Higher magnifications in METH treated animal indicated that the two does not overlap **(g-i)**. Scale bar=100 μm **(a-f)**, 20 μm **(g-i)**. **(B)** Number of DARPP32-positive neurons (mean ± SEM) were determined from cell counts in an area of 0.26 mm^2 for each of the four quadrants of the caudate putamen (CPu, dorsal-medial [DM], dorsal-lateral [DL], ventral-medial [VM], and ventral-lateral [VL]) in 11 animals per experimental group. * $p<0.05$ compared to corresponding regions of saline control.

4.4.3 Parvalbumin-containing GABA Interneurons

Various interneurons make up 10% of the neuronal population in the striatum. Their axonal projections remain within the striatum and each subtype is distinguished by its neurotransmitter content. Antibodies against the calcium binding protein, parvalbumin were used to assess METH (30 mg/kg, i.p.) effects on parvalbumin-containing GABA interneurons. No colocalization of parvalbumin and TUNEL-positive neurons was observed (Figure 4-9A). Despite this, immunoreactivity of parvalbumin-positive neurons was diminished (Figure 4-9A; d-f) and dendritic arbors appeared shorter (Figure 4-9A; j-l) in animals treated with METH (Figure 4-9; a-c, g-i). To detect the potential loss of some of these interneurons after METH exposure, cell counts of parvalbumin-positive neurons were performed in the four quadrants of the striatum. All four quadrants show a decrease. However, the dorsal region of the striatum where this GABAergic interneuron is concentrated was largely affected by METH treatment; resulting in 43.7% ± 5.5% decrease of the marker in the DM region and 49% ± 10.8 % in the DL region (Figure 4-8B).

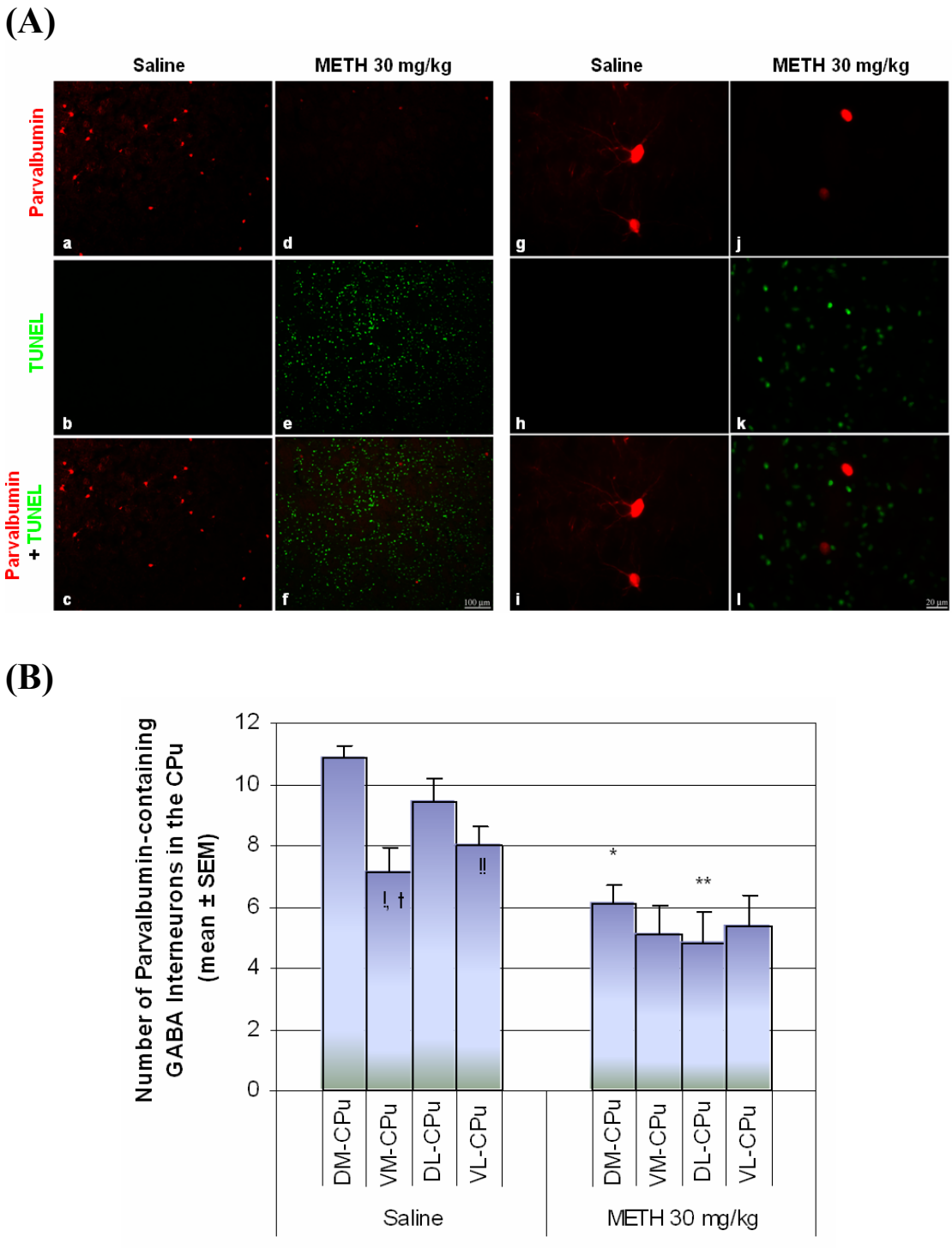

Figure 4-9. Loss of parvalbumin-containing GABA interneurons in the striatum neurons after methamphetamine treatment. Animals received a single injection of

methamphetamine (METH 30 mg/kg of body weight, i.p.) and were sacrificed 24 hours later. Striatal tissue sections were processed for immunohistofluorescence. **(A)** Double-labeled epifluorescent micrographs of striatal tissue stained with Cy3-labeled antibodies against parvalbumin and TUNEL with FITC-conjugated dUTP's in control **(a-c)** and METH treated animals **(d-i)**. Bottom panels **(c,f,I,l)** are overlays of both TUNEL and parvalbumin staining. Higher magnifications in METH treated animal indicated that the two does not overlap **(g-i)**, although cell bodies showed loss of dendritic arborization **(j-l)**. Scale bar=100 μm **(a-f)**, 20μm **(g-l)**. **(B)** Number of parvalbumin-positive neurons (mean ± SEM) were determined from cell counts in an area of 0.26 mm^2 for each of the four quadrants of the caudate putamen (CPu, dorsal-medial [DM], dorsal-lateral [DL], ventral-medial [VM], and ventral-lateral [VL]) in 11 animals per experimental group. A significant decrease is observed in the dorsal regions of the striatum * $p<0.0001$, ** $p< 0.005$, *** $p<0.05$ compared to corresponding regions of saline control. ! $p<0.0001$, !! $p<0.001$ compared to the DM region of saline. † $p<0.005$ compared to the DL region of saline.

4.4.4 Cholinergic Interneurons

Antibodies against choline acetyl transferase (ChAT) were used to assess the effect of METH (30 mg/kg, i.p.) on cholinergic interneurons. ChAT is an enzyme that catalyzes the transfer of the acetyl group of acetyl CoA to choline, forming acetylcholine. Similar to assessments with parvalbumin, no colocalization was observed between ChAT and TUNEL-positive neurons in the striatum (Figure 4-10A). No obvious change was seen in the morphology and the number of the cholinergic interneurons after METH treatment compared to control (Figure 4-10A). Cell counts of the cholinergic interneurons confirmed these neurons to be unaffected in the ventral portions of the striatum. However, the dorsal regions of the striatum showed loss of this neuronal cell type. This is most significant for the dorsal-medial portion of the striatum, which had a 28.9% ± 4.8% decrease from control (Figure 4-10B). It should be noted that these deficits were observed in the animals that displayed high levels of TUNEL.

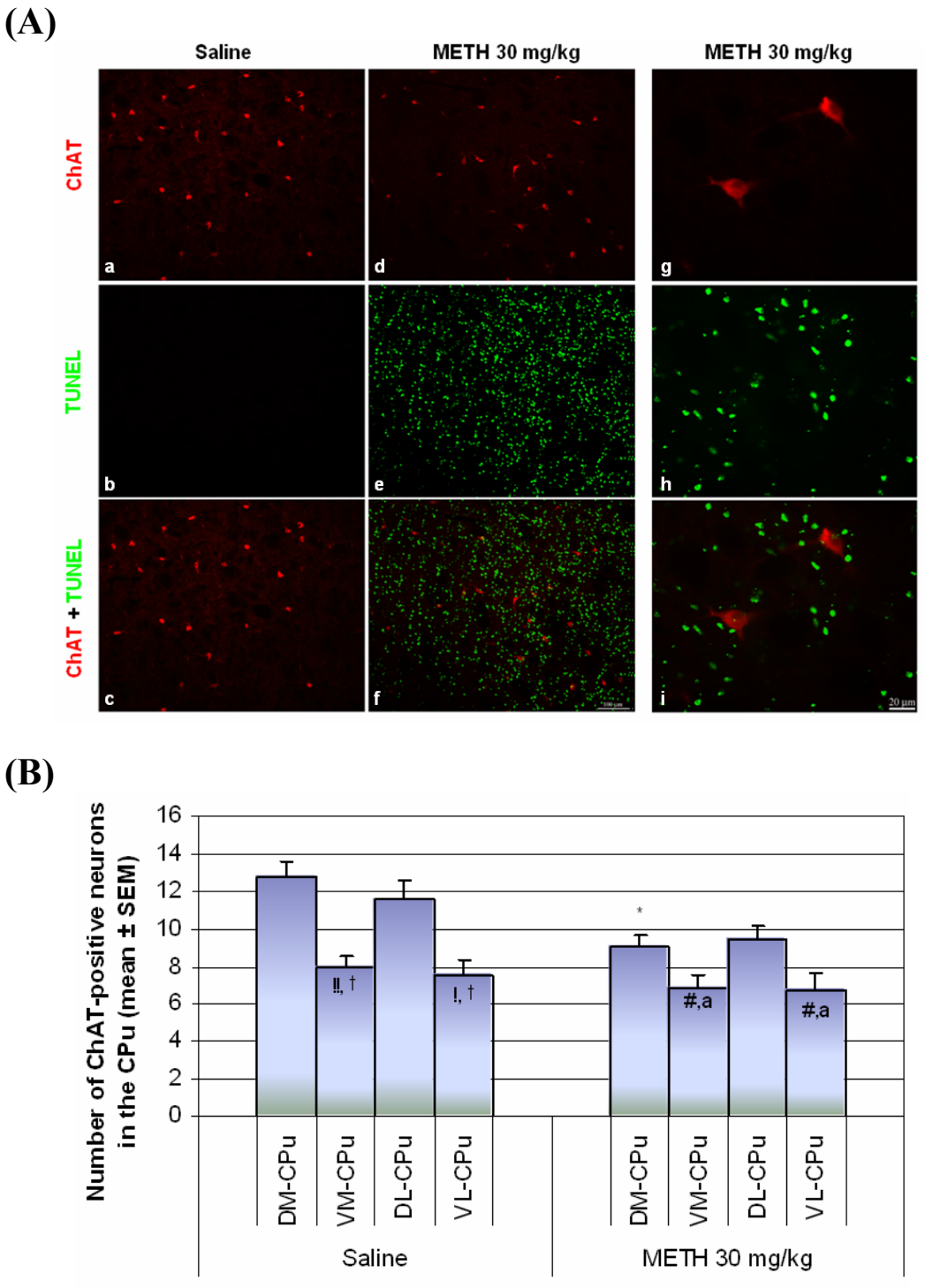

Figure 4-10. Loss of cholinergic interneurons in the striatum after methamphetamine treatment. Animals received a single injection of methamphetamine (METH 30 mg/kg of

body weight, i.p.) and were sacrificed 24 hours later. Striatal tissue sections were processed for immunohistofluorescence and TUNEL. **(A)** Double-labeled epifluorescent micrographs of striatal tissue stained with Cy3-labeled antibodies against choline acetyltransferase (ChAT) and TUNEL with FITC-conjugated dUTP's in control **(a-c)** and METH treated animals **(d-i)**. Bottom panels **(c,f,i)** are overlays of both TUNEL and ChAT staining. Higher magnifications in METH treated animal indicate that the two does not overlap **(g-i)**. Scale bar=100 μm **(a-f)**, 20 μm **(g-i)**. **(B)** Number of ChAT-positive neurons (mean ± SEM) were determined from cell counts in an area of 0.26 mm^2 for each of the four quadrants of the caudate putamen (CPu, dorsal-medial [DM], dorsal-lateral [DL], ventral-medial [VM], and ventral-lateral [VL]) in 8 animals per experimental group. A significant decrease is observed in the DM region of the striatum. * $p< 0.005$ compared to the corresponding regions of saline control. ! $p<0.0001$, † $p<0.005$ compared to the DL region of saline. !! $p<0.0005$ compared to DM region of saline. # $p<0.05$ compared to the DM of METH % $p<0.05$ compared to the DL region of METH.

4.4.5 Somatostatin Interneurons

Antibodies against somatostatin (SST) were used to assess the effect of METH (30 mg/kg, i.p.) on SST interneurons. No colocalization of immunofluorescence between SST and TUNEL-positive neurons was found (Figure 4-11A). Like the cholinergic interneurons, there is no obvious morphological change observable throughout the striatum. Cell counts in the four quadrants of the striatum did not reveal the loss of immunofluorescence for SST compared to controls (Figure 4-11B), suggesting that this population of striatal interneuron is refractory to METH treatment.

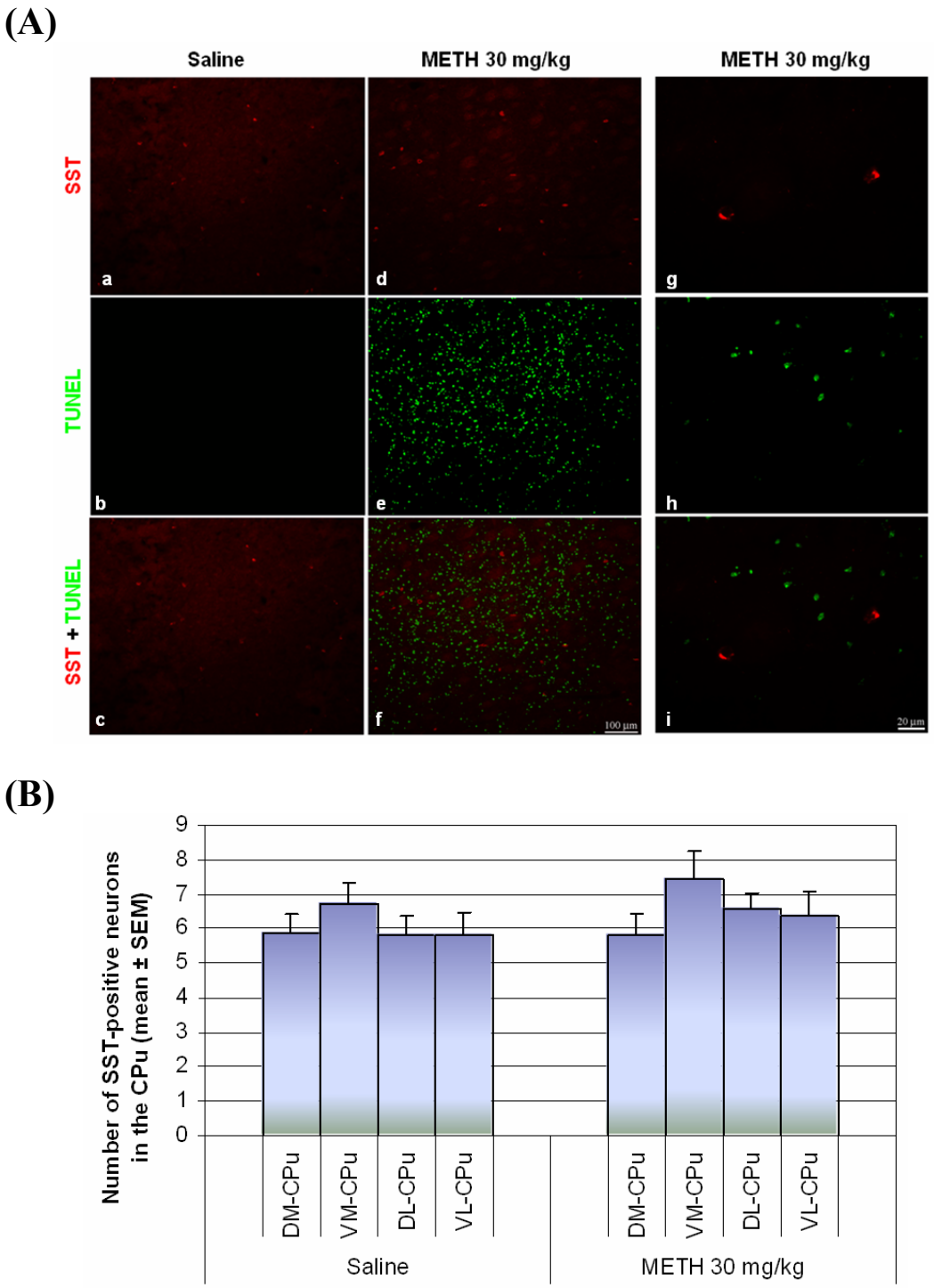

Figure 4-11. Somatostatin interneurons are spared from methamphetamine-induced cell death. Animals received a single injection of methamphetamine (METH 30 mg/kg of body

weight, i.p.) and were sacrificed 24 hours later. Striatal tissue sections were processed for immunohistofluorescence and TUNEL. **(A)** Double-labeled epifluorescent micrographs of striatal tissue stained with Cy3-labeled antibodies against somatostatin (SST) and TUNEL with FITC-conjugated dUTP's in control **(a-c)** and METH treated animals **(d-i)**. Bottom panels **(c,f,i)** are overlays of both TUNEL and SST staining. Higher magnifications in METH treated animal indicated that the two does not overlap **(g-i)**. Scale bar=100 μm **(a-f)**, 20 μm **(g-i)**. **(B)** Number of SST-positive neurons (mean ± SEM) were determined from cell counts in an area of 0.26 mm^2 for each of the four quadrants of the caudate putamen (CPu, dorsal-medial [DM], dorsal-lateral [DL], ventral-medial [VM], and ventral-lateral [VL]) in 8 animals per experimental group. No significance was observed between the two treatment groups or between the regions within the treatment groups.

4.5 Confirming Neuronal Loss

Loss of protein markers like DARPP32, parvalbumin, and ChAT were used to indirectly indicate the loss of these neuronal subtypes in the striatum 24 hours after METH administration. Since loss of these protein markers seen at 24 hours post METH administration may be due to METH-induced transient decreases in protein levels and not to the permanent loss of neurons in the striatum, Nissl staining was employed to assess for neuronal loss in the striatum. Nissl substance is found in nerve cell bodies and consists of rough endoplasmic reticulum and associated ribosomes. METH induced a significant reduction in Nissl-stained neurons in the striatum (Figure 4-12A). Cell counts of positive Nissl stained neurons in the four quadrants of the striatum confirmed this. METH caused decreases of 13-25% Nissl stained neurons compared to controls (Figure 4-12B). This reduction was also found in animals that did not have METH-induced TUNEL (*data not shown*). No significance was found between the four regions of the striatum.

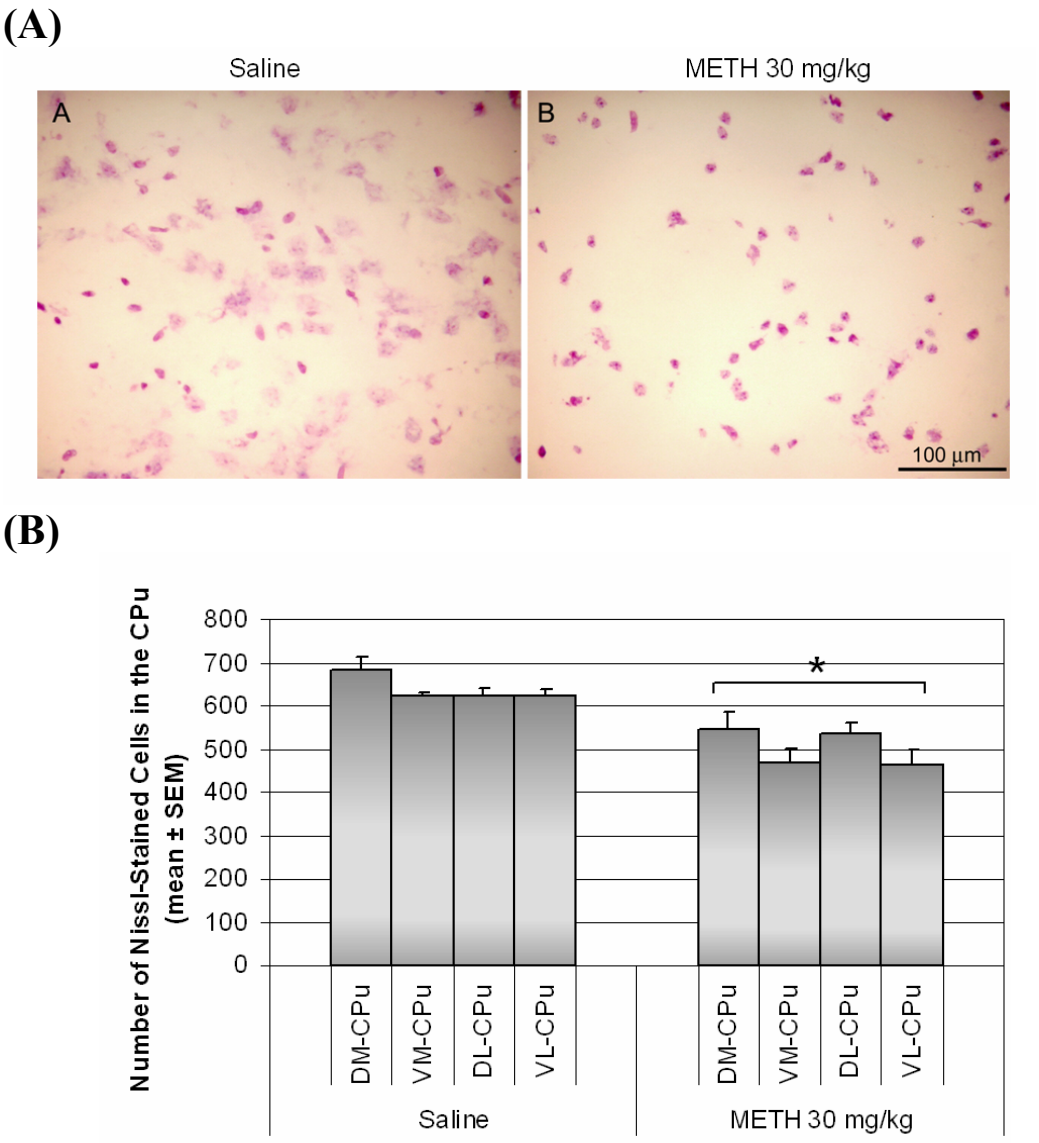

Figure 4-12. Loss of cell density in the striatum after methamphetamine treatment. Mice were treated with a single of methamphetamine (METH 30 mg/kg of body weight, i.p.) injection and sacrificed 24 hours later. Coronal sections of the striatum were stained with cresyl violet. (**Figure 4-12A**) Light micrographs of nissl staining in saline (**A**) and METH 30 mg/kg (**B**) treated animals. Scale bar=100 µm. (**Figure 4-12B**) Nissl-stained cells were counted on 20 µm thick coronal sections of the striatum in an area of 0.26 mm^2 for each of the four quadrants of the caudate-putamen (CPu, dorsal-medial [DM], dorsal-lateral [DL],

ventral-medial [VM], and ventral-lateral [VL]). Results represent the mean ± SEM number of cells counted in 10 animals per experimental group. *P<0.05 compared to controls of each corresponding striatal region. No significance was found between regions.

4.6 Discussion

METH-induced Cell Death: Issues of Paradigm, Dose, and Time

Characterization of METH-induced cell death in the striatum showed that peak levels of apoptosis, as detected by TUNEL, occur 24 hours after a high dose administration of METH (30 mg/kg of body weight, i.p.). The results have also shown that METH-induced apoptosis occured in specific neuronal populations of the striatum. Moreover, these postsynaptic effects occured prior to METH-induced depletion of DA nerve terminal markers of TH and DAT as well as METH-induced astrocytosis.

Both binge (10 mg/kg of body weight x 4 at 2 hour intervals, i.p.) and bolus (30 mg/kg of body weight, i.p.) schedules of METH administration induce striatal apoptosis; however, a single bolus administration is more effective and may be more suitable for studies in animal models that assess acute METH-induced striatal injury at sites postsynaptic to the nigrostriatal DA nerve terminals. The difference between the two paradigms may be in the concentration of METH accumulated in the brain. It is conceivable that the greater magnitude of apoptosis induced by the single high dose administration of METH is due to higher accumulated plasma and brain levels of

METH compared to the 4 x 10 mg/kg at 2 hour intervals schedule of drug administration. This is also evident in the significant elevation in the amount of TUNEL-positive neurons when increasing a single bolus dose from 20 to 30 mg/kg of body weight of METH. This is an important issue that needs to be investigated further. Also, consistent with the literature, a single high dose regiment of METH was shown here to be as effective as the binge schedule of METH in inducing deficits of DA terminal markers and reactive astrocytes in the striatum (Fukumura et al., 1998; Cappon et al., 2000; Yu et al., 2002). This schedule of dosing can simplify pharmacological studies involving METH-induced neural damage as it does not require the multiple dosing of intervening agents as with the binge paradigm. However, it was observed in this study that a single high dose schedule of METH does generate a higher mortality in the animals compared with the binge schedule (*data not shown*).

TUNEL is a late marker of apoptosis. It gives a positive signal after extensive nicks have accumulated on the DNA of apoptotic cells (Gavrieli et al., 1992). In the studies undertaken here, METH-induced TUNEL in the striatum was shown to consistently peak at 24 hours after METH administration; indicating that METH-induced apoptosis in the striatum is an acute event which happens soon after insult from the drug. In addition, Nissl-staining confirmed a 13-25% loss in striatal neurons at the 24 hour time point. This percentage represents neurons that are no longer present in the striatum at this time point and are not detected by TUNEL. Thus, METH-induced TUNEL-positive neurons detected at 24 hours represent a separate

set of neurons that are undergoing the final stages of neuronal cell death in the striatum. This also suggests that METH-induced cell death in the striatum may be a gradual or progressive process that occurs over an undetermined period of time soon after insult from the drug. This speculation may explain the large interanimal variability of TUNEL-positive neurons within a treatment group. It is possible that the interanimal variability observed is due to technical constraints which allowed only the observation of a fixed time point in a gradual apoptotic process; involving a network of multiple types of neurons where the death of one type of neuron may affect the death of another. This is supported by the loss of cell density observed in animals that do not have TUNEL-positive neurons (*data not shown*). Also, interanimal variability is not atypical in METH-induced striatal apoptosis. Although to a lesser degree, variability between animals has been reported for METH-induced depletion of DA terminal markers and METH-induced degenerating Fluoro-Jade B positive striatal cells using a binge of METH 10 mg/kg 4 x at 2-hour intervals (Pu et al., 1994; Yu et al., 2004).

Reports from Cadet et al. have indicated the detection of apoptosis by TUNEL peak at 3 days after the binge or single dose METH treatment (Deng and Cadet, 2000; Jayanthi et al., 2004). It is currently unclear what the reason is for this discrepancy in apoptosis peaks as detected by TUNEL. However, the same group reports early activation of apoptotic cascades. Release of AIF (apoptosis-inducing factor) from the mitochondria happens 30 minutes after METH administration and accumulation of proteolytic fragments of laminin A happens 8 hours after METH treatment (Jayanthi

et al., 2004). Also, upregulation of proapoptotic mitochondrial proteins like bax, bid, bad starts 1-2 hours after treatment and peaks at 16 hours in mice treated with a single high dose of METH (Jayanthi et al., 2001). Similarly, decreases of cytochrome C oxidase staining in rat striatal tissue was detected 2 hours after METH treatment, suggesting that METH-induced disruption of mitochondrial function occurs very soon after the administration of METH (Burrows et al., 2000). The results of METH-induced TUNEL peaking at 24 hours after METH treatment are consistent with an early onset of apoptosis, an event that may later lead to the weakening of the contacts between the dopaminergic terminals and the projection neurons of the striatum.

After examination of the temporal emergence of METH-induced neural damage at striatal nerve terminals and in striatal neurons, it was concluded that striatal deficits of TH, DAT, and induction of increased GFAP expression happens after METH-induced striatal apoptosis. This observation suggests the possibility that depletion of DA terminal markers may be causally associated or enhanced by striatal apoptosis. Loss of striatal neurons must render a significant number of dopaminergic synapses devoid of contacts, inducing the prominent expression of an astrocytic response later.

The increase of extracellular DA induced by METH can lead to the oxidative damage of proteins. In synaptosomal preparations, the auto-oxidation of DA leads to inhibition of DA uptake by the DAT (Berman et al., 1996; Whitehead et al., 2001) and inhibition of glutamate uptake by the glutamate transporter (Berman and Hastings, 1997). Additionally, in the presence of tyrosinase, DA induces the covalent

modification and inactivation of TH (Xu et al., 1998). These harmful effects of DA auto-oxidation may result from the covalent modification of cysteinyl residues of proteins. For example, intrastriatal injection of DA resulted in the accumulation of protein-bound cysteinyl DA 24 hours post-METH injection (Hastings et al., 1996). These findings may account in part for the inhibition of vesicular DA uptake observed *in vitro* soon after exposure to METH (Brown et al., 2000; Brown et al., 2002) and may lead to the instability of the terminals resulting in the loss of DAT and TH observed 24 hours after METH treatment.

METH-induced Cell Death: Issues of Selective Vulnerability and Refractoriness

The results of various histological and cell quantification assessments have now demonstrated that METH can cause toxic effects to specific neuronal subtypes postsynaptic to the dopaminergic nerve terminals in the striatum.

It was determined by double-labeling with TUNEL and NeuN, Nissl staining, and cell quantification experiments that METH induces apoptosis of some striatal neurons. However, immunohistological studies exhibited no colocalization of the selected striatal markers for medium spiny projection neurons (DARPP32) and interneurons (ChAT, SST and parvalbumin) with TUNEL-positive cells. This would initially suggest that these neuronal cells were not undergoing apoptosis. However, decreased numbers in the cell counts of these markers reported here confirm that injury has occurred. This might be interpreted as METH-induced transient down-

regulation of these protein markers and with time, protein expression will return to baseline levels. Yet significant loss of neurons indicated by Nissl staining and cell counts indicated that this interpretation is doubtful. Moreover, loss in the number of neurons assessed by Nissl staining (13-25%) and by protein immunohistochemistry (15-25%) corresponded to each other. Thus, the loss of protein markers can reflect the loss of their corresponding neurons in the striatum. It is believed that these noncolocalizations are due to temporal constraints in the apoptotic process. It is possible that by the time striatal neurons display METH-induced TUNEL-positivity, they will have accumulated extensive nicks in their DNA and their levels of molecular markers have dwindled below the limit of detection by commercial antibodies that were employed. On these premises, it is concluded that METH kills some striatal GABAergic projection neurons. METH also kills some striatal parvalbumin-containing GABA and some cholinergic interneurons in the dorsal regions of the striatum. Interestingly, SST interneurons are spared.

The results reported here are consistent with the pattern of striatal medium spiny neuron vulnerability and selective striatal interneuron robustness seen before in studies of Huntington's disease in humans, in animal models of Huntington's disease using excitotoxins and mitochondrial inhibitors, in ischemic models, and in other manipulations of the DA system (Uemura et al., 1990; Beal et al., 1991; Mitchell et al., 1994; Guyot et al., 1997; Mitchell et al., 1999). In early stages of Huntington's disease, enkephalin-positive neurons that lie in the dorsal-medial caudate nucleus are the most vulnerable (Vonsattel et al., 1985; Ellison et al., 1987), while cholinergic,

parvalbumin-containing GABA and SST interneurons were found to be spared (Ellison et al., 1987; Ferrante et al., 1987; Mitchell et al., 1999). Glutamate analogues such as quinolinic acid and kainic acid have been shown to induce excitotoxic lesions of striatal projection neurons (Beal et al., 1991; Qin et al., 1996) while sparing NADPH- diaphorase/SST/NPY/NOS-containing interneurons (Koh et al., 1986; Koh and Choi, 1988; Beal et al., 1991). Reports from models of ischemia where neuronal death is associated with excitotoxicity also indicate that NADPH-diaphorase/SST/NPY interneurons are spared while medium spiny projection neurons are vulnerable (Uemura et al., 1990). Very recently, a parallel study lent direct support to this study's findings, demonstrating METH-induced death of enkephalin-positive projection neurons and not the death of neuropeptide Y (NPY)/NOS-positive striatal interneurons (Thiriet et al., 2005).

The aberrant release of DA and glutamate in the striatum by METH sets off a complex and coordinated set of events which lead to nerve terminal degeneration and neuronal apoptosis. Augmented release of DA can accumulate in synapse and result in an increase production of free radicals. Excessive release of glutamate results in excitotoxicity via activation of ionotrophic NMDA and AMPA/KA receptors. Mapping studies have indicated that the majority of glutamate receptors are found on medium spiny neurons. These neurons contain the NMDA NR1 and NR2A/2b subunits in the striatum as well as AMPA GluR1, GluR2/3, and GluR4 subunits (Chen and Reiner, 1996; Chen et al., 1996; Chen et al., 1998; Hu et al., 2004; Wang et al., 2004). The NMDA NR1 subunit is also found on all striatal neurons in the

human striatum (Kuppenbender et al., 2000). Amphetamine exposure can increase the phosphorylation of NMDA receptor NR1 subunit on dynorphin-containing projection neurons (Liu et al., 2004). Cholinergic interneurons and half of the GABAergic parvalbumin-containing interneurons express NMDA NR2A/2B R while SST interneurons do not (Landwehrmeyer et al., 1995; Chen and Reiner, 1996; Chen et al., 1996). Receptor subunit composition plays a key role in determining the functional properties of glutamate receptors, including their permeability to calcium and susceptibility to excitotoxic insults. AMPA glutamate receptors that have the GluR2 subunit are more impermeable to Ca^{2+} influx while AMPA glutamate receptors with the subunits GluR1 and GluR4 are more Ca^{2+} permeable (Cicchetti et al., 1999). These data suggest that all striatal neurons have NMDA receptors, but each subpopulation has different subunit compositions that may affect striatal function as well as selective vulnerability.

Activation of the NMDA receptor in the striatum leads to the activation of nitric oxide synthase (NOS) (Szabo, 1996a), which results in the synthesis of the diffusible second messenger nitric oxide (NO), an agent that has been associated with damage of surrounding neurons in the brain (Dawson et al., 1991; Dawson et al., 1994). This would imply that activation of SST interneurons which also contain NOS can contribute to the vulnerability of its neighboring medium spiny projection neurons via NO. The question now remains how this interneuron may be protected against its own intracellular NO production after activation. It has been suggested that the robustness seen in interneurons may be due to the differential localization of free

radical scavengers in different striatal neurons. In the rhesus monkey, striatal interneurons are enriched in copper-zinc-dependent superoxide dismutase (CuZnSOD) and/or manganese superoxide dismutase (MnSOD) (Medina et al., 1996). *In vitro* studies with pheochromocytoma-derived PC12 cell line resistant to NO was also shown to be enriched in MnSOD gene expression (Gonzalez-Zulueta et al., 1998). In rats, MnSOD was also found colocalized to ChAT and SST-containing neurons (Inagaki et al., 1991). In addition, NOS-containing interneurons in the cortex, which were found to be resistant in ischemia, also co-expressed the antioxidative enzymes MnSOD, CuZnSOD, heme oxygenase-2 and cytosolic glutathione peroxidase. This enhanced antioxidant expression was accompanied by a strong perinuclear presence of the antiapoptotic bcl-2 protein (Bidmon et al., 2001). Furthermore, transgenic mice overexpressing the human CuZnSOD showed attenuation to METH-induced cell death and neurotoxicity (Cadet et al., 1994; Deng and Cadet, 2000).

Chapter 5

Involvement of the Neurokinin-1 Receptor in Methamphetamine-induced Cell Death in the Striatum

5.1 Effects of Systemic Receptor Blockade

A pharmacological approach was taken to evaluate the involvement of the neurokinin-1 (NK-1) receptor in methamphetamine (METH)-induced cell death by the use of a highly selective nonpeptide NK-1 receptor antagonist, 17-hydroxy-17-ethynyl-5-androstano[3,2-b]pyrimido[1,2-a]benzimidazole (WIN 51,708) (See figure 5-1).

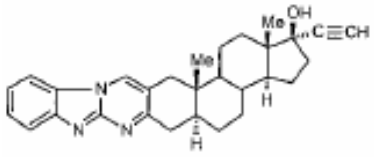

WIN 51,708

Figure 5-1. Structure of nonpeptide NK-1 receptor antagonist, WIN 51,708.

(Quartara and Maggi, 1997; Lazareno et al., 2002)

This antagonist displays high affinity for the rodent NK-1 receptor (Ki=21nM for rat NK-1 receptor) (Quartara and Maggi, 1997; Lazareno et al., 2002) and was shown to protect against METH-induced depletions of dopamine (DA) nerve terminal markers (Yu et al., 2002).

5.1.1 Dose Response

The effects of the high affinity, rodent specific, NK-1 receptor antagonist, WIN 51,708, was tested at various doses to assess its effects on METH-induced cell death in the striatum. Striatal apoptosis is assessed with TUNEL 24 hours after METH (30 mg/kg of body weight, i.p.) administration. WIN 51,708 was administered by intraperitoneal injections at 2.5, 5, 10, 20, or 30 mg/kg of body weight 30 minutes prior to the administration of METH. METH induced 18-22% of TUNEL-positive neurons. Pretreatment with WIN 51,708 offered dose-dependent protection of METH-induced TUNEL-positive neurons up to 10 mg/kg of body weight; the most effective doses being 5 and 10 mg/kg (Figure 5-2A). Prior dosing of the NK-1 receptor antagonist at 2.5, 5, or 10 mg/kg reduced METH-induced TUNEL-positive neurons from 18-22% to 6-12%, 2-5% and 3-5% respectively in the four quadrants of the striatum (Figure 5-2B). These lower doses of the antagonist also reduced the number of animals that had METH-induced TUNEL-positive neurons (Figure 5-2C). Increased doses of WIN 51,708 at 20 or 30 mg/kg of body weight given prior to METH treatment did not attenuate METH's effects. Instead, it began losing its

protective effects on METH-induced apoptosis in a dose dependent manner. Pretreatment with WIN 51,708 at 20 or 30 mg/kg of body weight resulted in 10-16% and 13-25% of TUNEL-positive neurons respectively (Figure 5-2B). It also resulted in an increase number of animals who had METH-induced TUNEL-positive neurons compared to prior treatment with lower doses of the antagonist (Figure 5-2C). Antagonist treatment alone had no effect on TUNEL-positive staining (Figure 5-2A-C).

(A)

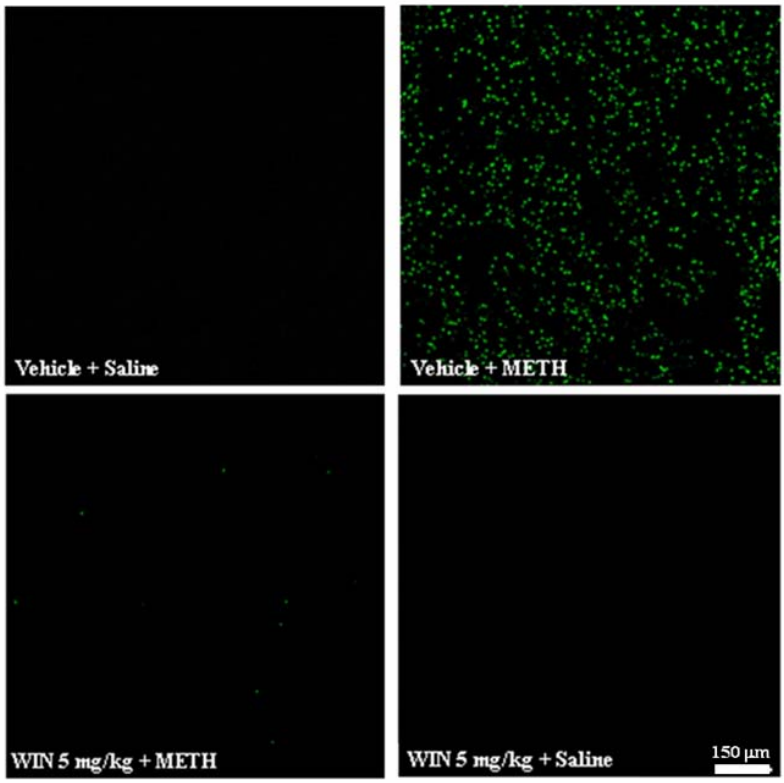

Figure 5-2 continues on next page→

(B)

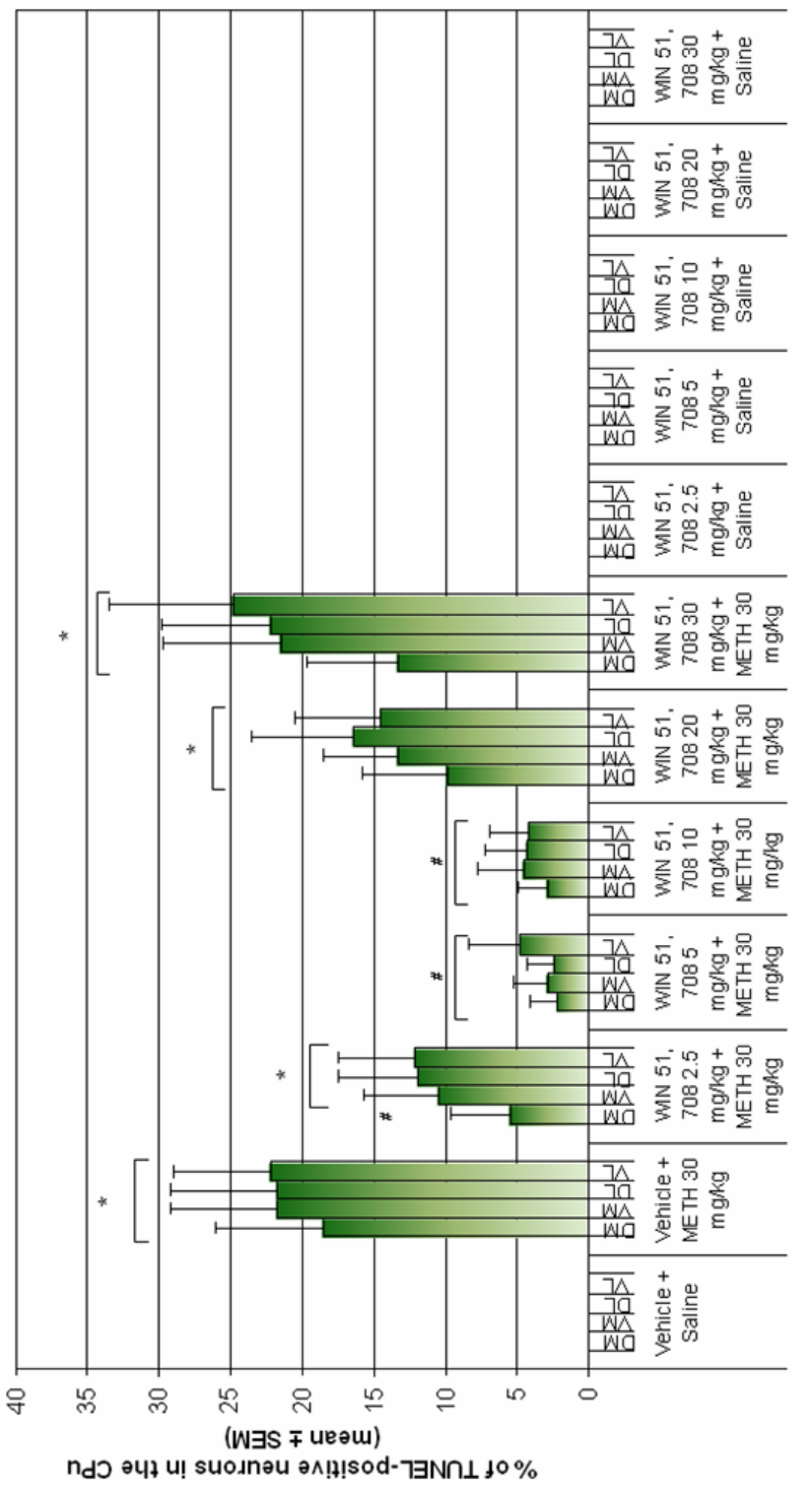

Figure 5-2 continues on next page→

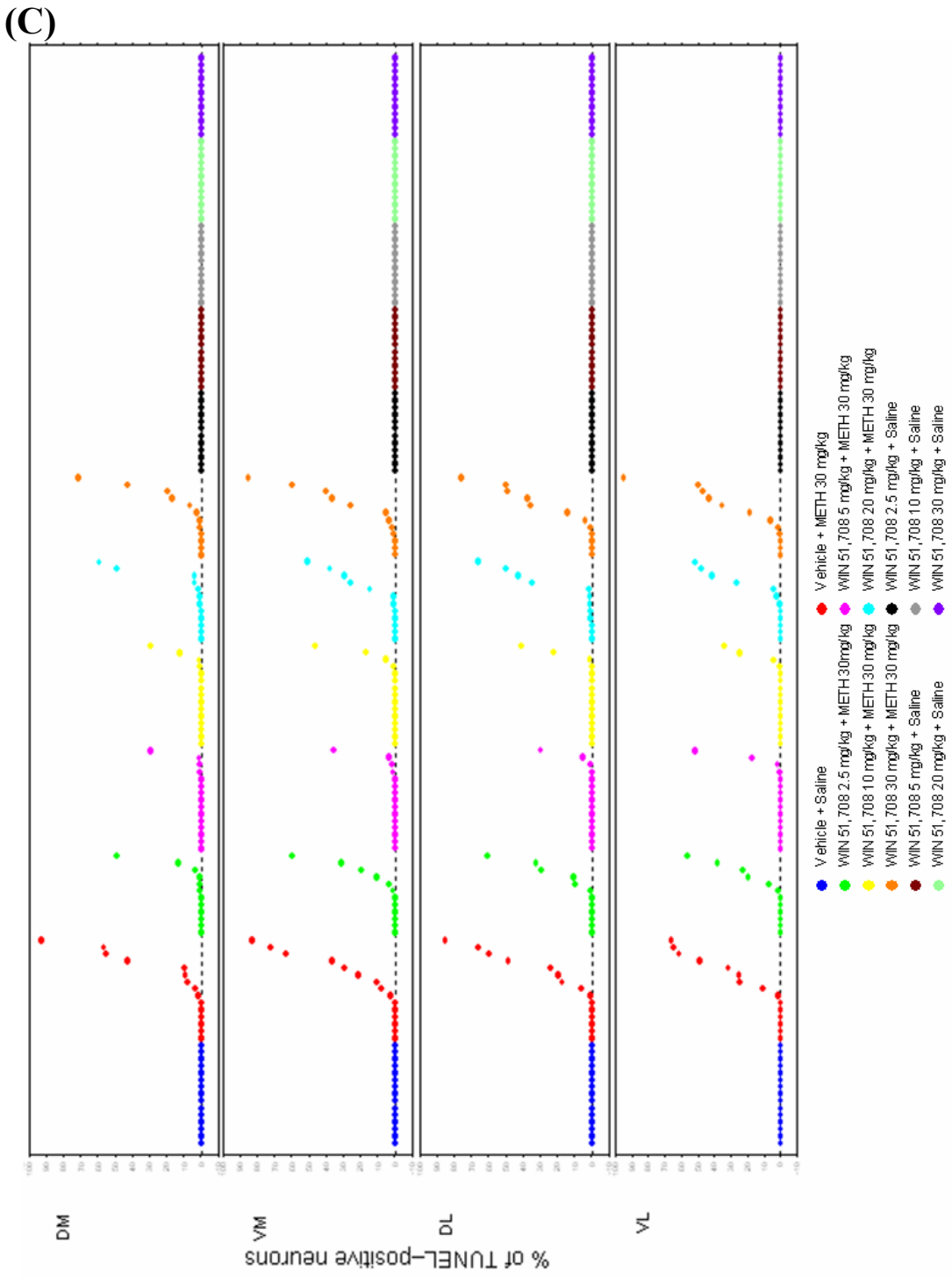

Figure 5-2. Pretreatment with NK-1 receptor antagonist, WIN 51,708, attenuates METH-induced cell death in the adult male ICR mouse striatum. Mice received a single

intraperitoneal (i.p.) injection of the NK-1 receptor antagonist, WIN 51, 708 (2.5, 5, 10, 20 or 30 mg/kg of body weight), 30 minutes prior to METH treatment (30 mg/kg of body weight, i.p.). Cell death is detected on striatal tissue sections by TUNEL 24 hours post METH treatment. **(A)** Confocal micrographs of TUNEL staining in the caudate putamen (CPu). Scale bar = 150µm. **(B)** Percent of TUNEL-positive neurons (mean ± SEM) were determined from cell counts in an area of 0.26mm^2 for each of the four quadrants of the caudate putamen (CPu, dorsal-medial [DM], dorsal-lateral [DL], ventral-medial [VM], and ventral-lateral [VL]). * $p<0.05$ compared to corresponding regions of Vehicle + Saline. # $p<0.05$ compared to corresponding regions of Vehicle + METH 30mg/kg. Antagonist alone did not induce positive TUNEL-labeling. **(C)** Scattergraphs indicate percent of TUNEL-positive neurons for each animal within each treatment group. Each dot represents one animal. ● Vehicle + Saline, ● Vehicle + METH 30 mg/kg, ● WIN 51,708 2.5 mg/kg + METH 30 mg/kg, ● WIN 51,708 5 mg/kg + METH 30 mg/kg, ● WIN 51,708 10 mg/kg + METH 30 mg/kg, ● WIN 51,708 20 mg/kg + METH 30 mg/kg, ● WIN 51,708 30 mg/kg + METH 30 mg/kg, ● WIN 51,708 2.5 mg/kg + Saline, ● WIN 51,708 5 mg/kg + Saline, ● WIN 51,708 10 mg/kg + Saline, ● WIN 51,708 20 mg/kg + Saline, ● WIN 51,708 30 mg/kg + Saline. n=12-15 per experimental group.

5.1.2 Hyperthermia

METH treatment produces hyperthermia in rodents (Sandoval et al., 2000) and in humans (Kalant and Kalant, 1975) which can contribute to and exacerbate its lethal and toxic effects (LaVoie and Hastings, 1999a; Xie et al., 2000). Since some protective pharmacological agents against METH-induced neurotoxicity have been shown to suppress hyperthermia (Albers and Sonsalla, 1995), WIN 51,708's (5 mg/kg of body weight, i.p.) ability to suppress METH-induced elevation of body temperature was assessed. Body core temperature was measured with a mouse rectal probe every hour starting from two hours prior to METH treatment until hyperthermia subsided. Ambient room temperature was also recorded at these times and maintained between 20-22°C. Temperature was taken immediately prior to any treatment.

Core body temperatures elevated from 36.3°C to 39.2°C one hour after a single injection of METH (30 mg/kg of body weight, i.p.). This elevation in body temperature was sustained for four consecutive hours. Concurrent administration of METH and WIN 51,708 failed to prevent METH-induced hyperthermia. In contrast, concurrent administration induced a short transient hypothermic response 6 hours after drug administration. Administration of WIN 51,708 alone had no significant effects on core body temperature. (See Figure 5-3).

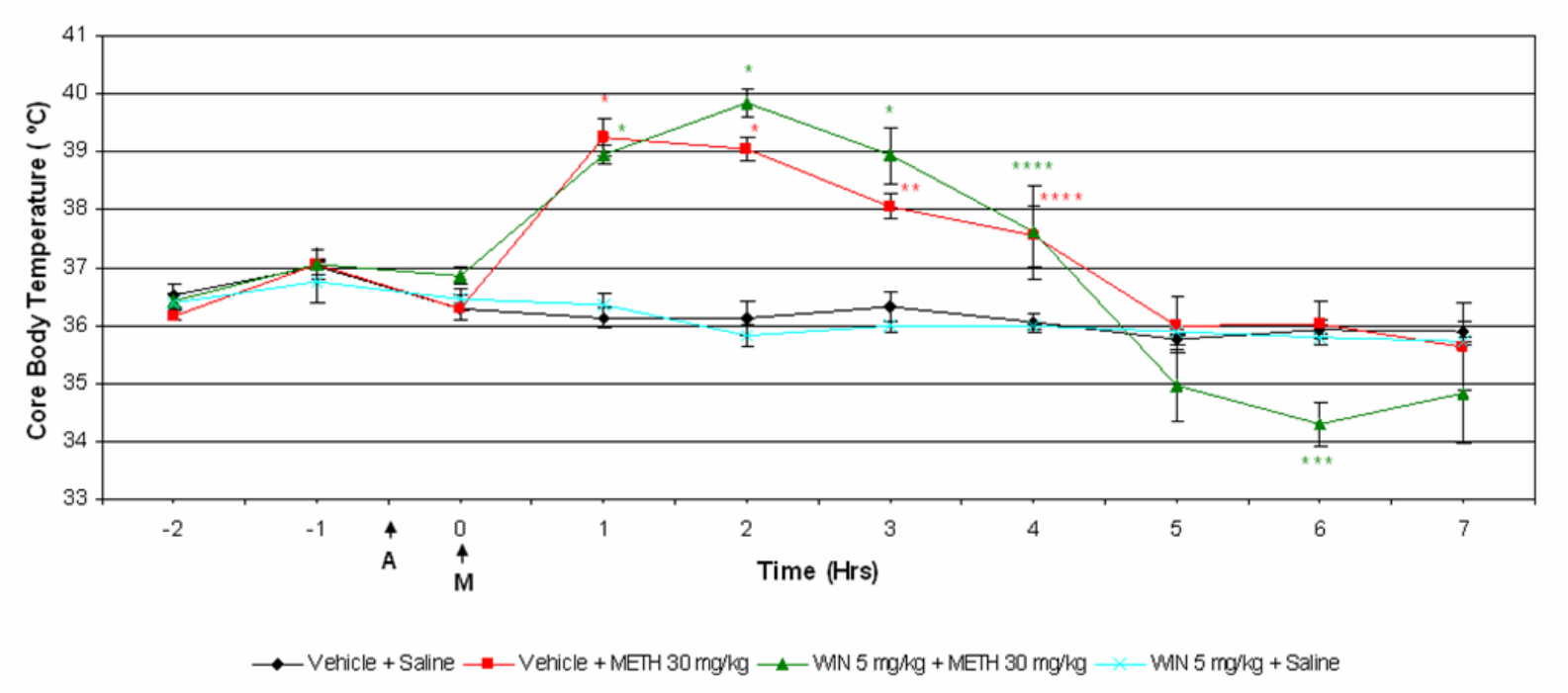

Figure 5-3. Neurokinin-1 receptor antagonist, WIN 51,708, protects against methamphetamine-induced apoptosis without suppression of methamphetamine-induced hyperthermia. Rectal temperature was measured every hour, starting from 2 hrs prior to METH injection (30mg/kg, i.p.). Antagonist (5 mg/kg, i.p.) was given 30 minutes prior to METH treatment. Ambient room temperature was maintained at 20-22 °C. No statistical difference was found in METH-induced elevation of body temperature between animals treated with Vehicle + METH 30 mg/kg and animals treated with WIN 51, 708 5 mg/kg + METH 30 mg/kg. The results are expressed as mean ± SEM of six animals. * $p<0.0001$, ** $p\leq0.0005$, *** $p\leq0.001$, **** $p<0.05$ compared with vehicle + saline controls. A=Antagonist, M=METH

5.1.3 Peroxynitrite

One mechanism by which METH induces neural damage is via the generation of reactive oxygen and nitrogen species such as superoxide (O_2^-) (Cadet and Brannock, 1998), nitric oxide (NO) (Itzhak et al., 2000), and peroxynitrite ($ONOO^-$) (Imam et al., 1999b) from the oxidation of catecholamines and from the activation of endogenous cellular pathways (See Chapter 1.2.5.1). $ONOO^-$ is a potent oxidant formed by the reaction of NO with the O_2^- anion and has been shown to nitrate protein tyrosine residues, causing cellular dysfunctions, DNA damage, and apoptosis (Koppenol et al., 1992; Beckman and Koppenol, 1996). The presence of 3-nitrotyrosine (3NT) on proteins can be used as a marker for $ONOO^-$ formation *in vivo* (Beckman et al., 1994; Beckman and Koppenol, 1996).

Substance P (SP) agonists have been shown to release both DA and glutamate in the striatum (Reid et al., 1990a; Tremblay et al., 1992). Administration of NK-1 antagonists significantly reduce DA release in the striatum (Kraft et al., 2001; Noailles and Angulo, 2002); allowing for less DA to be oxidized in the synapse. Furthermore, since the NK-1 receptor is found on SST interneurons containing nNOS (Li et al., 2001; Li et al., 2002b), it is postulated that signaling through the NK-1 receptor will lead to the activation of NO production. Since suppression of reactive oxygen and nitrogen species have been shown to protect against METH induced damage, and the NK-1 receptor exerts modulatory actions on the dopaminergic and glutamatergic systems where METH acts to generate oxidative stress (See Chapter

1.2.5.1), the NK-1 receptor antagonist was tested to see whether its protection against METH-induced cell death was due, in part, to its ability to suppress the formation of $ONOO^-$.

High performance liquid chromatography (HPLC) was used to assess whether blockade of NK-1 receptor signaling can alter the oxidative stress caused by METH treatment. METH (30mg/kg of body weight, i.p.) administration resulted in significant production of 3-NT in the striatum 24 hours after treatment. Administration of the NK-1 receptor antagonist, WIN 51,708 (5mg/kg of body weight, i.p.) 30 minutes prior to METH administration abrogated METH-induced increases in 3NT. (See Figure 5-4).

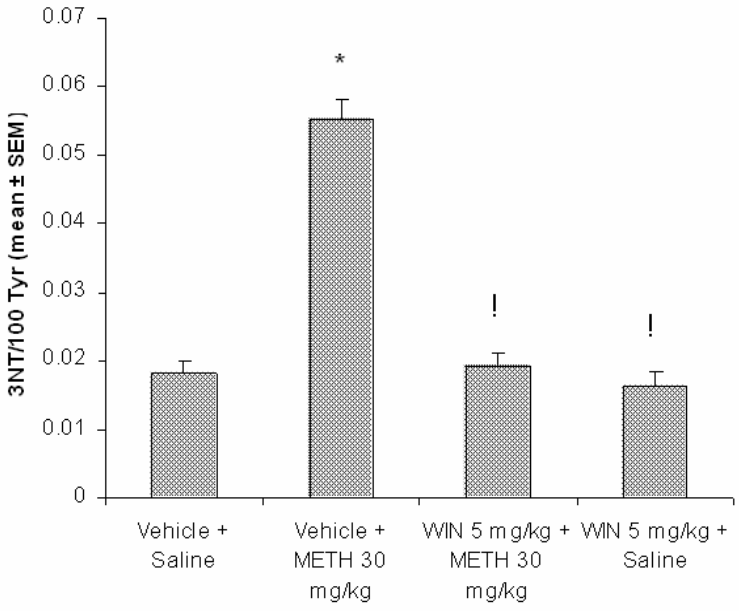

Figure 5-4. Effects of neurokinin-1 receptor antagonist, WIN 51, 708, on 3-nitrotyrosine (3-NT) levels in the adult male ICR mouse striatum. 3NT was detected in the caudate

putamen using electrochemical HPLC 24 hours post-METH (30mg/kg of body weight, i.p.) treatment. Treatment with Vehicle + METH, 30mg/kg caused significant increases in 3-NT as compared to Vehicle + Saline treated animals. Pretreatment with WIN 51,708 (5mg/kg. i.p., 30 minutes prior to METH) reduced METH-induced levels of 3NT to control levels. Antagonist alone had no effect. * $p<0.0001$as compared to Vehicle + Saline controls. ! $p<0.0001$ as compared to Vehicle + METH 30mg/kg. 3-NT values were represented as 3-NT per 100 Tyrosine (Tyr). n=8-10 per experimental group.

5.2 Effects of Local Receptor Ablation

SP and the NK-1 receptor are abundantly found in the mammalian central and peripheral nervous systems. Both have affinities for other peptides and receptors within the tachykinin peptide and receptor family. Thus, systemic administration of receptor antagonists for the NK-1 receptor will have unknown extraneous effects on the monoaminergic and glutamatergic systems that are not within control and will limit the understanding of local actions of the receptor within the striatum. In order to confirm the protection from METH-induced cell death seen in the striatum with systemic application of the NK-1 receptor antagonist, WIN 51,708 and to establish a firm role for the NK-1 receptor in signaling METH-induced cell death within the striatum, a selective NK-1 agonist, [Sar^{9},$Met(O_2)^{11}$]substance P, conjugated to saporin (SSP-SAP) was employed. Intrastriatal microinjections of SSP-SAP selectively removed NK-1 receptor-expressing interneurons within the striatum.

In the striatum, NK-1 receptors are expressed on cholinergic and SST-containing interneurons (Kaneko et al., 1993; Li et al., 2001; Li et al., 2002b). These receptors are internalized upon exposure to METH (Wang et al, unpublished data) through the binding of its ligand SP (Mantyh et al., 1995a; Mantyh et al., 1995b), which is released via a dopamine D1 receptor mechanism (for review see Angulo and McEwen, 1994). Saporin (SAP) is a ribosome inactivating protein from the perennial plant *Saponaria officinalis*. By itself, SAP is not permeable to cell membranes. When conjugated to the NK-1 receptor agonist [Sar^9,$Met(O_2)^{11}$]substance P (SSP-SAP), it can selectively bind NK-1 receptor-expressing cells. Once bound, this receptor-ligand complex gets into the cell via receptor internalization. This allows for selective ablation of NK-1 receptor-expressing cells in the striatum while preserving all other striatal cells (Wiley and Lappi, 1999) and leaving the rest of the basal ganglia circuitry intact.

5.2.1 Establishing the SSP-SAP model

First, the ability of [Sar^9,$Met(O_2)^{11}$]substance P conjugated to a ribosome-inactivating protein, saporin, (SSP-SAP) to effectively ablate the NK-1 receptor-expressing interneurons was determined. Animals were given ipsilateral intrastriatal injections of [Sar^9,$Met(O_2)^{11}$]substance P-saporin (SSP-SAP [4ng, 1 µl volume]) and contralateral intrastriatal injections of saporin (SAP [4ng, 1 µl volume]).

Immunohistochemistry was then used to assess for the presence of NK-1 receptor and the various striatal neurons 3 weeks after microinjections of SSP-SAP into the striatum.

5.2.1.1 Removal of Neurokinin-1 Receptors

Intrastriatal injections of SSP-SAP effectively ablated NK-1 receptors in the striatum (See figure 5-5B) 3 weeks after exposure. SSP-SAP injected into the ipsilateral striatum is devoid of NK-1 receptor staining (See figure 5-5B, d, f) while staining on the SAP-injected contralateral striatum remained intact (See figure 5-5B, c, e). SAP microinjected alone into the striatum had no effect on the levels of NK-1 receptor expression (See figure 5-5A).

5.2.1.2 Selective Ablation of Neurokinin-1 Receptor-expressing Interneurons

Immunostaining for choline acetyltransferase (ChAT), somatostatin (SST), parvalbumin, and dopamine and cyclic adenosine 3',5'-monophosphate-regulated phosphoprotein, 32 kDa (DARPP32) was used to evaluate if SSP-SAP can specifically and effectively ablate only cholinergic and SST interneurons, which express the NK-1 receptor, and not GABAergic interneurons and projection neurons, which do not express the NK-1 receptor. Intrastriatal injections of SSP-SAP

specifically and effectively ablated NK-1 receptor-expressing cholinergic and SST interneurons, since ipsilateral SSP-SAP injections into the striatum caused removal of ChAT (a marker for cholinergic interneurons) and SST immunoreactivity (See figure 5-6; a', b'). Parvalbumin (a marker for GABAergic interneurons) and DARPP32 (a marker for GABAergic projections neurons) immunoreactivity was unaffected by SSP-SAP, indicating that GABAergic interneurons and projection neurons remained intact after microinjections of SSP-SAP into the striatum (See figure 5-6; c-d,c'-d').

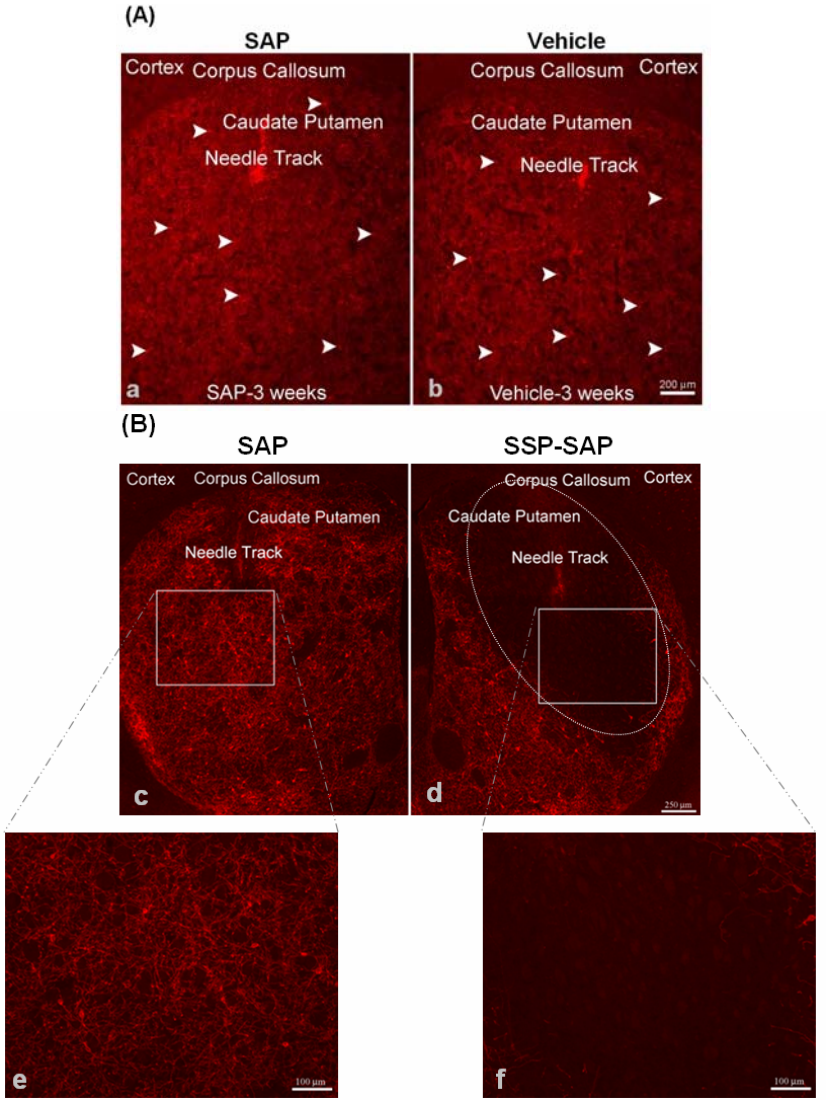

Figure 5-5. Ablation of striatal neurokinin-1 receptor-expressing neurons using [Sar^{9},Met(O$_2$)^{11}]substance P-saporin (SSP-SAP). Animals are intrastriatally injected with [Sar^{9},Met(O$_2$)^{11}]substance P-saporin (SSP-SAP [4ng, 1 µl volume]) (**b,d,f**) or vehicle (1 µl volume) (**b**) and saporin (SAP [4ng, 1 µl volume]) on the contralateral side (**a,c,e**). Three weeks later animals were sacrificed and striatal tissue sections are immunostained with antibodies against the neurokinin-1 (NK-1) receptor. Microinjection of SAP alone does not affect NK-1 receptor immunoreactivity in the striatum (**A**). SSP-SAP effectively removed NK-1 receptors in the striatum (**B; d, f**). High magnification clearly shows NK-1 receptor

immunoreactivity is absent (**e-f**). White dotted circle indicates region lacking NK-1 receptors. White arrows examples of NK-1 receptor staining. Scale bars=100 μm (**e-f**), 200 μm (**a-b**), 250 μm (**c-d**).

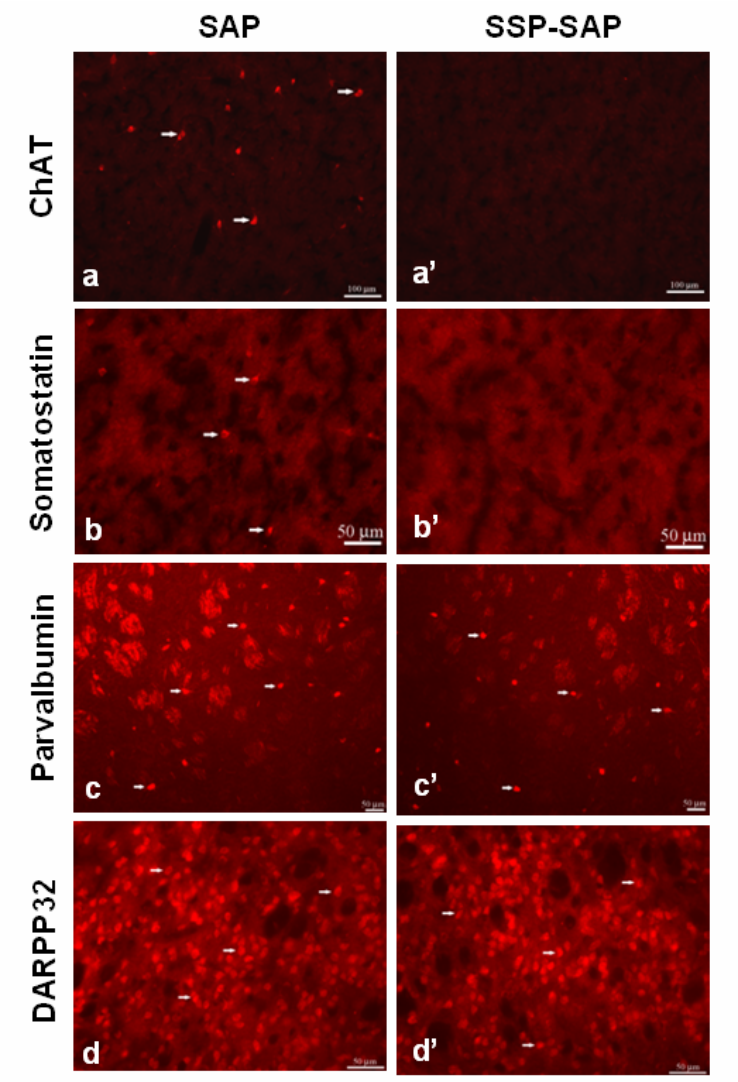

Figure 5-6. [Sar^{9},Met(O$_2$)^{11}]substance P-saporin (SSP-SAP) injections produced cell-specific ablation of striatal cholinergic and somatostatin interneurons in the mouse

striatum. Animals are intrastriatally injected with [Sar^{9},$Met(O_2)^{11}$]substance P-saporin (SSP-SAP [4 ng, 1 µl volume]) (**a'-d'**) and saporin (SAP [4 ng, 1 µl volume]) on the contralateral side (**a-d**). Coronal tissue sections of the striatum were immunostained with antibodies against choline acetyltransferase (ChAT) (**a,a'**), somatostatin (**b,b'**), parvalbumin (**c,c'**), or DARPP32 (**d,d'**) three weeks after microinjections. White arrows point to examples of stained neurons. Intrastriatal injection of SSP-SAP selectively ablates neurokinin-1 receptor expressing cholinergic (**a'**) and somatostatin (**b'**) interneurons while parvalbumin (**c'**) and DARPP32 (**d'**) neurons are unaffected. Intrastrial injection of SAP alone does not affect any of the neuronal population assessed (**a-d**). Scale bars=100 µm (**a,a'**) and 50 µm (**b-d, b'-d'**).

5.2.2 Effects of Local Receptor Ablation

A bolus dose of METH (30mg/kg of body weight, i.p.) was administered to animals 3 week after receiving an ipsilateral intrastriatal microinjection of SSP-SAP. Animals were sacrificed 24 hours later and processed for immunofluorescence of NK-1 receptors and TUNEL. Intrastriatal injections of SSP-SAP effectively ablated NK-1 receptors in the striatum (Figure 5-7; a'). In the absence of NK-1 receptor-immunoreactivity, there was no detectable METH-induced cell death as analyzed by TUNEL (Figure 5-7; b'). In contrast, the contralateral control side where NK-1 receptor immunostaining was unaffected by SAP microinjections (Figure 5-7; a) had considerably more METH-induced apoptosis (Figure 5-7; b).

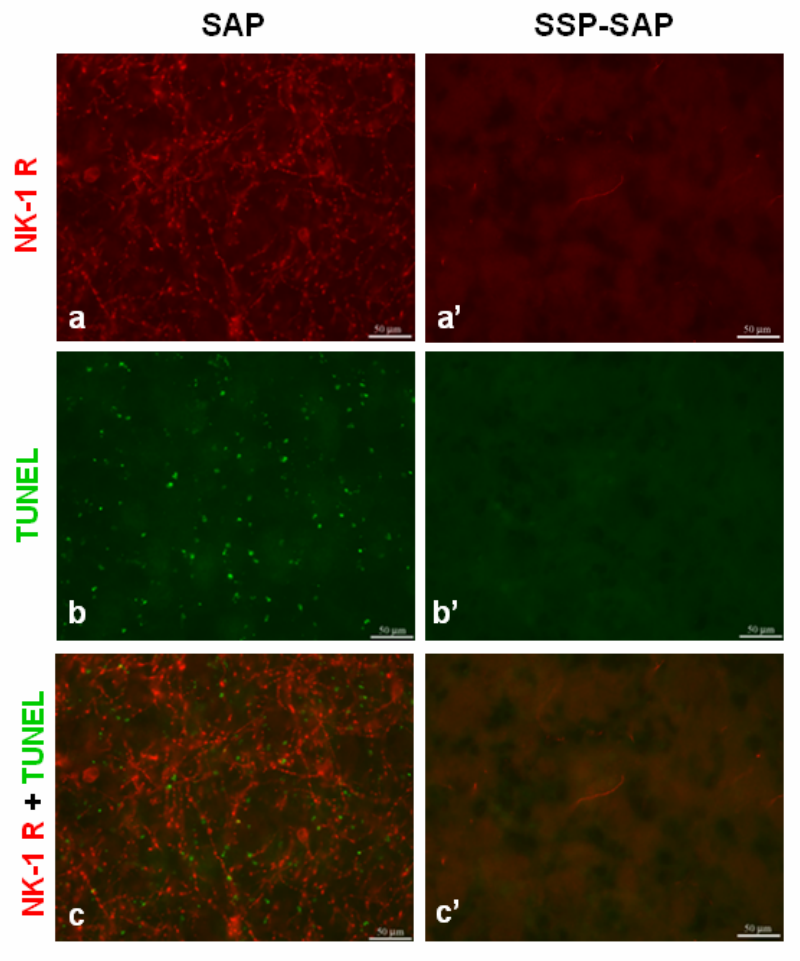

Figure 5-7. Striatal ablation of NK-1 receptor-expressing neurons prevents methamphetamine-induced cell death in the striatum. Animals received intrastriatal injections of [Sar^{9},$Met(O_2)^{11}$]substance P-saporin (SSP-SAP [4 ng, 1 µl volume]) (**a'-c'**) and saporin (SAP [4 ng, 1 µl volume]) on the contralateral side (**a-c**). Three weeks following intrastriatal surgery, animals received a single intraperitoneal injection of METH (30 mg/kg of body weight). The animals are then sacrificed 1 day later METH treatment. Striatal sections were double-labeled with antibodies against NK-1 receptors and TUNEL. Local ablation of striatal NK-1 receptor-expressing striatal interneurons conferred protection from METH-induced cell death on the ipsilateral side (**a'-c'**). No protection was observed on the contralateral side receiving only SAP (**a-c**). Scale bars=50 µm

5.3 Discussion

The results demonstrate that pharmacological blockade of the NK-1 receptor is protective against METH-induced cell death and METH-induced increases of $ONOO^-$ in the striatum. These protective effects are seen without the suppression of METH-induced hyperthermia. Administration of the NK-1 receptor antagonist, WIN 51,708, alone does not affect the levels of METH-induced TUNEL, hyperthermia, or $ONOO^-$. It is therefore unlikely that the protection seen with the antagonist is due to altered regulation of the DA system alone to offset METH's deleterious effects. Also, the protection afforded by the NK-1 receptor antagonist suggests that the receptor is involved in the coordinated METH-induced deleterious mechanisms that lead to neuronal loss in the striatum. In addition, removal of interneurons that express the NK-1 receptors in the striatum protects against METH-induced cell death in the striatum, indicating that the apoptosis of some striatal neurons induced by METH requires the signaling of these interneurons which express NK-1 receptors.

The role of elevated body temperature has been a critical component in METH-induced neural damage. Increases in core body temperature by induced METH correlate directly to the subsequent decreases in striatal dopaminergic markers (Yuan et al., 2005). Elevation in body temperature increases in DAT function (Xie et al., 2000) and may enhance METH-induced neural damage by amplification of a DAT-dependent neurotoxic cascade (Callahan et al., 2001). The enzymatic oxidation of DA is temperature sensitive (LaVoie and Hastings, 1999a). Thus, elevated body

temperature induced by METH could increase the formation of reactive oxidative species (Cubells et al., 1994; Giovanni et al., 1995; Yamamoto and Zhu, 1998). It has been reported that lowering the ambient temperature or administration of pharmacological agents which suppress the hyperthermic response by METH can significantly reduced METH-induced neurotoxicity (Bowyer et al., 1992; Bowyer et al., 1993; Ali et al., 1994; Miller and O'Callaghan, 1994; Imam et al., 1999b). However, the results from this study demonstrated the protection conferred by the NK-1 receptor antagonist, WIN 51,708, is independent of the hyperthermic response induced by METH. This reinforces the current view that METH-induced hyperthermia alone is not sufficient to produce neural damage but may enhance an animal's suspectiblity to neural damage by METH (Ali et al., 1994).

The underlying mechanisms by which the NK-1 receptor mediates METH-induced apoptosis and striatal output are unknown. However, based on accumulating reports from anatomical, functional, and molecular studies of the tachykinin system and striatal degeneration from chemical insults and in neurodegenerative disease, mechanistic implications can be made based on its position in the striatum, its interactions with DA and glutamate, and its influence on the production of reactive free radicals.

Anatomically, SP and the NK-1 receptor are located in the center of the striatal circuit (See figure 1-2); capable of influencing the actions of classical neurotransmitters, such as DA, glutamate, and acetylcholine which are involved in striatal output. Reciprocally, these classical neurotransmitters can influence the

actions of the tachykinin system in the striatum. METH can induce the release of DA and subsequently activate DA receptors. Activation of DA receptors have been shown to significantly increase striatonigral SP-like immunoreactivity and preprotachykinin messenger RNA in the striatum (Li et al., 1987), suggesting that release of DA by METH can trigger the release of SP. Since intranigral injections of SP has been shown to increase striatal DA release (Reid et al., 1990b; Reid et al., 1990a; Reid et al., 1991), release of SP can amplify DA signals from a reciprocal nigrostriatal feed-forward loop via the activation of NK-1 receptors (See figure 1-2). This is supported by several pharmacological studies where NK-1 antagonists attenuated psychostimulant-induced and DA agonist-induced increases in striatal DA release and in motor behavior (Reid et al., 1990b; Kraft et al., 2001; Noailles and Angulo, 2002; Bishop and Walker, 2004; Krolewski et al., 2005).

Additionally, SP can regulate the DA release indirectly via local circuits within the striatum. An *in vivo* microdialysis study showed local application of the NK-1 antagonist, CP-96,345 decreased the elevation of acetylcholine induced by the D1 agonist SKF 38393 (Anderson et al., 1994). This indicates that acetylcholine release is mediated by SP acting on NK-1 receptors located on striatal cholinergic interneurons (Guzman et al., 1993; Kaneko et al., 1993). Acetylcholine can then stimulate the release of DA and glutamate through acetylcholine receptors found on dopaminergic terminals and glutamatergic terminals, respectively (Calabresi et al., 1996; Hamada et al., 2004). Thus, it is speculated that METH-induced DA release can lead to the stimulation of acetylcholine release via the actions of SP and the NK-1

receptor. Acetylcholine release in turn may further activate pathways that potentiate METH's injury to the striatum.

The mechanisms by which DA and DA analogues induce injury in the striatum are complicated by the actions of glutamate. *In vivo* microdialysis studies in rats indicate that glutamate is released following the immediate release of METH-induced DA (Abekawa et al., 1994; Stephans and Yamamoto, 1994). Stimulating the release of glutamate can further activate presynaptic NMDA/AMPA receptors on dopaminergic terminals, further potentiating the release of DA (Glowinski et al., 1988; Hamada et al., 2004). Excessive activation of glutamate receptors by increased levels of glutamate can cause an overload of Ca^{2+} influx through glutamate-gated ion channels which lead to neuronal excitotoxicity and cell death in the brain (Choi, 1988; Beal, 1992a; Nakanishi, 1992). Stimulation of NMDA receptors also leads to the activation of NOS, a Ca^{2+}/calmodulin-dependent enzyme, resulting in NO production and release and ensuing damage of surrounding neurons (Szabo, 1996a). NO can act synergistically with catecholamines to induce single and double stranded DNA breaks (Yoshie and Ohshima, 1997). NO can also oxidize catecholamines to form quinone derivatives, which leads to the generation of O_2^- by the quinone/hydroquinone redox system. O_2^- then reacts rapidly with NO to form the strong $ONOO^-$ oxidant (Yoshie and Ohshima, 1997; Riobo et al., 2002).

It is unclear what underlying mechanisms are involved with the delayed release of glutamate in the striatum. However, there are various lines of evidence that point toward the involvement of SP and the NK-1 receptor signaling in glutamate

transmission. It has been demonstrated that intranigral injection of SP can cause striatal glutamate release (Reid et al., 1990a). In addition, NMDA-evoked glutamate release was found to be dependent on striatal SP and required the activation of the NK-1 receptors (Marti et al., 2005). In the spinal cord, SP increases intracellular Ca^{2+} concentrations (Rusin et al., 1993) and enhances the response of glutamate (Cumberbatch et al., 1995). NK-1 receptor antagonism reduces the infarct size of focal cerebral ischemia (Yu et al., 1997), a condition that induces significant increases in the expression of PPT-A mRNA and NK-1 receptors on glutamatergic cells in the cortex (Stumm et al., 2001). In the hippocampus, drug-induced excitotoxicity has also been associated with the NK-1 receptor. *In vitro* experiments showed SP can increase the release of glutamate from hippocampal slices (Liu et al., 1999a). Also, intracerebroventricular injections of SP fragments can induce a dose-dependent upregulation of the NMDA receptor subunit transcripts in the hippocampus (Zhou et al., 2000). SP also contributes to status epilepticus while NK-1 receptor antagonist reduces kainic acid-induced seizures (Zachrisson et al., 1998; Liu et al., 1999a). Moreover, mice lacking the preprotachykinin-A gene encoding for SP prevents kainite-induced seizures and neuronal death in the hippocampus (Liu et al., 1999b). Thus, SP and the NK-1 receptor may contribute to METH-induced cell death, in part, through its influences on an excitotoxic glutamatergic system.

A common underlying mechanism that mediates METH-induced DA and glutamate damage to striatal neurons is oxidative stress from the production of reactive oxygen-based and nitrogen-based free radicals. DA can generate hydroxyl

(OH^-) radicals and through its enzymatic degradation by monoamine oxidase result in the formation of hydrogen peroxide (H_2O_2) and superoxide (O_2^-) free radicals (Cadet and Brannock, 1998). Glutamate, via activation of glutamate receptors, can also produce reactive oxygen species through its release of arachidonic acid (Dumuis et al., 1988) and generate nitrite oxide (NO) through its activation of nitric oxide synthase (NOS) (Christopherson et al., 1999). NO can react with O_2^- to form peroxynitrate ion ($ONOO^-$). These free radicals can diffuse across cellular membranes to induce lipid peroxidation, DNA strand breaks, cysteine oxidation, as well as tyrosine and tryptophan nitration; all of which are deleterious to the normal function of the neuron. In the striatum, SP-containing medium spiny projection neurons have direct projections onto NOS-containing striatal interneurons where NK-1 receptors are colocalized (Li et al., 2001; Li et al., 2002b). This observation supports the claim that 1) NOS-positive neurons are under the influences of SP and 2) activation of the NK-1 receptor leads to the synthesis and release of NO following METH-induced SP release. In line with this speculation, anatomical evidence in the cortex show reciprocal signaling between SP-containing neurons and neighboring NK-1 receptor-expressing NOS-positive neurons (Vruwink et al., 2001). Thus, activation of the NK-1 receptor by SP may be contributing to the METH-induced convergence and aggravation of oxidative stress signals; stemming from 1) the production of NO by interneurons, NMDA receptor activation and surrounding astroglia, from 2) the oxidation of accumulated DA, and from 3) the generation of $ONOO^-$. Results from this study which demonstrate the abrogation of increased levels of METH-induced

$ONOO^-$ by the NK-1 receptor antagonist (See Chapter 5.1.3 and Figure 5-4) and protection of METH-induced cell death by removal of the NK-1 receptor-expressing interneurons that produce NO supports this speculation (See Chapter 5.2.2 and Figure 5-7).

It is postulated that METH may be inducing damage at dopaminergic terminals and the death of specific neuronal cell types in the striatum through its ability to induce SP release from SP-containing GABAergic projections. Excessive release of SP can activate NK-1 receptors to set in motion convergent signals which produce and release NO from SST/NOS-containing interneurons (See Figure 5-8). METH-induced DA release can cause the subsequent release of SP from axonal collaterals of SP-containing GABAergic projections in the striatum. SP can bind to NK-1 receptors located on SST/NOS-containing interneurons to activate the production and release of NO. In addition, METH-induced DA release can cause the subsequent release of SP from striatonigral SP-containing GABAergic projections in the substantia nigra (SN). SP can bind to NK-1 receptors located in the SN to activate the release of glutamate in the striatum through a thalamocortical loop. Release of glutamate in the striatum can also lead to the production and subsequent release of NO through its activation of NMDA receptors located on SST/NOS-containing interneurons. Glutamate may also further poteniate the release of NO by exacerbating DA release from dopaminergic terminals. NO released from SST/NOS interneurons can interact with oxidizing DA metabolites to aggravate oxidative stress and readily diffuse across membranes to damage surrounding GABAergic projection neurons,

GABAergic interneurons, and cholinergic interneurons in the striatum. SST/NOS-containing interneurons may be protected by its own high levels of NO through its enriched expression of free radical scavengers (See Chapter 4.6 for further discussion).

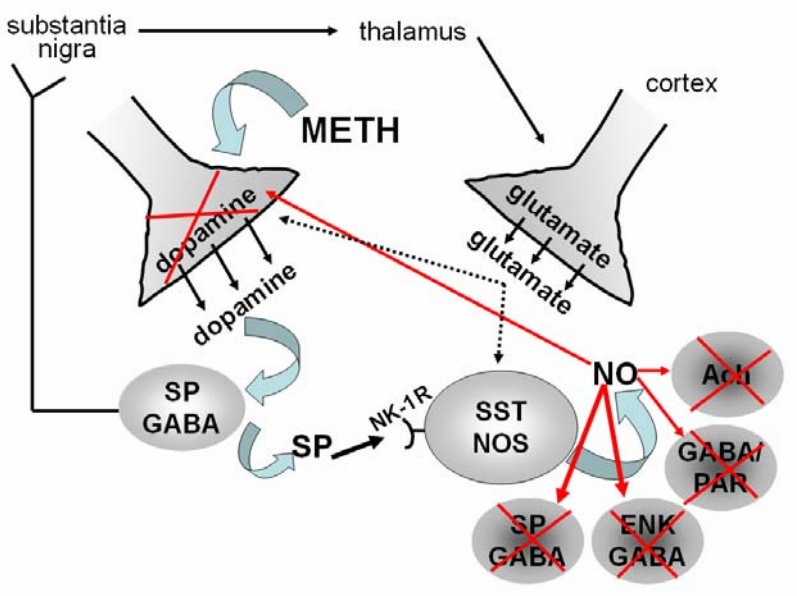

Figure 5-8. Schematic illustration of a postulated model of methamphetamine-induced selective neuronal cell death in the striatum involving the activation of the neurokinin-1 (NK-1) receptor. Augmented release of dopamine (DA) induced by METH stimulates excessive release of substance P (SP) from the axonal collaterals of SP-containing projection neurons of the striatum. This excessive release of SP activates NK-1 receptors on nitric oxide synthase (NOS)-expressing somatostatin (SST) interneurons. Release of nitric oxide (NO) from SST interneurons can damage to dopaminergic terminals and surrounding GABAergic projection neurons, GABAergic interneurons, and cholinergic interneurons. In addition, SP may activate the release of glutamate via a nigral-thalamo-cortical loop. Release of glutamate in the striatum can further cause the release of NO through NMDA receptors and through its potentiation of DA release from dopaminergic nerve terminals.

Chapter 6

Conclusions

There is considerable evidence to demonstrate that methamphetamine (METH) is toxic to the striatum. METH affects monoaminergic nerve terminals, depleting striatal dopamine (DA) levels, tyrosine hydroxylase, and dopamine transporters (Davidson et al., 2001). Contributing to these accumulated findings on the neural damaging effects of METH and on the neuroplasticity of the striatum, the present study has provided direct histological evidence of METH-induced neuronal loss and neuronal apoptosis in select neuronal populations in the striatum. This is an acute event occurring prior to the damage of monoaminergic terminals 24 hours after METH exposure. Specifically, METH causes the death of striatal projection neurons and some GABAergic and cholinergic interneurons. Interneurons containing SST do not degenerate with METH exposure. This pattern of neuronal damage is similar to that seen in the early stages of Huntington's disease when its pathology is largely limited to the loss of striatal projections neurons (Albin et al., 1992; Hedreen and Folstein, 1995). Likewise, METH-induced toxicity at the DA terminals resembles the

lost of striatal DA and progressive degeneration of DA cell bodies in Parkinson's disease. Thus, the actions of METH represent a model of striatal injury which can reflect the dysfunctions seen in these neurodegenerative diseases. The fact that 34 million people use METH emphasizes the importance of clarifying its underlying mechanisms and in order to find neuroprotective interventions.

The underlying mechanisms of the deleterious effects of METH are extremely complex and involve a multifaceted and coordinated set of events which has, for the most part, included the dopaminergic and glutamatergic systems and oxidative stress. Contributing to the research on mechanisms of action by METH and on the role of tachykinins in the basal ganglia, the present study has identified, through pharmacological approaches, the role of NK-1 receptor's contribution to striatal vulnerability. Blockade of the NK-1 receptor as well as removal of interneurons which express the receptor protected against METH-induced cell death. Blockade of the receptor also prevented the generation of METH-induced peroxynitrite free radicals in the striatum. Suppression of hyperthermia was excluded in the interpretation of the NK-1 receptor antagonist's protective effects. These findings offer a new approach to finding therapeutic interventions for drug addictions and for a number of neurodegenerative diseases, including Parkinson's disease and Huntington's chorea. Ultimately, the greater goal of the research undertaken here is to gain further understanding into the role of the tachykinins, particularly SP and the NK-1 receptor, within the basal ganglia circuitry under conditions relevant to the

consumption of METH in our population and its relevance to neurological degenerative diseases.

REFERENCES

(2001) 21 CFR 1308.12. In: Physician's Desk Reference. Montvale, NJ: Medical Economics Co.

Abekawa T, Ohmori T, Koyama T (1994) Effects of repeated administration of a high dose of methamphetamine on dopamine and glutamate release in rat striatum and nucleus accumbens. Brain Res 643:276-281.

Albers DS, Sonsalla PK (1995) Methamphetamine-induced hyperthermia and dopaminergic neurotoxicity in mice: pharmacological profile of protective and nonprotective agents. J Pharmacol Exp Ther 275:1104-1114.

Albertson TE, Derlet RW, Van Hoozen BE (1999) Methamphetamine and the expanding complications of amphetamines. West J Med 170:214-219.

Albin RL, Reiner A, Anderson KD, Penney JB, Young AB (1990) Striatal and nigral neuron subpopulations in rigid Huntington's disease: implications for the functional anatomy of chorea and rigidity-akinesia. Ann Neurol 27:357-365.

Albin RL, Reiner A, Anderson KD, Dure LSt, Handelin B, Balfour R, Whetsell WO, Jr., Penney JB, Young AB (1992) Preferential loss of striato-external pallidal projection neurons in presymptomatic Huntington's disease. Ann Neurol 31:425-430.

Alexander GE, DeLong MR, Strick PL (1986) Parallel organization of functionally segregated circuits linking basal ganglia and cortex. Annu Rev Neurosci 9:357-381.

Ali SF, Imam SZ, Itzhak Y (2005) Role of Peroxynitrite in Methamphetamine-Induced Dopaminergic Neurodegeneration and Neuroprotection by Antioxidants and Selective NOS Inhibitors. Ann N Y Acad Sci 1053:97-98.

Ali SF, Martin JL, Black MD, Itzhak Y (1999) Neuroprotective role of melatonin in methamphetamine- and 1-methyl-4-phenyl-1,2,3,6-tetrahydropyridine-induced dopaminergic neurotoxicity. Ann N Y Acad Sci 890:119.

Ali SF, Newport GD, Holson RR, Slikker W, Jr., Bowyer JF (1994) Low environmental temperatures or pharmacologic agents that produce hypothermia decrease methamphetamine neurotoxicity in mice. Brain Res 658:33-38.

Anderson JJ, Kuo S, Chase TN, Engber TM (1994) Dopamine D1 receptor-stimulated release of acetylcholine in rat striatum is mediated indirectly by activation of striatal neurokinin1 receptors. J Pharmacol Exp Ther 269:1144-1151.

Anglin MD, Burke C, Perrochet B, Stamper E, Dawud-Noursi S (2000) History of the methamphetamine problem. J Psychoactive Drugs 32:137-141.

Angulo JA, McEwen BS (1994) Molecular aspects of neuropeptide regulation and function in the corpus striatum and nucleus accumbens. Brain Res Brain Res Rev 19:1-28.

Aosaki T, Kawaguchi Y (1996) Actions of substance P on rat neostriatal neurons in vitro. J Neurosci 16:5141-5153.

Araneda R, Bustos G (1989) Modulation of dendritic release of dopamine by N-methyl-D-aspartate receptors in rat substantia nigra. J Neurochem 52:962-970.

Arundine M, Tymianski M (2004) Molecular mechanisms of glutamate-dependent neurodegeneration in ischemia and traumatic brain injury. Cell Mol Life Sci 61:657-668.

Axt KJ, Molliver ME (1991) Immunocytochemical evidence for methamphetamine-induced serotonergic axon loss in the rat brain. Synapse 9:302-313.

Bannon MJ, Elliott PJ, Bunney EB (1987) Striatal tachykinin biosynthesis: regulation of mRNA and peptide levels by dopamine agonists and antagonists. Brain Res 427:31-37.

Baruch P, Artaud F, Godeheu G, Barbeito L, Glowinski J, Cheramy A (1988) Substance P and neurokinin A regulate by different mechanisms dopamine release from dendrites and nerve terminals of the nigrostriatal dopaminergic neurons. Neuroscience 25:889-898.

Beal MF (1992a) Mechanisms of excitotoxicity in neurologic diseases. Faseb J 6:3338-3344.

Beal MF (1992b) Role of excitotoxicity in human neurological disease. Curr Opin Neurobiol 2:657-662.

Beal MF, Ferrante RJ, Swartz KJ, Kowall NW (1991) Chronic quinolinic acid lesions in rats closely resemble Huntington's disease. J Neurosci 11:1649-1659.

Beal MF, Kowall NW, Ellison DW, Mazurek MF, Swartz KJ, Martin JB (1986) Replication of the neurochemical characteristics of Huntington's disease by quinolinic acid. Nature 321:168-171.

Beckman JS, Koppenol WH (1996) Nitric oxide, superoxide, and peroxynitrite: the good, the bad, and ugly. Am J Physiol 271:C1424-1437.

Beckman JS, Chen J, Ischiropoulos H, Crow JP (1994) Oxidative chemistry of peroxynitrite. Methods Enzymol 233:229-240.

Berman SB, Hastings TG (1997) Inhibition of glutamate transport in synaptosomes by dopamine oxidation and reactive oxygen species. J Neurochem 69:1185-1195.

Berman SB, Hastings TG (1999) Dopamine oxidation alters mitochondrial respiration and induces permeability transition in brain mitochondria: implications for Parkinson's disease. J Neurochem 73:1127-1137.

Berman SB, Zigmond MJ, Hastings TG (1996) Modification of dopamine transporter function: effect of reactive oxygen species and dopamine. J Neurochem 67:593-600.

Bidmon HJ, Emde B, Kowalski T, Schmitt M, Mayer B, Kato K, Asayama K, Witte OW, Zilles K (2001) Nitric oxide synthase-I containing cortical interneurons co-express antioxidative enzymes and anti-apoptotic Bcl-2 following focal ischemia: evidence for direct and indirect mechanisms towards their resistance to neuropathology. J Chem Neuroanat 22:167-184.

Bishop C, Walker PD (2004) Intranigral antagonism of neurokinin 1 and 3 receptors reduces intrastriatal dopamine D1 receptor-stimulated locomotion in the rat. Brain Res 1023:126-133.

Bolam JP, Ingham CA, Izzo PN, Levey AI, Rye DB, Smith AD, Wainer BH (1986) Substance P-containing terminals in synaptic contact with cholinergic neurons in the neostriatum and basal forebrain: a double immunocytochemical study in the rat. Brain Res 397:279-289.

Bolanos JP, Almeida A, Stewart V, Peuchen S, Land JM, Clark JB, Heales SJ (1997) Nitric oxide-mediated mitochondrial damage in the brain: mechanisms and implications for neurodegenerative diseases. J Neurochem 68:2227-2240.

Bowyer JF, Tank AW, Newport GD, Slikker W, Jr., Ali SF, Holson RR (1992) The influence of environmental temperature on the transient effects of methamphetamine on dopamine levels and dopamine release in rat striatum. J Pharmacol Exp Ther 260:817-824.

Bowyer JF, Gough B, Slikker W, Jr., Lipe GW, Newport GD, Holson RR (1993) Effects of a cold environment or age on methamphetamine-induced dopamine release in the caudate putamen of female rats. Pharmacol Biochem Behav 44:87-98.

Bowyer JF, Davies DL, Schmued L, Broening HW, Newport GD, Slikker W, Jr., Holson RR (1994) Further studies of the role of hyperthermia in methamphetamine neurotoxicity. J Pharmacol Exp Ther 268:1571-1580.

Brookes PS, Bolanos JP, Heales SJ (1999) The assumption that nitric oxide inhibits mitochondrial ATP synthesis is correct. FEBS Lett 446:261-263.

Brown JM, Hanson GR, Fleckenstein AE (2000) Methamphetamine rapidly decreases vesicular dopamine uptake. J Neurochem 74:2221-2223.

Brown JM, Riddle EL, Sandoval V, Weston RK, Hanson JE, Crosby MJ, Ugarte YV, Gibb JW, Hanson GR, Fleckenstein AE (2002) A single methamphetamine administration rapidly decreases vesicular dopamine uptake. J Pharmacol Exp Ther 302:497-501.

Burrows KB, Gudelsky G, Yamamoto BK (2000) Rapid and transient inhibition of mitochondrial function following methamphetamine or 3,4-methylenedioxymethamphetamine administration. Eur J Pharmacol 398:11-18.

Cadet JL, Brannock C (1998) Free radicals and the pathobiology of brain dopamine systems. Neurochem Int 32:117-131.

Cadet JL, Ordonez SV, Ordonez JV (1997) Methamphetamine induces apoptosis in immortalized neural cells: protection by the proto-oncogene, bcl-2. Synapse 25:176-184.

Cadet JL, Jayanthi S, Deng X (2003) Speed kills: cellular and molecular bases of methamphetamine-induced nerve terminal degeneration and neuronal apoptosis. Faseb J 17:1775-1788.

Cadet JL, Sheng P, Ali S, Rothman R, Carlson E, Epstein C (1994) Attenuation of methamphetamine-induced neurotoxicity in copper/zinc superoxide dismutase transgenic mice. J Neurochem 62:380-383.

Calabresi P, De Murtas M, Bernardi G (1997a) The neostriatum beyond the motor function: experimental and clinical evidence. Neuroscience 78:39-60.

Calabresi P, Pisani A, Mercuri NB, Bernardi G (1996) The corticostriatal projection: from synaptic plasticity to dysfunctions of the basal ganglia. Trends Neurosci 19:19-24.

Calabresi P, Pisani A, Centonze D, Bernardi G (1997b) Synaptic plasticity and physiological interactions between dopamine and glutamate in the striatum. Neurosci Biobehav Rev 21:519-523.

Callahan BT, Cord BJ, Yuan J, McCann UD, Ricaurte GA (2001) Inhibitors of Na(+)/H(+) and Na(+)/Ca(2+) exchange potentiate methamphetamine-induced dopamine neurotoxicity: possible role of ionic dysregulation in methamphetamine neurotoxicity. J Neurochem 77:1348-1362.

Cappon GD, Pu C, Vorhees CV (2000) Time-course of methamphetamine-induced neurotoxicity in rat caudate-putamen after single-dose treatment. Brain Res 863:106-111.

Carlsson M, Carlsson A (1990) Interactions between glutamatergic and monoaminergic systems within the basal ganglia--implications for schizophrenia and Parkinson's disease. Trends Neurosci 13:272-276.

Centonze D, Gubellini P, Bernardi G, Calabresi P (1999) Permissive role of interneurons in corticostriatal synaptic plasticity. Brain Res Brain Res Rev 31:1-5.

CEWG (2005) Epidemiologic Trends in Drug Abuse-Advance Report. In: Community Epidemiology Work Group.

Chapman DE, Hanson GR, Kesner RP, Keefe KA (2001) Long-term changes in basal ganglia function after a neurotoxic regimen of methamphetamine. J Pharmacol Exp Ther 296:520-527.

Chen Q, Reiner A (1996) Cellular distribution of the NMDA receptor NR2A/2B subunits in the rat striatum. Brain Res 743:346-352.

Chen Q, Veenman CL, Reiner A (1996) Cellular expression of ionotropic glutamate receptor subunits on specific striatal neuron types and its implication for striatal vulnerability in glutamate receptor-mediated excitotoxicity. Neuroscience 73:715-731.

Chen Q, Veenman L, Knopp K, Yan Z, Medina L, Song WJ, Surmeier DJ, Reiner A (1998) Evidence for the preferential localization of glutamate receptor-1 subunits of AMPA receptors to the dendritic spines of medium spiny neurons in rat striatum. Neuroscience 83:749-761.

Cho AK, Melega WP, Kuczenski R, Segal DS (2001) Relevance of pharmacokinetic parameters in animal models of methamphetamine abuse. Synapse 39:161-166.

Choi DW (1988) Calcium-mediated neurotoxicity: relationship to specific channel types and role in ischemic damage. Trends Neurosci 11:465-469.

Christopherson KS, Hillier BJ, Lim WA, Bredt DS (1999) PSD-95 assembles a ternary complex with the N-methyl-D-aspartic acid receptor and a bivalent neuronal NO synthase PDZ domain. J Biol Chem 274:27467-27473.

Cicchetti F, Gould PV, Parent A (1996) Sparing of striatal neurons coexpressing calretinin and substance P (NK1) receptor in Huntington's disease. Brain Res 730:232-237.

Cicchetti F, Vinet J, Beach TG, Parent A (1999) Differential expression of alpha-amino-3-hydroxy-5-methyl-4-isoxazolepropionate receptor subunits by calretinin-immunoreactive neurons in the human striatum. Neuroscience 93:89-97.

Cook CE, Jeffcoat AR, Sadler BM, Hill JM, Voyksner RD, Pugh DE, White WR, Perez-Reyes M (1992) Pharmacokinetics of oral methamphetamine and effects of repeated daily dosing in humans. Drug Metab Dispos 20:856-862.

Cook CE, Jeffcoat AR, Hill JM, Pugh DE, Patetta PK, Sadler BM, White WR, Perez-Reyes M (1993) Pharmacokinetics of methamphetamine self-administered to human subjects by smoking S-(+)-methamphetamine hydrochloride. Drug Metab Dispos 21:717-723.

Cubells JF, Rayport S, Rajendran G, Sulzer D (1994) Methamphetamine neurotoxicity involves vacuolation of endocytic organelles and dopamine-dependent intracellular oxidative stress. J Neurosci 14:2260-2271.

Cumberbatch MJ, Chizh BA, Headley PM (1995) Modulation of excitatory amino acid responses by tachykinins and selective tachykinin receptor agonists in the rat spinal cord. Br J Pharmacol 115:1005-1012.

Davidson C, Gow AJ, Lee TH, Ellinwood EH (2001) Methamphetamine neurotoxicity: necrotic and apoptotic mechanisms and relevance to human abuse and treatment. Brain Res Brain Res Rev 36:1-22.

Dawson TM, Zhang J, Dawson VL, Snyder SH (1994) Nitric oxide: cellular regulation and neuronal injury. Prog Brain Res 103:365-369.

Dawson VL, Dawson TM, London ED, Bredt DS, Snyder SH (1991) Nitric oxide mediates glutamate neurotoxicity in primary cortical cultures. Proc Natl Acad Sci U S A 88:6368-6371.

DEA (2005) Drug Trafficking in the United States. Methamphetamine Section. In: United States Drug Enforcement Administration.

DeLong MR, Alexander GE, Georgopoulos AP, Crutcher MD, Mitchell SJ, Richardson RT (1984) Role of basal ganglia in limb movements. Hum Neurobiol 2:235-244.

Deng X, Cadet JL (1999) Methamphetamine administration causes overexpression of nNOS in the mouse striatum. Brain Res 851:254-257.

Deng X, Cadet JL (2000) Methamphetamine-induced apoptosis is attenuated in the striata of copper-zinc superoxide dismutase transgenic mice. Brain Res Mol Brain Res 83:121-124.

Deng X, Wang Y, Chou J, Cadet JL (2001) Methamphetamine causes widespread apoptosis in the mouse brain: evidence from using an improved TUNEL histochemical method. Brain Res Mol Brain Res 93:64-69.

Deng YP, Albin RL, Penney JB, Young AB, Anderson KD, Reiner A (2004) Differential loss of striatal projection systems in Huntington's disease: a quantitative immunohistochemical study. J Chem Neuroanat 27:143-164.

Denninger JW, Marletta MA (1999) Guanylate cyclase and the .NO/cGMP signaling pathway. Biochim Biophys Acta 1411:334-350.

Dumuis A, Sebben M, Haynes L, Pin JP, Bockaert J (1988) NMDA receptors activate the arachidonic acid cascade system in striatal neurons. Nature 336:68-70.

Eisch AJ, Marshall JF (1998) Methamphetamine neurotoxicity: dissociation of striatal dopamine terminal damage from parietal cortical cell body injury. Synapse 30:433-445.

Eisch AJ, Schmued LC, Marshall JF (1998) Characterizing cortical neuron injury with Fluoro-Jade labeling after a neurotoxic regimen of methamphetamine. Synapse 30:329-333.

El Daly E, Chefer V, Sandill S, Shippenberg TS (2000) Modulation of the neurotoxic effects of methamphetamine by the selective kappa-opioid receptor agonist U69593. J Neurochem 74:1553-1562.

Ellinwood EH, Jr., Kilbey MM (1980) Fundamental mechanisms underlying altered behavior following chronic administration of psychomotor stimulants. Biol Psychiatry 15:749-757.

Ellison DW, Beal MF, Mazurek MF, Malloy JR, Bird ED, Martin JB (1987) Amino acid neurotransmitter abnormalities in Huntington's disease and the quinolinic acid animal model of Huntington's disease. Brain 110 (Pt 6):1657-1673.

Ellison G, Eison MS, Huberman HS, Daniel F (1978) Long-term changes in dopaminergic innervation of caudate nucleus after continuous amphetamine administration. Science 201:276-278.

Emonson DL, Vanderbeek RD (1995) The use of amphetamines in U.S. Air Force tactical operations during Desert Shield and Storm. Aviat Space Environ Med 66:260-263.

Ernst T, Chang L, Leonido-Yee M, Speck O (2000) Evidence for long-term neurotoxicity associated with methamphetamine abuse: A 1H MRS study. Neurology 54:1344-1349.

Ferrante RJ, Beal MF, Kowall NW, Richardson EP, Jr., Martin JB (1987) Sparing of acetylcholinesterase-containing striatal neurons in Huntington's disease. Brain Res 411:162-166.

Ferrante RJ, Kowall NW, Beal MF, Richardson EP, Jr., Bird ED, Martin JB (1985) Selective sparing of a class of striatal neurons in Huntington's disease. Science 230:561-563.

Fischer JF, Cho AK (1979) Chemical release of dopamine from striatal homogenates: evidence for an exchange diffusion model. J Pharmacol Exp Ther 208:203-209.

Franklin KBJ, Paxinos G (1997) The Mouse Brain in Stereotaxic Coordinates. New York: Academic Press.

Frost DO, Cadet JL (2000) Effects of methamphetamine-induced neurotoxicity on the development of neural circuitry: a hypothesis. Brain Res Brain Res Rev 34:103-118.

Fukui K, Nakajima T, Kariyama H, Kashiba A, Kato N, Tohyama I, Kimura H (1989) Selective reduction of serotonin immunoreactivity in some forebrain regions of rats induced by acute methamphetamine treatment; quantitative morphometric analysis by serotonin immunocytochemistry. Brain Res 482:198-203.

Fukumura M, Cappon GD, Pu C, Broening HW, Vorhees CV (1998) A single dose model of methamphetamine-induced neurotoxicity in rats: effects on neostriatal monoamines and glial fibrillary acidic protein. Brain Res 806:1-7.

Gavrieli Y, Sherman Y, Ben-Sasson SA (1992) Identification of programmed cell death in situ via specific labeling of nuclear DNA fragmentation. J Cell Biol 119:493-501.

Gerfen CR (1992) The neostriatal mosaic: multiple levels of compartmental organization in the basal ganglia. Annu Rev Neurosci 15:285-320.

Giovanni A, Liang LP, Hastings TG, Zigmond MJ (1995) Estimating hydroxyl radical content in rat brain using systemic and intraventricular salicylate: impact of methamphetamine. J Neurochem 64:1819-1825.

Giros B, Jaber M, Jones SR, Wightman RM, Caron MG (1996) Hyperlocomotion and indifference to cocaine and amphetamine in mice lacking the dopamine transporter. Nature 379:606-612.

Glowinski J, Cheramy A, Romo R, Barbeito L (1988) Presynaptic regulation of dopaminergic transmission in the striatum. Cell Mol Neurobiol 8:7-17.

Gonzalez-Zulueta M, Ensz LM, Mukhina G, Lebovitz RM, Zwacka RM, Engelhardt JF, Oberley LW, Dawson VL, Dawson TM (1998) Manganese superoxide dismutase protects nNOS neurons from NMDA and nitric oxide-mediated neurotoxicity. J Neurosci 18:2040-2055.

Guyot MC, Hantraye P, Dolan R, Palfi S, Maziere M, Brouillet E (1997) Quantifiable bradykinesia, gait abnormalities and Huntington's disease-like striatal lesions in rats chronically treated with 3-nitropropionic acid. Neuroscience 79:45-56.

Guzman RG, Kendrick KM, Emson PC (1993) Effect of substance P on acetylcholine and dopamine release in the rat striatum: a microdialysis study. Brain Res 622:147-154.

Halkitis PN, Parsons JT, Stirratt MJ (2001) A double epidemic: crystal methamphetamine drug use in relation to HIV transmission among gay men. J Homosex 41:17-35.

Hamada M, Higashi H, Nairn AC, Greengard P, Nishi A (2004) Differential regulation of dopamine D1 and D2 signaling by nicotine in neostriatal neurons. J Neurochem 90:1094-1103.

Hanson GR, Rau KS, Fleckenstein AE (2004) The methamphetamine experience: a NIDA partnership. Neuropharmacology 47 Suppl 1:92-100.

Hanson GR, Letter AA, Merchant K, Gibb JW (1986) Comparison of responses by striatonigral substance P and neurokinin A systems to methamphetamine treatment. Peptides 7:983-987.

Hardmsn JG, Limbird LEE (1996) Goodman and Gilman's the Pharmacological Basis of Therapeutics, 9th ed. Edition. New York, NY: McGraw Hill.

Harvey DC, Lacan G, Melegan WP (2000) Regional heterogeneity of dopaminergic deficits in vervet monkey striatum and substantia nigra after methamphetamine exposure. Exp Brain Res 133:349-358.

Hastings TG, Lewis DA, Zigmond MJ (1996) Role of oxidation in the neurotoxic effects of intrastriatal dopamine injections. Proc Natl Acad Sci U S A 93:1956-1961.

Heales SJ, Bolanos JP, Stewart VC, Brookes PS, Land JM, Clark JB (1999) Nitric oxide, mitochondria and neurological disease. Biochim Biophys Acta 1410:215-228.

Hedreen JC, Folstein SE (1995) Early loss of neostriatal striosome neurons in Huntington's disease. J Neuropathol Exp Neurol 54:105-120.

Hickey MA, Chesselet MF (2003) Apoptosis in Huntington's disease. Prog Neuropsychopharmacol Biol Psychiatry 27:255-265.

Hirata H, Ladenheim B, Carlson E, Epstein C, Cadet JL (1996) Autoradiographic evidence for methamphetamine-induced striatal dopaminergic loss in mouse brain: attenuation in CuZn-superoxide dismutase transgenic mice. Brain Res 714:95-103.

Hof PR, Young WG, Bloom FE, Belichenko PV, Celio MR (2000) Comparative Cytoarchitectonic Altas of the C57Bl/6 and 129/Sv Mouse Brains: Elsevier.

Hokfelt T, Kellerth JO, Nilsson G, Pernow B (1975) Substance p: localization in the central nervous system and in some primary sensory neurons. Science 190:889-890.

Hong R, Matsuyama E, Nur K (1991) Cardiomyopathy associated with the smoking of crystal methamphetamine. Jama 265:1152-1154.

Hotchkiss AJ, Gibb JW (1980) Long-term effects of multiple doses of methamphetamine on tryptophan hydroxylase and tyrosine hydroxylase activity in rat brain. J Pharmacol Exp Ther 214:257-262.

Hotchkiss AJ, Morgan ME, Gibb JW (1979) The long-term effects of multiple doses of methamphetamine on neostriatal tryptophan hydroxylase, tyrosine hydroxylase, choline acetyltransferase and glutamate decarboxylase activities. Life Sci 25:1373-1378.

Hu HJ, Chen LW, Yung KK, Chan YS (2004) Differential expression of AMPA receptor subunits in substance P receptor-containing neurons of the caudate-putamen of rats. Neurosci Res 49:281-288.

Hynd MR, Scott HL, Dodd PR (2004) Glutamate-mediated excitotoxicity and neurodegeneration in Alzheimer's disease. Neurochem Int 45:583-595.

Imam SZ, Ali SF (2000) Selenium, an antioxidant, attenuates methamphetamine-induced dopaminergic toxicity and peroxynitrite generation. Brain Res 855:186-191.

Imam SZ, Newport GD, Islam F, Slikker W, Jr., Ali SF (1999a) Selenium, an antioxidant, protects against methamphetamine-induced dopaminergic neurotoxicity. Brain Res 818:575-578.

Imam SZ, Islam F, Itzhak Y, Slikker W, Jr., Ali SF (2000) Prevention of dopaminergic neurotoxicity by targeting nitric oxide and peroxynitrite: implications for the prevention of methamphetamine-induced neurotoxic damage. Ann N Y Acad Sci 914:157-171.

Imam SZ, Crow JP, Newport GD, Islam F, Slikker W, Jr., Ali SF (1999b) Methamphetamine generates peroxynitrite and produces dopaminergic neurotoxicity in mice: protective effects of peroxynitrite decomposition catalyst. Brain Res 837:15-21.

Imam SZ, Itzhak Y, Cadet JL, Islam F, Slikker W, Jr., Ali SF (2001) Methamphetamine-induced alteration in striatal p53 and bcl-2 expressions in mice. Brain Res Mol Brain Res 91:174-178.

Inagaki S, Suzuki K, Taniguchi N, Takagi H (1991) Localization of Mn-superoxide dismutase (Mn-SOD) in cholinergic and somatostatin-containing neurons in the rat neostriatum. Brain Res 549:174-177.

Itzhak Y, Ali SF (1996) The neuronal nitric oxide synthase inhibitor, 7-nitroindazole, protects against methamphetamine-induced neurotoxicity in vivo. J Neurochem 67:1770-1773.

Itzhak Y, Martin JL, Ail SF (2000) nNOS inhibitors attenuate methamphetamine-induced dopaminergic neurotoxicity but not hyperthermia in mice. Neuroreport 11:2943-2946.

Itzhak Y, Gandia C, Huang PL, Ali SF (1998) Resistance of neuronal nitric oxide synthase-deficient mice to methamphetamine-induced dopaminergic neurotoxicity. J Pharmacol Exp Ther 284:1040-1047.

Jayanthi S, Deng X, Bordelon M, McCoy MT, Cadet JL (2001) Methamphetamine causes differential regulation of pro-death and anti-death Bcl-2 genes in the mouse neocortex. Faseb J 15:1745-1752.

Jayanthi S, Deng X, Noailles PA, Ladenheim B, Cadet JL (2004) Methamphetamine induces neuronal apoptosis via cross-talks between endoplasmic reticulum and mitochondria-dependent death cascades. Faseb J 18:238-251.

Jolkkonen J, Jenner P, Marsden CD (1995) Glutamatergic regulation of striatal peptide gene expression in rats. J Neural Transm Park Dis Dement Sect 10:187-198.

Jones E, Mikula S, Trotts I, Stone J (2005) Brain Map.org. In. http://brainmaps.org/index.php?action=viewslides&dirname=HBP/mus.musculus/C57m1/C57m1/

Kalant H, Kalant OJ (1975) Death in amphetamine users: causes and rates. Can Med Assoc J 112:299-304.

Kaneko T, Shigemoto R, Nakanishi S, Mizuno N (1993) Substance P receptor-immunoreactive neurons in the rat neostriatum are segregated into somatostatinergic and cholinergic aspiny neurons. Brain Res 631:297-303.

Kashihara K, Hamamura T, Okumura K, Otsuki S (1990) Effect of MK-801 on endogenous dopamine release in vivo. Brain Res 528:80-82.

Kelley AE, Stinus L, Iversen SD (1979) Behavioural activation induced in the rat by substance P infusion into ventral tegmental area: implication of dopaminergic A10 neurones. Neurosci Lett 11:335-339.

Kelley AE, Cador M, Stinus L (1985) Behavioral analysis of the effect of substance P injected into the ventral mesencephalon on investigatory and spontaneous motor behavior in the rat. Psychopharmacology (Berl) 85:37-46.

Kita T, Wagner GC, Nakashima T (2003) Current research on methamphetamine-induced neurotoxicity: animal models of monoamine disruption. J Pharmacol Sci 92:178-195.

Kiyatkin EA (2005) Brain hyperthermia as physiological and pathological phenomena. Brain Res Brain Res Rev 50:27-56.

Kiyatkin EA, Brown PL (2004) Modulation of physiological brain hyperthermia by environmental temperature and impaired blood outflow in rats. Physiol Behav 83:467-474.

Kogan FJ, Nichols WK, Gibb JW (1976) Influence of methamphetamine on nigral and striatal tyrosine hydroxylase activity and on striatal dopamine levels. Eur J Pharmacol 36:363-371.

Koh JY, Choi DW (1988) Cultured striatal neurons containing NADPH-diaphorase or acetylcholinesterase are selectively resistant to injury by NMDA receptor agonists. Brain Res 446:374-378.

Koh JY, Peters S, Choi DW (1986) Neurons containing NADPH-diaphorase are selectively resistant to quinolinate toxicity. Science 234:73-76.

Koppenol WH, Moreno JJ, Pryor WA, Ischiropoulos H, Beckman JS (1992) Peroxynitrite, a cloaked oxidant formed by nitric oxide and superoxide. Chem Res Toxicol 5:834-842.

Kraft M, Noailles P, Angulo JA (2001) Substance P modulates cocaine-evoked dopamine overflow in the striatum of the rat brain. Ann N Y Acad Sci 937:121-131.

Kramer MS, Cutler N, Feighner J, Shrivastava R, Carman J, Sramek JJ, Reines SA, Liu G, Snavely D, Wyatt-Knowles E, Hale JJ, Mills SG, MacCoss M, Swain CJ, Harrison T, Hill RG, Hefti F, Scolnick EM, Cascieri MA, Chicchi GG, Sadowski S, Williams AR, Hewson L, Smith D, Carlson EJ, Hargreaves RJ, Rupniak NM (1998) Distinct mechanism for antidepressant activity by blockade of central substance P receptors. Science 281:1640-1645.

Krause JE, Hershey AD, Dykema PE, Takeda Y (1990) Molecular biological studies on the diversity of chemical signalling in tachykinin peptidergic neurons. Ann N Y Acad Sci 579:254-272.

Krebs MO, Trovero F, Desban M, Gauchy C, Glowinski J, Kemel ML (1991a) Distinct presynaptic regulation of dopamine release through NMDA receptors in striosome- and matrix-enriched areas of the rat striatum. J Neurosci 11:1256-1262.

Krebs MO, Desce JM, Kemel ML, Gauchy C, Godeheu G, Cheramy A, Glowinski J (1991b) Glutamatergic control of dopamine release in the rat striatum: evidence for presynaptic N-methyl-D-aspartate receptors on dopaminergic nerve terminals. J Neurochem 56:81-85.

Krolewski DM, Bishop C, Walker PD (2005) Intrastriatal dopamine D1 receptor agonist-mediated motor behavior is reduced by local neurokinin 1 receptor antagonism. Synapse 57:1-7.

Kuppenbender KD, Standaert DG, Feuerstein TJ, Penney JB, Jr., Young AB, Landwehrmeyer GB (2000) Expression of NMDA receptor subunit mRNAs in neurochemically identified projection and interneurons in the human striatum. J Comp Neurol 419:407-421.

Landwehrmeyer GB, Standaert DG, Testa CM, Penney JB, Jr., Young AB (1995) NMDA receptor subunit mRNA expression by projection neurons and interneurons in rat striatum. J Neurosci 15:5297-5307.

LaVoie MJ, Hastings TG (1999a) Dopamine quinone formation and protein modification associated with the striatal neurotoxicity of methamphetamine: evidence against a role for extracellular dopamine. J Neurosci 19:1484-1491.

LaVoie MJ, Hastings TG (1999b) Peroxynitrite- and nitrite-induced oxidation of dopamine: implications for nitric oxide in dopaminergic cell loss. J Neurochem 73:2546-2554.

Lazareno S, Popham A, Birdsall NJ (2002) Analogs of WIN 62,577 define a second allosteric site on muscarinic receptors. Mol Pharmacol 62:1492-1505.

Li JL, Kaneko T, Mizuno N (2001) Colocalization of neuronal nitric oxide synthase and neurokinin-1 receptor in striatal interneurons in the rat. Neurosci Lett 310:109-112.

Li JL, Kaneko T, Mizuno N (2002a) Synaptic association of dopaminergic axon terminals and neurokinin-1 receptor-expressing intrinsic neurons in the striatum of the rat. Neurosci Lett 324:9-12.

Li JL, Dong YL, Kaneko T, Mizuno N (2002b) Direct projections from substance P-containing neurons to nitric oxide synthase-containing interneurons in the rat striatum. Neurosci Lett 318:133-136.

Li JL, Wang D, Kaneko T, Shigemoto R, Nomura S, Mizuno N (2000) Relationship between neurokinin-1 receptor and substance P in the striatum: light and electron microscopic immunohistochemical study in the rat. J Comp Neurol 418:156-163.

Li SJ, Sivam SP, McGinty JF, Huang YS, Hong JS (1987) Dopaminergic regulation of tachykinin metabolism in the striatonigral pathway. J Pharmacol Exp Ther 243:792-798.

Liang NY, Rutledge CO (1982) Evidence for carrier-mediated efflux of dopamine from corpus striatum. Biochem Pharmacol 31:2479-2484.

Liu H, Mazarati AM, Katsumori H, Sankar R, Wasterlain CG (1999a) Substance P is expressed in hippocampal principal neurons during status epilepticus and plays a critical role in the maintenance of status epilepticus. Proc Natl Acad Sci U S A 96:5286-5291.

Liu H, Cao Y, Basbaum AI, Mazarati AM, Sankar R, Wasterlain CG (1999b) Resistance to excitotoxin-induced seizures and neuronal death in mice lacking the preprotachykinin A gene. Proc Natl Acad Sci U S A 96:12096-12101.

Liu Z, Mao L, Parelkar NK, Tang Q, Samdani S, Wang JQ (2004) Distinct expression of phosphorylated N-methyl-D-aspartate receptor NR1 subunits by projection neurons and interneurons in the striatum of normal and amphetamine-treated rats. J Comp Neurol 474:393-406.

Lorez H (1981) Fluorescence histochemistry indicates damage of striatal dopamine nerve terminals in rats after multiple doses of methamphetamine. Life Sci 28:911-916.

Lukas SE (1985) Amphetamine:Danger in the Fast Lane. New York: Chelsea House Publishers.

Maggi CA (1995) The mammalian tachykinin receptors. Gen Pharmacol 26:911-944.

Maggi CA, Schwartz TW (1997) The dual nature of the tachykinin NK1 receptor. Trends Pharmacol Sci 18:351-355.

Mantyh PW, Allen CJ, Ghilardi JR, Rogers SD, Mantyh CR, Liu H, Basbaum AI, Vigna SR, Maggio JE (1995a) Rapid endocytosis of a G protein-coupled receptor: substance P evoked internalization of its receptor in the rat striatum in vivo. Proc Natl Acad Sci U S A 92:2622-2626.

Mantyh PW, DeMaster E, Malhotra A, Ghilardi JR, Rogers SD, Mantyh CR, Liu H, Basbaum AI, Vigna SR, Maggio JE, et al. (1995b) Receptor endocytosis and dendrite reshaping in spinal neurons after somatosensory stimulation. Science 268:1629-1632.

Marino MJ, Valenti O, Conn PJ (2003) Glutamate receptors and Parkinson's disease: opportunities for intervention. Drugs Aging 20:377-397.

Marti M, Mela F, Bianchi C, Beani L, Morari M (2002) Striatal dopamine-NMDA receptor interactions in the modulation of glutamate release in the substantia nigra pars reticulata in vivo: opposite role for D1 and D2 receptors. J Neurochem 83:635-644.

Marti M, Manzalini M, Fantin M, Bianchi C, Della Corte L, Morari M (2005) Striatal glutamate release evoked in vivo by NMDA is dependent upon ongoing neuronal activity in the substantia nigra, endogenous striatal substance P and dopamine. J Neurochem 93:195-205.

McCann UD, Ricaurte GA (2004) Amphetamine neurotoxicity: accomplishments and remaining challenges. Neurosci Biobehav Rev 27:821-826.

McCann UD, Wong DF, Yokoi F, Villemagne V, Dannals RF, Ricaurte GA (1998) Reduced striatal dopamine transporter density in abstinent methamphetamine and methcathinone users: evidence from positron emission tomography studies with [11C]WIN-35,428. J Neurosci 18:8417-8422.

Medina L, Figueredo-Cardenas G, Reiner A (1996) Differential abundance of superoxide dismutase in interneurons versus projection neurons and in matrix versus striosome neurons in monkey striatum. Brain Res 708:59-70.

Melega WP, Williams AE, Schmitz DA, DiStefano EW, Cho AK (1995) Pharmacokinetic and pharmacodynamic analysis of the actions of D-amphetamine and D-methamphetamine on the dopamine terminal. J Pharmacol Exp Ther 274:90-96.

Melega WP, Lacan G, Harvey DC, Huang SC, Phelps ME (1998) Dizocilpine and reduced body temperature do not prevent methamphetamine-induced neurotoxicity in the vervet monkey: [11C]WIN 35,428 - positron emission tomography studies. Neurosci Lett 258:17-20.

Migheli R, Godani C, Sciola L, Delogu MR, Serra PA, Zangani D, De Natale G, Miele E, Desole MS (1999) Enhancing effect of manganese on L-DOPA-induced apoptosis in PC12 cells: role of oxidative stress. J Neurochem 73:1155-1163.

Miller DB, O'Callaghan JP (1994) Environment-, drug- and stress-induced alterations in body temperature affect the neurotoxicity of substituted amphetamines in the C57BL/6J mouse. J Pharmacol Exp Ther 270:752-760.

Mitchell IJ, Cooper AJ, Griffiths MR (1999) The selective vulnerability of striatopallidal neurons. Prog Neurobiol 59:691-719.

Mitchell IJ, Lawson S, Moser B, Laidlaw SM, Cooper AJ, Walkinshaw G, Waters CM (1994) Glutamate-induced apoptosis results in a loss of striatal neurons in the parkinsonian rat. Neuroscience 63:1-5.

Moore RY, Bhatnagar RK, Heller A (1971) Anatomical and chemical studies of a nigro-neostriatal projection in the cat. Brain Res 30:119-135.

Mullen RJ, Buck CR, Smith AM (1992) NeuN, a neuronal specific nuclear protein in vertebrates. Development 116:201-211.

Murtra P, Sheasby AM, Hunt SP, De Felipe C (2000) Rewarding effects of opiates are absent in mice lacking the receptor for substance P. Nature 405:180-183.

Nakanishi S (1992) Molecular diversity of glutamate receptors and implications for brain function. Science 258:597-603.

Namiki M, Mori T, Sawaguchi T, Ito S, Suzuki T (2005) Underlying mechanism of combined effect of methamphetamine and morphine on lethality in mice and therapeutic potential of cooling. J Pharmacol Sci 99:168-176.

Nash JF, Yamamoto BK (1992) Methamphetamine neurotoxicity and striatal glutamate release: comparison to 3,4-methylenedioxymethamphetamine. Brain Res 581:237-243.

Noailles PA, Angulo JA (2002) Neurokinin receptors modulate the neurochemical actions of cocaine. Ann N Y Acad Sci 965:267-273.

Nwanze E, Jonsson G (1981) Amphetamine neurotoxicity on dopamine nerve terminals in the caudate nucleus of mice. Neurosci Lett 26:163-168.

O'Dell SJ, Weihmuller FB, Marshall JF (1992) MK-801 prevents methamphetamine-induced striatal dopamine damage and reduces extracellular dopamine overflow. Ann N Y Acad Sci 648:317-319.

Ogata A (1919) Constitution of ephedrine-Desoxyephedrine. J Pharm Soc Jpn 451:751.

ONDCP (2001) The economic costs of drug abuse in the United States. In: Office of National Drug Control Policy.

Otsuka M, Yoshioka K (1993) Neurotransmitter functions of mammalian tachykinins. Physiol Rev 73:229-308.

Parent A, Mackey A, De Bellefeuille L (1983) The subcortical afferents to caudate nucleus and putamen in primate: a fluorescence retrograde double labeling study. Neuroscience 10:1137-1150.

Patacchini R, Lecci A, Holzer P, Maggi CA (2004) Newly discovered tachykinins raise new questions about their peripheral roles and the tachykinin nomenclature. Trends Pharmacol Sci 25:1-3.

Perez JA, Jr., Arsura EL, Strategos S (1999) Methamphetamine-related stroke: four cases. J Emerg Med 17:469-471.

Pu C, Vorhees CV (1995) Protective effects of MK-801 on methamphetamine-induced depletion of dopaminergic and serotonergic terminals and striatal astrocytic response: an immunohistochemical study. Synapse 19:97-104.

Pu C, Fisher JE, Cappon GD, Vorhees CV (1994) The effects of amfonelic acid, a dopamine uptake inhibitor, on methamphetamine-induced dopaminergic terminal degeneration and astrocytic response in rat striatum. Brain Res 649:217-224.

Qin ZH, Wang Y, Chase TN (1996) Stimulation of N-methyl-D-aspartate receptors induces apoptosis in rat brain. Brain Res 725:166-176.

Quartara L, Maggi CA (1997) The tachykinin NK1 receptor. Part I: ligands and mechanisms of cellular activation. Neuropeptides 31:537-563.

Raiteri M, Cerrito F, Cervoni AM, Levi G (1979) Dopamine can be released by two mechanisms differentially affected by the dopamine transport inhibitor nomifensine. J Pharmacol Exp Ther 208:195-202.

Rawson RA, Anglin MD, Ling W (2002) Will the methamphetamine problem go away? J Addict Dis 21:5-19.

Reid MS, Herrera-Marschitz M, Ungerstedt U (1991) Effects of intranigral substance P and neurokinin A injections on extracellular dopamine levels measured with microdialysis in the striatum and frontoparietal cortex of rats. J Neurochem 57:970-974.

Reid MS, Herrera-Marschitz M, Kehr J, Ungerstedt U (1990a) Striatal dopamine and glutamate release: effects of intranigral injections of substance P. Acta Physiol Scand 140:527-537.

Reid MS, Herrera-Marschitz M, Hokfelt T, Ohlin M, Valentino KL, Ungerstedt U (1990b) Effects of intranigral substance P and neurokinin A on striatal dopamine release--I. Interactions with substance P antagonists. Neuroscience 36:643-658.

Reid MS, Herrera-Marschitz M, Hokfelt T, Lindefors N, Persson H, Ungerstedt U (1990c) Striatonigral GABA, dynorphin, substance P and neurokinin A modulation of nigrostriatal dopamine release: evidence for direct regulatory mechanisms. Exp Brain Res 82:293-303.

Reiner A, Albin RL, Anderson KD, D'Amato CJ, Penney JB, Young AB (1988) Differential loss of striatal projection neurons in Huntington disease. Proc Natl Acad Sci U S A 85:5733-5737.

Ricaurte GA, Schuster CR, Seiden LS (1980) Long-term effects of repeated methylamphetamine administration on dopamine and serotonin neurons in the rat brain: a regional study. Brain Res 193:153-163.

Ricaurte GA, Seiden LS, Schuster CR (1983) Increased dopamine metabolism in the rat neostriatum after toxic doses of d-methylamphetamine. Neuropharmacology 22:1383-1388.

Ricaurte GA, Seiden LS, Schuster CR (1984) Further evidence that amphetamines produce long-lasting dopamine neurochemical deficits by destroying dopamine nerve fibers. Brain Res 303:359-364.

Ricaurte GA, Guillery RW, Seiden LS, Schuster CR, Moore RY (1982) Dopamine nerve terminal degeneration produced by high doses of methylamphetamine in the rat brain. Brain Res 235:93-103.

Richards JR, Johnson EB, Stark RW, Derlet RW (1999) Methamphetamine abuse and rhabdomyolysis in the ED: a 5-year study. Am J Emerg Med 17:681-685.

Richfield EK, Maguire-Zeiss KA, Vonkeman HE, Voorn P (1995) Preferential loss of preproenkephalin versus preprotachykinin neurons from the striatum of Huntington's disease patients. Ann Neurol 38:852-861.

Richfield EK, Vonsattel JP, MacDonald ME, Sun Z, Deng YP, Reiner A (2002) Selective loss of striatal preprotachykinin neurons in a phenocopy of Huntington's disease. Mov Disord 17:327-332.

Riobo NA, Schopfer FJ, Boveris AD, Cadenas E, Poderoso JJ (2002) The reaction of nitric oxide with 6-hydroxydopamine: implications for Parkinson's disease. Free Radic Biol Med 32:115-121.

Riviere GJ, Gentry WB, Owens SM (2000) Disposition of methamphetamine and its metabolite amphetamine in brain and other tissues in rats after intravenous administration. J Pharmacol Exp Ther 292:1042-1047.

Rusin KI, Bleakman D, Chard PS, Randic M, Miller RJ (1993) Tachykinins potentiate N-methyl-D-aspartate responses in acutely isolated neurons from the dorsal horn. J Neurochem 60:952-960.

Saka E, Graybiel AM (2003) Pathophysiology of Tourette's syndrome: striatal pathways revisited. Brain Dev 25 Suppl 1:S15-19.

SAMHSA (2005) 2004 National Survey on Drug Abuse and Health:National Findings. In: Substance Abuse and Mental Health Services Administration.

Sandoval V, Hanson GR, Fleckenstein AE (2000) Methamphetamine decreases mouse striatal dopamine transporter activity: roles of hyperthermia and dopamine. Eur J Pharmacol 409:265-271.

Schmidt CJ, Ritter JK, Sonsalla PK, Hanson GR, Gibb JW (1985) Role of dopamine in the neurotoxic effects of methamphetamine. J Pharmacol Exp Ther 233:539-544.

Seiden LS, Fischman MW, Schuster CR (1976) Long-term methamphetamine induced changes in brain catecholamines in tolerant rhesus monkeys. Drug Alcohol Depend 1:215-219.

Seiden LS, Sabol KE, Ricaurte GA (1993) Amphetamine: effects on catecholamine systems and behavior. Annu Rev Pharmacol Toxicol 33:639-677.

Sidman RL, Kosaras B, Misra B, Senft S (2005) High Resolution Mouse Brain Atlas. In. http://www.hms.harvard.edu/ research/brain/atlas.html.

Simantov R, Blinder E, Ratovitski T, Tauber M, Gabbay M, Porat S (1996) Dopamine-induced apoptosis in human neuronal cells: inhibition by nucleic acids antisense to the dopamine transporter. Neuroscience 74:39-50.

Singer HS, Minzer K (2003) Neurobiology of Tourette's syndrome: concepts of neuroanatomic localization and neurochemical abnormalities. Brain Dev 25 Suppl 1:S70-84.

Sonsalla PK, Gibb JW, Hanson GR (1986) Nigrostriatal dopamine actions on the D2 receptors mediate methamphetamine effects on the striatonigral substance P system. Neuropharmacology 25:1221-1230.

Sonsalla PK, Nicklas WJ, Heikkila RE (1989) Role for excitatory amino acids in methamphetamine-induced nigrostriatal dopaminergic toxicity. Science 243:398-400.

Stephans SE, Yamamoto BK (1994) Methamphetamine-induced neurotoxicity: roles for glutamate and dopamine efflux. Synapse 17:203-209.

Stumm G, Schlegel J, Schafer T, Wurz C, Mennel HD, Krieg JC, Vedder H (1999) Amphetamines induce apoptosis and regulation of bcl-x splice variants in neocortical neurons. Faseb J 13:1065-1072.

Stumm R, Culmsee C, Schafer MK, Krieglstein J, Weihe E (2001) Adaptive plasticity in tachykinin and tachykinin receptor expression after focal cerebral ischemia

is differentially linked to gabaergic and glutamatergic cerebrocortical circuits and cerebrovenular endothelium. J Neurosci 21:798-811.

Sulzer D, Rayport S (1990) Amphetamine and other psychostimulants reduce pH gradients in midbrain dopaminergic neurons and chromaffin granules: a mechanism of action. Neuron 5:797-808.

Sulzer D, Maidment NT, Rayport S (1993) Amphetamine and other weak bases act to promote reverse transport of dopamine in ventral midbrain neurons. J Neurochem 60:527-535.

Sulzer D, Pothos E, Sung HM, Maidment NT, Hoebel BG, Rayport S (1992) Weak base model of amphetamine action. Ann N Y Acad Sci 654:525-528.

Sulzer D, Chen TK, Lau YY, Kristensen H, Rayport S, Ewing A (1995) Amphetamine redistributes dopamine from synaptic vesicles to the cytosol and promotes reverse transport. J Neurosci 15:4102-4108.

Szabo C (1996a) Physiological and pathophysiological roles of nitric oxide in the central nervous system. Brain Res Bull 41:131-141.

Szabo C (1996b) DNA strand breakage and activation of poly-ADP ribosyltransferase: a cytotoxic pathway triggered by peroxynitrite. Free Radic Biol Med 21:855-869.

Thiriet N, Jayanthi S, McCoy M, Ladenheim B, Lud Cadet J (2001) Methamphetamine increases expression of the apoptotic c-myc and L-myc genes in the mouse brain. Brain Res Mol Brain Res 90:202-204.

Thiriet N, Deng X, Solinas M, Ladenheim B, Curtis W, Goldberg SR, Palmiter RD, Cadet JL (2005) Neuropeptide Y protects against methamphetamine-induced neuronal apoptosis in the mouse striatum. J Neurosci 25:5273-5279.

Thompson PM, Hayashi KM, Simon SL, Geaga JA, Hong MS, Sui Y, Lee JY, Toga AW, Ling W, London ED (2004) Structural abnormalities in the brains of human subjects who use methamphetamine. J Neurosci 24:6028-6036.

Tremblay L, Kemel ML, Desban M, Gauchy C, Glowinski J (1992) Distinct presynaptic control of dopamine release in striosomal- and matrix-enriched areas of the rat striatum by selective agonists of NK1, NK2, and NK3 tachykinin receptors. Proc Natl Acad Sci U S A 89:11214-11218.

Tsao LI, Ladenheim B, Andrews AM, Chiueh CC, Cadet JL, Su TP (1998) Delta opioid peptide [D-Ala2,D-leu5]enkephalin blocks the long-term loss of dopamine transporters induced by multiple administrations of methamphetamine: involvement of opioid receptors and reactive oxygen species. J Pharmacol Exp Ther 287:322-331.

Uemura K, Aki T, Yamaguchi K, Yoshida K (2003) Protein kinase C-epsilon protects PC12 cells against methamphetamine-induced death: possible involvement of suppression of glutamate receptor. Life Sci 72:1595-1607.

Uemura Y, Kowall NW, Beal MF (1990) Selective sparing of NADPH-diaphorase-somatostatin-neuropeptide Y neurons in ischemic gerbil striatum. Ann Neurol 27:620-625.

UNODC (2003) Global Illicit drug trends 2003. In. New York: United Nations Office on Drugs and Crime.

Varner KJ, Ogden BA, Delcarpio J, Meleg-Smith S (2002) Cardiovascular responses elicited by the "binge" administration of methamphetamine. J Pharmacol Exp Ther 301:152-159.

Vezzani A, Forloni GL, Serafini R, Rizzi M, Samanin R (1991) Neurodegenerative Effects Induced by Chronic Infusion of Quinolinic Acid in Rat Striatum and Hippocampus. Eur J Neurosci 3:40-46.

Villemagne V, Yuan J, Wong DF, Dannals RF, Hatzidimitriou G, Mathews WB, Ravert HT, Musachio J, McCann UD, Ricaurte GA (1998) Brain dopamine neurotoxicity in baboons treated with doses of methamphetamine comparable to those recreationally abused by humans: evidence from [11C]WIN-35,428 positron emission tomography studies and direct in vitro determinations. J Neurosci 18:419-427.

Vonsattel JP, Myers RH, Stevens TJ, Ferrante RJ, Bird ED, Richardson EP, Jr. (1985) Neuropathological classification of Huntington's disease. J Neuropathol Exp Neurol 44:559-577.

Vruwink M, Schmidt HH, Weinberg RJ, Burette A (2001) Substance P and nitric oxide signaling in cerebral cortex: anatomical evidence for reciprocal signaling between two classes of interneurons. J Comp Neurol 441:288-301.

Wagner GC, Ricaurte GA, Seiden LS, Schuster CR, Miller RJ, Westley J (1980) Long-lasting depletions of striatal dopamine and loss of dopamine uptake sites following repeated administration of methamphetamine. Brain Res 181:151-160.

Wang WW, Cao R, Rao ZR, Chen LW (2004) Differential expression of NMDA and AMPA receptor subunits in DARPP-32-containing neurons of the cerebral cortex, hippocampus and neostriatum of rats. Brain Res 998:174-183.

Weihmuller FB, O'Dell SJ, Marshall JF (1992) MK-801 protection against methamphetamine-induced striatal dopamine terminal injury is associated with attenuated dopamine overflow. Synapse 11:155-163.

Whitehead RE, Ferrer JV, Javitch JA, Justice JB (2001) Reaction of oxidized dopamine with endogenous cysteine residues in the human dopamine transporter. J Neurochem 76:1242-1251.

Wiley RG, Lappi DA (1999) Targeting neurokinin-1 receptor-expressing neurons with [Sar9,Met(O2)11 substance P-saporin. Neurosci Lett 277:1-4.

Wilson JM, Kalasinsky KS, Levey AI, Bergeron C, Reiber G, Anthony RM, Schmunk GA, Shannak K, Haycock JW, Kish SJ (1996) Striatal dopamine nerve terminal markers in human, chronic methamphetamine users. Nat Med 2:699-703.

Woolf CJ, Doubell TP (1994) The pathophysiology of chronic pain--increased sensitivity to low threshold A beta-fibre inputs. Curr Opin Neurobiol 4:525-534.

Woolverton WL, Ricaurte GA, Forno LS, Seiden LS (1989) Long-term effects of chronic methamphetamine administration in rhesus monkeys. Brain Res 486:73-78.

Xie T, McCann UD, Kim S, Yuan J, Ricaurte GA (2000) Effect of temperature on dopamine transporter function and intracellular accumulation of methamphetamine: implications for methamphetamine-induced dopaminergic neurotoxicity. J Neurosci 20:7838-7845.

Xu Y, Stokes AH, Roskoski R, Jr., Vrana KE (1998) Dopamine, in the presence of tyrosinase, covalently modifies and inactivates tyrosine hydroxylase. J Neurosci Res 54:691-697.

Yamamoto BK, Zhu W (1998) The effects of methamphetamine on the production of free radicals and oxidative stress. J Pharmacol Exp Ther 287:107-114.

Yoshie Y, Ohshima H (1997) Synergistic induction of DNA strand breakage caused by nitric oxide together with catecholamine: implications for neurodegenerative disease. Chem Res Toxicol 10:1015-1022.

Yu J, Cadet JL, Angulo JA (2002) Neurokinin-1 (NK-1) receptor antagonists abrogate methamphetamine-induced striatal dopaminergic neurotoxicity in the murine brain. J Neurochem 83:613-622.

Yu J, Wang J, Cadet JL, Angulo JA (2004) Histological evidence supporting a role for the striatal neurokinin-1 receptor in methamphetamine-induced neurotoxicity in the mouse brain. Brain Res 1007:124-131.

Yu Z, Cheng G, Huang X, Li K, Cao X (1997) Neurokinin-1 receptor antagonist SR140333: a novel type of drug to treat cerebral ischemia. Neuroreport 8:2117-2119.

Yuan J, Hatzidimitriou G, Suthar P, Mueller M, McCann U, Ricaurte G (2005) Relationship between temperature, dopaminergic neurotoxicity and plasma drug concentrations in methamphetamine-treated squirrel monkeys. J Pharmacol Exp Ther.

Zachrisson O, Lindefors N, Brene S (1998) A tachykinin NK1 receptor antagonist, CP-122,721-1, attenuates kainic acid-induced seizure activity. Brain Res Mol Brain Res 60:291-295.

Zhang Y, Landas K, Mueller H, Angulo JA (1997) Progressive augmentation of striatal and accumbal preprotachykinin mRNA levels by chronic treatment with methamphetamine and effect of concurrent administration of the N-methyl-D-aspartate receptor antagonist MK-801. Neuropharmacology 36:325-334.

Zhou Q, Le Greves P, Ragnar F, Nyberg F (2000) Intracerebroventricular injection of the N-terminal substance P fragment SP(1-7) regulates the expression of the N-methyl-D-aspartate receptor NR1, NR2A and NR2B subunit mRNAs in the rat brain. Neurosci Lett 291:109-112.